ICFA Beam Dynamics Newsletter, No. 20

Editors in chief
K. Hirata and J.M. Jowett

Editors
W. Chou, S. Ivanov, H. Mais, J. Wei, D.H. Whittum, and C. Zhang

August 1999

Contents

1: Foreword

John Jowett john.jowett@cern.ch CERN

This issue of the Newsletter is the first to be prepared under a new editorial scheme. Readers will have noticed that the list of editors on our cover page is much longer than it used to be. In the old scheme each of the three editors was principally responsible for one issue per year. The larger team will now take it in turn to be principal editors of an issue. The idea behind this is not merely to distribute the (entirely voluntary) workload over more members of the ICFA Beam Dynamics Panel. Rather, we hope that it will imbue the Newsletter with their individual ideas and approaches and provide more varied reading. The grandly titled "Editors-in-Chief" will coordinate and maintain continuity.

The present Newsletter gives every indication that this arrangement will produce the goods. Weiren Chou, the principal editor of this issue, has produced a Newsletter with a large section devoted to the theme of high-intensity, high-brightness hadron beams. As one of the most active researchers in this field, he is in an excellent position to compile a comprehensive survey of activities from contacts world-wide. The regular Newsletter features continue to be present and, of course, your contributions—activity reports, letters to the editors, announcements of beam dynamics events and so on—are welcome for future issues. We hope that all members of the beam dynamics community will feel they can contact their nearest Panel Member and propose a contribution.

2: From the Editor

Weiren Chou chou@adcon.fnal.gov Fermilab

When the readers receive this issue of the Newsletter, you will have noticed that it is almost twice as thick as previous ones. This is because it contains a special section of high intensity high brightness hadron beams. This is a field that has been very active in recent years. In the high energy physics (HEP) community, high brightness is an essential requirement of synchrotrons that serve as injectors to hadron-hadron or hadron-lepton colliders (Tevatron, HERA and LHC). The newest medium energy proton synchrotron, the Main Injector at Fermilab, will increase the Tevatron luminosity by at least a factor of five. Since mid-1990s, the HEP community has also become more and more interested in very high intensity proton machines. For example, a proton driver that would deliver intense short proton bunches to the target for muon production. These muons will then be used in a neutrino factory and/or a muon collider for HEP experiments. In the nuclear physics (NP) community, on the other hand, high flux of protons is always in demand. The approval of the Spallation Neutron Source (SNS) means the first large accelerator project in the US after the demise of the SSC that reaches one billion US dollars scale. Another big project, the Japan Hadron Facility (JHF), is expected to start full construction soon. In Europe, an European Spallation Source (ESS) is under design. Moreover, existing facilities, *e.g.,* the ISIS, PSR, AGS, KEK PS, CERN PSB, PS and SPS, are all having various levels of upgrades for performance improvement. Considerable amount of work in this field is also taking place at other labs such as the ANL, PPPL and BINP. This issue is a collection of reports of these activities. Each report contains a description of parameters, key technical issues and their solutions, as well as open issues that need solutions.

In this special section, five tables of high intensity high brightness proton machines are included. These tables are compiled and maintained by the ICFA Working Group during the last three years. I hope the readers will find them useful.

In addition to the special section, the readers will find in this issue a number of interesting workshop reports, activity reports, accelerator summer course, new doctoral theses and announcements of forthcoming workshops and schools. Two recent ICFA panel and working group meeting minutes are also enclosed.

I am pleased to receive a letter from Alvin Tollestrup. Alvin is a well-known veteran in the HEP community. He played a major role in the construction of the world's first superconducting collider Tevatron. He was also the first spokesperson of the detector CDF, in which the top quark was found. He received numerous awards, including the prestige National Medal of Technology from the then US president Bush. His letter addresses an important question, which is faced by the whole HEP community today. Namely, what is the next machine to build after the LHC? He expresses his opinions, which, almost certainly, will stimulate interesting discussions in our community.

I would like to express my sincere gratitude to the ICFA Working Group. Most members of this group contributed to the special section of this issue. Kohji Hirata and John Jowett provided much needed help throughout the editing process. I am also greatly obliged to Joshua Talley. He carefully read the manuscripts, converted them to LaTex when needed, re-typed the tables, corrected errors, put them on the web, and pieced everything together. His hard work produced this Newsletter that you are reading. Enjoy!

3: Letters to the Editors

3.1 From A. Tollestrup

Alvin Tollestrup alvin@fnal.gov Fermilab

How to Choose and What to Do!

How should we choose the next machine to build? This is an emotionally loaded question and the answer has many variations depending on the respondent. We need to begin a dialog now on how to make this decision that is so critical for the future of our field. My fundamental premise is that first we must know the energy scale that the machine must address. This is a radically different constraint than the ones we have worked with in the past. Let me revisit our past briefly.

When I was a graduate student at CalTech, the definition of "high energy" was shifting from the world of nuclear resonances at the few MeV level to that of the cyclotrons and synchrotrons at a few hundred MeV. The field was solidly grounded in the universities. Everyone could have a machine! There WAS a definitive energy scale, that of the pion mass, but we were finding it by trial and error. Machines below this threshold for new physics languished and machines well above that prospered. The failures mattered locally, of course, but not globally. Machines were cheap and could be built by professors and their graduate students.

Contrast that scenario with the present environment. We have noisy proponents of electron colliders, muon colliders, and very large hadron colliders. The cost of any of these machines will certainly approach the limit of what the world community is willing to spend on our esoteric field. A "wrong choice" will spell disaster for our future. A "right choice" may pay rich dividends. How do we choose?

If we look to the future, Run II at the Tevatron will furnish the first chance to find new physics, unless LEP manages to pull the Higgs out of the box in the near future. Suppose the low mass Higgs turned up in the next five years. Would that set the energy scale for a new lepton collider? The answer depends on who your favorite theoretical soothsayer is but if the Tevatron turns up the LSP of SUSY, that would set the scale and we should be prepared. First, we must start now the basic R & D needs to be done on long lead time projects necessary for upgrading the luminosity (and energy, modestly?) of the Tevatron. That machine will be our only window till the LHC comes on line, and we must be ready to exploit this machine to its utmost without shutting it down for long periods.

Second, there will be a "feeding frenzy" for a low energy lepton collider. The choice will probably be between a TESLA-type technology and the x-band technology of the NLC. We should educate ourselves now about these options in order to be in a position to make this choice rapidly and we are fortunate that this is already underway. I will assume that the technology for these machines is portable and not tied to a specific site and that the politics will allow a free choice. Some of the important general considerations will be:

1. Cost and financial support. Obviously an overwhelming consideration that I will leave others to discuss!

2. Is the technology in place? Is the R & D really done?

3. How long will it take to commission and reach design luminosity? This is a crucial point. We will want this machine in a hurry, and a long commissioning time will not be acceptable. Complexity of the design will matter. Does the larger aperture of TESLA with its attendant relaxed restrictions make for more rapid commissioning? Or does the SCRF have a whole new set of problems that must be dealt with?

4. What role does luminosity play in the choice? TESLA advertises a factor of three more in this important number. A third of a year for an experiment to find extra dimensions instead of a year sounds attractive.

5. Will it be possible to make a free choice, or will political and geographical considerations force major compromises?

There are many other questions to be addressed, including the ability to increase the machine's energy and luminosity. However, if the Tevatron discovers SUSY, the "energy scale" will be low and perhaps we should look at this as the first exploratory machine and hence leave the question of higher energy to the future. Perhaps the hardware could be used as part of a future complex that would capitalize on the CLIC-like technology. Or perhaps if the choice is for a TESLA-like machine, it could be reconfigured as the final accelerator for a muon collider. The future will tell.

Suppose that the Tevatron does not discover SUSY. The next step then will be up to the LHC. Our theoretical friends tell us that machine will surely reveal the underlying mysteries of the TeV-scale universe. What should we be doing in the meantime? We have a lot of work to do in the next 10 years!

We must devote much more effort to accelerator science. We must bring the universities back into this field. The idea must be dispelled that the "Accelerator Fairy" is going to bless us with the next machine on the Livingston curve. The main challenge for the next 50 years will be accelerators...not detectors. Large scale accelerator experiments at the major laboratories must include professors and their graduate students and make use of the technology base at the universities for instrumentation. This has become a well established modus operandi for large experiments like CDF, D0, and the LEP experiments. This will not be easy: the funding agencies, the laboratories and the universities all have conceptual problems with this proposal.

What experiments do we need? The goal should be to develop the various accelerator scenarios to the point where they would be ready for construction when LHC makes the big discovery. If the energy scale is high, then the muon collider and CLIC may be desired options. I find the recent developments at CLIC very appealing, but much experimental work must be done before such a machine could be built. The muon collider needs to be made "real" or killed. I like the present effort because the experimental program to demonstrate cooling has drawn in the university community creating a nice amalgam of accelerator types and experimental people. I also like it because there is physics at each stage of its development. Using the cooled muons for making neutrino beams would be a nice spin-off. SCRF is obviously a hot topic for the future that on a longer time scale may have some surprising payoffs.

A major challenge for the x-band machines as well as for all the other options is to get the cost down. However, on this point I'm pessimistic ..... any of the machines we are considering are going to cost a lot. The solution will have to involve spreading the costs out in time as well as geographically. Finally, we mustn't forget the hadron collider. If some of the more recent ideas of quantum gravity becoming strong at the weak scale should prove to be the way the universe is made, then the

VLHC may well be the machine of choice. Although we may know and understand this technology better than any of the others, it is also true that the cost of an LHC-like extension to 100 TeV would have a prohibitive cost. Perhaps the low-field version being studied at FNAL is an answer, but like the other options will take an enormous development effort to bring the cost down.

So I believe there is plenty to do! We have a beautiful transition period, when a young physicist can spend time in the ongoing particle physics program, and more senior ones can also start to engage themselves with the machines of our future. I have concentrated here on the near term; but, as I mentioned above this is not the major problem for our future. We must have higher energy, and so the possibility of lasers, plasmas, and ”whatevers” that are in their embryonic stage must be encouraged with funding and support. We must put more of our resources into our future. There is no Accelerator Fairy!

4: Special Section - High Intensity High Brightness Hadron Beams

4.1 KEK PS Beam Intensity Upgrade Program and Its Result

Ken Takayama takayama@post.kek.jp KEK, Japan

4.1.1 Introduction

Since 1976, the KEK 12-GeV Proton Synchrotron has delivered proton beams to a wide variety of physics experiments. The accelerator comprises two 750-keV Cockcroft-Walton accelerators, a 40-MeV drift tube linac (Linac), a 500-MeV fast-cycling synchrotron (Booster), and a 12-GeV synchrotron (Main Ring). The Main Ring stacks nine beam pulses from the Booster during the injection porch, and delivers 12-GeV proton beams to two experimental halls as a dc-current beam spill in slow-extraction.

In 1994, the long-baseline neutrino-oscillation experiment using the 12-GeV PS and Super KAMIOKANDE, which demands a total number of protons of 10^{20} on target in a time period of three years, has been approved by the program advisory committee. It has been proposed that the MR should operate at a repetition rate of 0.5 Hz with 6×10^{12} ppp to meet this beam requirement. For this purpose, the MR beam intensity upgrade program was internally authorized in 1995 and several task forces started activities [1].

First of all, the task force tried to realize what is the achievable limit of the beam intensity in the MR. Obviously, beam current of 5.0-6.0 $\times 10^{11}$ per bunch at injection, which had been nominal before 1995, is much less than that of the space-charge limit. Nevertheless, a beam intensity beyond this value is not acceptable because beam loss would be serious at a transition and other loss could not be avoided just after beginning acceleration.

4.1.2 Microwave Instability

After extensive observations, it has turned out that the former beam loss is caused by eruptive longitudinal emittance blow-up just after transition crossing (TC) due to a serious microwave instability (MI). The characteristic features in the observed instability are summarized as follows: (1) it never evolves to an observable level before TC, (2) it grows from the bunch-tail portion, (3) just after TC it dramatically starts to grow within 1 msec near 1GHz, (4) then a substantial fraction goes away from the bunch-center. As a result of MAFIA simulations and impedance measurements at a test bench, the beam-position monitors (BPM) and cavity-like vacuum chambers (CVC) located at every lattice quadrupole magnet were identified to dominate the narrow-band impedance source capable of driving the M.I. in the range of 0.7 - 1.4 GHz. In order to consistently explain the experimental results, a proton-klystron model has been proposed [2], where highly resonant structures are periodically distributed along the beam-path and wake fields excited by the bunch-head can affect the bunch-tail, member change in a global-scale between the bunch-head and -tail scarcely occurs near the transition energy, the interaction between a proton bunch and resonant structures is quite analogous to that in a klystron driven by electron beams, all of excited resonant structures can be regarded as being idling cavities, and build-up of the wakes in each resonant structure is treated in a formulation of the forced excitation of a damped harmonic-oscillator.

During the summer shutdown of 1996, two-thirds of highly resonant impedance devices (BPM and CVC) were replaced by newly designed ones; meanwhile, the other one-third were left because of the high residual radiation level. The new BPM is an electrostatic type. Its Rshunt/Q is reduced by a factor of 2 or 3 according to a MAFIA calculation. The resonant frequency of the dominant mode moves to 342 MHz. In the new CVC the original cavity-like structure is discarded and the evacuation port is shielded by RF slits. As a result, the magnitude of the resonant impedance is negligibly small. The emittance blow-up ratio was measured in the same way. Certainly, the emittance blow-up ratio has notably decreased, as expected, although the MI itself is still observed to evolve at some level [3].

4.1.3 Head-tail Instability

Another serious beam loss has been confirmed to result from a head-tail instability by extensive experiments [4]. It has turned out that the eddy-current-induced sextupole fields in the rectangular shaped vacuum pipe in the main bending magnets play a crucial role in the head-tail instability at the beginning of acceleration. The eddy current effects were verified by actual field measurements and chromaticity measurements involving different field-rampings [5].

The eddy current-induced sextupole field in the vacuum pipe in the main bending magnets forces the horizontal chromaticity into shifting from negative to positive values at the beginning of acceleration. Then, longitudinal modes l = 0, 1 and 2 become unstable. Especially the mode l = 0 is fatal. The chromaticity change is proportional to (dB/dt)/B if it comes from an eddy current. In the KEK PS dB/dt saturates at 2.3 T/s, while B increases as the beam is accelerated. Therefore, the chromaticity change is larger for a lower energy. That is why the instability tends to occur just after acceleration starts. The theoretically predicted chromaticity is indicated by the solid and dashed lines, assuming nominal chromaticity control and an analytic eddy current-model. The observed chromaticity is given by symbols as a function of time counted from acceleration start. the global feature of the temporal variation of the observed chromaticity is very similar to that of the theoretically predicted one.

A growth-rate measurement has suggested that the main sources of the coupling impedances are the kickers and the resistive wall [5]. Coupling impedance measurements for the existing injection kickers and newly installed extraction kickers were performed using a copper wire of 1mm in diameter. The measured impedances have been compared with the magnitude of the impedance calculated by using the standard theory of travelling-wave kickers, and have been confirmed to be in good agreement with each other in the low-frequency region of $f < 15$ MHz of current interest.

In order to suppress the Head-Tail instability, Landau damping due to octupole magnet fields has been employed, in addition to further careful chromaticity control to prevent the horizontal chromaticity from shifting into a positive region. Octupole magnets are located along the ring with fourfold symmetry so as to minimize any reduction in the dynamic aperture.

4.1.4 Bunch Shaping

Most of collective instabilities depend on the local beam density. It has been well-known that mitigation of the local beam density is quite effective to avoid any collective instabilities. In the KEK PS, bunch shaping by artificial beam blowup in the longitudinal direction was quite effective to relax any undesired instabilities, such as the microwave instability at TC where the local beam density in

the longitudinal direction becomes maximum over the entire acceleration period. So far, two sorts of bunch-shaping techniques have been attempted.

One is a technique [6] in which the quadrupole oscillation mode in the longitudinal motion is enhanced by introducing a positive feedback in the voltage-feedback system before TC, yielding a substantial blowup of the longitudinal emittance. Since this method resorts on communication between beam, itself, and accelerating devices with a positive feed-back, the performance was not very reliable. In some case, emittance blowup was observed to extend to a level beyond the RF bucket size with undesired deep filamentation structures, which used to be harmful for slow-extraction beam spills. Although this method had lead to the intensity record in the MR before the intensity upgrade program started, it was discarded in the task work responsible for realizing more stable machine operation with an expected beam intensity.

Instead, a method modulating the RF voltage by band-limited white signals has been attempted by the task. Through computer simulations and analytic considerations [7], a uniform distribution in a bounded area of the longitudinal phase space has been known to be achieved by introducing parametric quadrupole resonances for the desired amplitude. The mechanism is rather simple: a particle resonates at one band of the modulation frequency and changes its amplitude where the resonate frequency shifts due to a phase nonlinearity of the RF voltage; the particle then starts to resonate at another frequency in the same band. This resonant dynamics continues until the particle arrives at the outer boundary that is covered with the band width. Although the control of longitudinal beam emittance was not perfect, a substantial reduction in the line density before transition has been practically achieved. The maximum value and smoothness in the line density is sufficiently enough to prevent any rapid growth of the microwave instability or a temporal defect in the current low-level system, such as tripping of synchonization just after TC, that sometime occurs in the case of a narrow bunch.

4.1.5 Tune Optimization

Fast ($<$ msec), medium ($<$ a few msec), and slow loss ($<$ 50 msec) at the injection stage strongly depend on a set of betatron tunes in both directions beyond a beam intensity of 6.0×10^{11} per bunch [8]. Fast loss is resulted from betatron mismatching and rapid emittance blowup due to space-charge forces coupled with the dynamic aperture determined by octupole fields, providing Landau damping. At this moment it is unknown to what the later loss can be attributed. However, a speculation that weak nonlinear resonances coupled with beam-core breathing (envelope oscillation) may drive a substantial fraction of the halo to the outer edge during a relatively long time period is likely.

4.1.6 Current Status of the Machine

The intensity per bunch decreases by 23% 3 msec after injection, due to the above mentioned reason. The survival rate just at acceleration start (P2) is about 82%. 92% of the beam which arrives at P2 can survive up to the end of acceleration (P3). Noted there is a slow loss at the beginning of acceleration and a slight loss at TC through acceleration. The over-all acceleration rate from injection to the end of acceleration in the MR is 58beam intensity is 6.2×10^{12} ppp, which meets the demand from the experimental group.

Sources of serious beam loss downstream in time have been practically removed, as mentioned above. Now, the maximum accelerated beam intensity is determined by the surviving beam in-

tensity at the end of the injection stage. A systematic study focusing on beam loss at injection is scheduled from this Fall.

References

[1] H.Sato and Crew of the Intensity Upgrade Study, "Intensity Upgrade Studies at the KEK-PS," Proc. of the 1997 PAC, 1009, (1998).

[2] K.Takayama, D.Arakawa, J.Kishiro, K.Koba, and M.Yoshii, "Microwave Instability at Transition Crossing: Experiments and a Proton-Klystron Model," Phys. Rev. Letts, 78, 871 (1997).

[3] K.Takayama, D.Arakawa, J.Kishiro, K.Koba, T.Toyama, and M.Yoshii, "Microwave Instability at Transition Crossing in the KEK-PS," Proc. of the 1997 PAC, 1548, (1998).

[4] T.Toyama, D.Arakawa, S.Igarashi, J.Kishiro, K.Koba, and K.Takayama, "Beam Loss at the Beginning of Acceleration in the KEK-PS Main Ring," Proc. of the 1997 PAC, 1599, (1998).

[5] T.Toyama, D.Arakawa, S.Igarashi, J.Kishiro, E.Nakamura, and K.Takayama, "The Eddy-current induced Head-Tail Instability in the KEK-PS," Proc. of the 1999 PAC.

[6] S.Ninomiya, private communication (1995).

[7] T.Toyama, to be submitted into Nuclear Instruments and Methods in Physics Research.

[8] M.Shirakata, private communication (1999).

4.2 Japan Hadron Project (JHF) Update

Y. Mori yoshiharu.mori@kek.jp KEK
S. Machida shinji.machida@kek.jp National Laboratory for High Energy Physics

4.2.1 Outline of the Joint Project

There was a big change of the JHF project last fall. It was decided to merge two major accelerator projects in Japan, one is the JHF and other is the Neutron Science Project (NSP). The new home of the join project will be JAERI Tokai, about 70km north east of KEK tsukuba [1].

The specifications of the accelerator complex do not differ much from the one for the JHF. The main synchrotron energy is 50 GeV with an average current of 15 μA (it was 10 μA before). The beam current will be increased in future by increasing a repetition rate. As an injector of the main synchrotron and also as a high intensity primary proton source for neutron, meson, and unstable nuclear physics, the 3 GeV booster synchrotron with 333 μA (it was 200 μA before) will be constructed. The output energy of the injector linac will be 400 MeV in order to ease space charge effects at the injection of the booster. The linac beam will be also used for the accelerator-driven nuclear waste transmutation system. For that purpose, the beam is further accelerated to 600 MeV. The portion between 400 and 600 MeV will be a superconducting linac with a pulsed operation. Figure 4.1 shows the layout of the accelerator complex of the Joint Project.

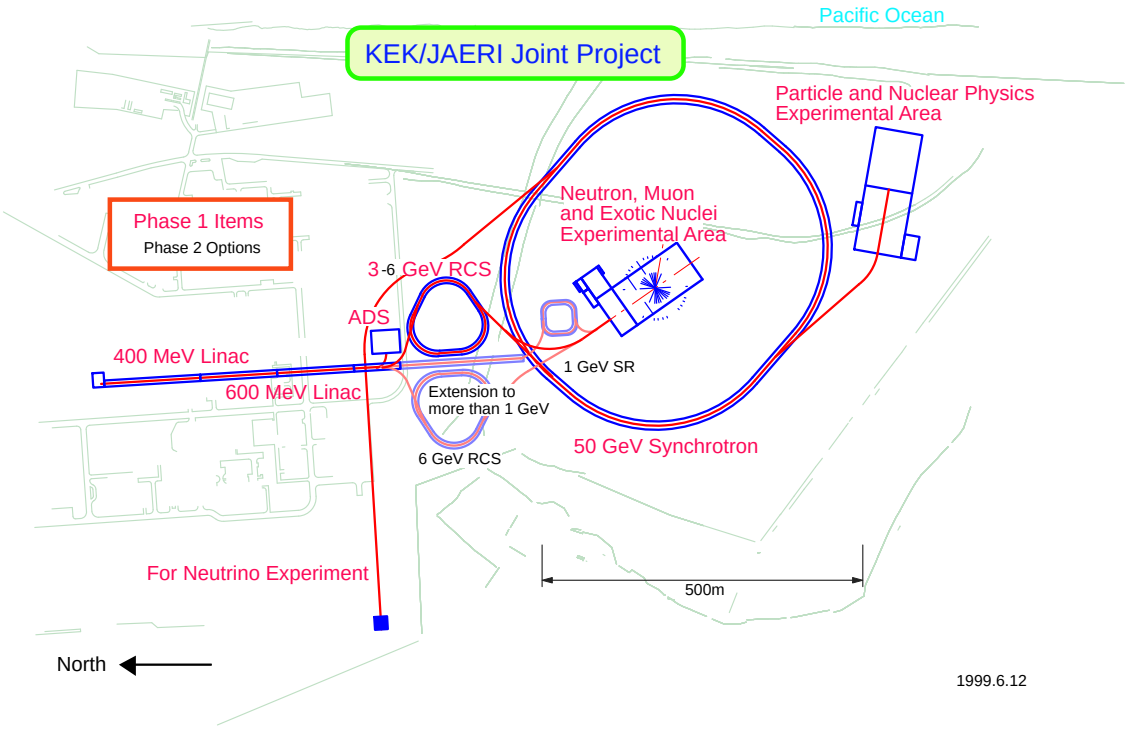

Figure 4.1: Layout of the accelerator complex of the Joint Project. The facilities with parentheses are for the future upgrade.

Although the NSP assumed originally a combination of a 1.5 GeV linac and a storage ring as a high intensity proton source, we decided to choose a synchrotron for the role. First of all, it has to be an injector for the main 50 GeV synchrotron. The linac output energy of 1 to 1.5 GeV is too low for the injection of the main synchrotron. Thus, the intermediate booster is necessary in any case.

Secondly, we think it is a big advantage to lower the injection energy of the high intensity ring in order to reduce radio activation. Since the beam loss should occur mainly at injection energy, the energy deposit by inevitable beam loss is scaled with injection energy if the same amount of particles is injected.

In fact, we can reduce the beam intensity per pulse in order to have the same amount of output beam power, simply because output energy of a synchrotron can be higher than that of a storage ring. That makes the third reason to choose a synchrotron.

Table 1. Main Parameters of the 50 GeV synchrotron

beam intensity	3.2×10^{14} ppp
repetition	0.3 Hz
average beam current	15.6μA
beam power	0.78 MW
circumference	1488 m
magnetic rigidity	12.76-170 Tm
typical tune	(21.8, 16.3)
momentum compaction factor	-0.001

rf frequency	1.82-1.87 MHz
circulating beam current	9.3-9.6 A
rf voltage	300 kV
beam emittance at injection	54πmm-mrad
beam emittance at extraction	4.1πmm-mrad

Table 2. Main Parameters of the 3 GeV synchrotron

beam intensity	8×10^{13} ppp
repetition	25 Hz
average beam current	333μA
beam power	1.0 MW
circumference	298 m
magnetic rigidity	3.18-12.76 Tm
rf frequency	1.34-1.82 MHz
circulating beam current	8.6-11.7 A
rf voltage	450 kV
beam emittance at injection	220πmm-mrad
beam emittance at extraction	54πmm-mrad

4.2.2 Space Charge Effects

Space charge is always a concern, especially at the injection of an accelerator. The synchrotrons of JHF have stringent beam loss specifications just as other high intensity synchrotrons and storage rings. More quantitative understanding of space charge effects on beam loss is essential for the success of those machines.

Space charge effects are studied mostly by multi-particle tracking code, Simpsons [2]. There are mainly two goals we want to achieve. One is the detailed analysis of the stability of a beam core. The other is to identify the source of a beam halo in a synchrotron. Here we briefly mention the status of studies of the beam core stability.

In order to study the beam core stability, we are mostly looking at the coherent modes and its resonance with lattice imperfections. The coherent quadrupole mode is nothing but a envelope mode. Although Sacherer pointed out the importance of coherent modes on the stability of a beam core in his thesis in 1968 [3], not many people were aware of it.

With the multi-particle tracking, we first reproduced the prediction of Sacherer for the envelope oscillations and their resonance conditions with a half-integer resonance. The emittance growth and beam loss occur when the incoherent tune shift further goes down below the resonance by a factor of $5/4\Delta\nu_{inc}$. Those results are more or less independent of the detailed particle distributions. That is a consistent result with another paper by Sacherer stating that the same envelope equations hold in the rms beam size and they are insensitive to the actual distributions [4].

It is not obvious whether the higher order resonances are also governed by the higher order coherent modes. There are also several related questions such as 1) how the frequency of higher

order modes relates with the incoherent tune shift in a 2D and 3D beam? 2) is it independent of the detailed particle distributions?

Our preliminary tracking results show the emittance growth and beam loss occur when the coherent mode frequency satisfies a resonance condition even for the sextupole and octupole driving resonances.

Although that study has been done for a coasting beam, it is shown that the 3D envelope equations give the quite similar coherent mode frequency as far as the transverse modes are concerned. That is the case when a 2D beam with the aspect ratio (longitudinal bunch length/transverse beam size) is not comparable to unity [5]. Since a bunched beam in a synchrotron is fairly long in longitudinal direction, the 2D model of a beam is adequate to derive most physics of space charge effects in a synchrotron.

4.2.3 High Gradient RF Cavity

As we have already reported in several papers, a new type of an rf cavity with Magnetic Alloy (MA) is developed. An accelerating gradient of 50 kV/m is demonstrated and higher record is expected without much difficulty. The high gradient means the reduction of the physical space necessary for rf cavities as well as the impedance seen by the circulating beam. More complete description on the development of the cavity can be found in the reference [6] [7].

Recently, beam tests have been carried out with the MA cavities installed in operational synchrotrons. One is the MA loaded barrier bucket cavity in the AGS at BNL and the other the single gap high gradient cavity in the HIMAC at NIRS (Chiba in Japan). The MA cavity at BNL provides an rf voltage of 40 kV with a single-sinusoidal 2 MHz barrier pulse. This cavity is a low-Q system, which is superior to any other system for barrier applications. The power dissipation is 60 kW average, which has been realized with relatively small power amplifier. The cavity responses fast and creates an arbitrary waveform on the gap, because of low-Q characteristics. For transient beam loading compensations, the system applied a feed-forward system. Picked-up bunch current signals are fed directly into drive amplifier after appropriate amplitude correction and phase matching. The feed-forward system works well and stable for intense AGS proton beam. Proton beam of 3×10^{13} ppp with 5 transfers has been accumulated in the manner of longitudinal barrier gymnastics and accelerated with success, so far. The experimental details of barrier bucket using the MA cavity is reported in the reference [8].

The HIMAC is a heavy ion synchrotron for medical use. Several ions such as He, C, Ne, and Si are accelerated from 6MeV/u to 800 MeV/u. One of the challenges for the MA cavity in the HIMAC is the acceleration without a frequency tuning loop. The accelerating frequency is swept from 1 MHz to 8 MHz for a heavy ion such as Si. Because of the broadband nature, once a frequency pattern is programmed at a low level rf system, the MA cavity provides an enough gap voltage throughout the whole frequency range.

In fact, there is a small variation of the output voltage depending on frequency. That is due to the gain characteristics of a driver amplifier. One can obtain, however, a constant voltage curve by simply pre-programming a voltage pattern.

Another beam study taking an advantage of the broadband nature is the beam stacking and acceleration with multi-harmonics of an rf. Since the cavity impedance is equally high at the second and third harmonics frequency as the fundamental, several harmonics components can be applied into one rf cavity at once. With second harmonics, the bunching factor is improved from 0.28 to

0.40 and the reduction of beam loss is manifest.

A combination of more number of harmonics makes the accelerating voltage even a saw-tooth shape [9]. The linear region of the rf bucket is widen, which can be observed as a small spread of synchrotron frequency. A bunch rotation of a mismatched beam with smaller dp/p at the beginning shows less filamentation after several synchrotron oscillations.

(The home page of the JHF Accelerator is `http://hadron.tanashi.kek.jp/index.html`)

References

[1] The proposal of the Join Project will be ready soon.

[2] S. Machida et al., Proc. of PAC99.

[3] F.J. Sacherer, Ph.D. thesis, UCRL-18454, 1968.

[4] F.J. Sacherer, IEEE Trans. on Nucl. Sci., Vol. NS-18, No. 3, 1971.

[5] T. Uesugi et al., Proc. of PAC99.

[6] Y. Mori et al., Proc. of EPAC98.

[7] C. Ohmori et al., Proc. of PAC99.

[8] M. Fujieda et al., Proc. of PAC99.

[9] M. Yamamoto et al., Proc. of PAC99.

4.3 Spallation Neutron Source Related Activities at the BNL

Jie Wei `wei1@bnl.gov` Collider Accelerator Dept.
Brookhaven National Laboratory

The Spallation Neutron Source (SNS) is designed to meet the growing need for new tools that will deepen our understanding in materials science, life science, chemistry, fundamental and nuclear physics, earth and environmental sciences, and engineering sciences. During the past months, accelerator physics activities on the Spallation Neutron Source Project at the Brookhaven National Laboratory have been focusing on a completely alternative scenario based on Rapid-Cycling-Synchrotrons (RCS),[1] generally believed to be more cost-effective than a full-energy LINAC-accumulator ring design (LAR). [2] The study, on the contrary, led to the conclusion that stringent beam loss limit of a 2 MW-source requires a design of the RCS rings that are technically challenging and consequently less cost-effective. After reaching this conclusion, our physics group re-focused on design optimization of the present full-energy LINAC-accumulator ring. [3]

4.3.1 Rapid-Cycling-Synchrotron design study

The SNS is based on an accelerator producing an average beam power of 2 MW at a repetition rate of 60 Hz. The nominal accelerator complex (LAR) consists of the source and the front end, a 1 GeV full-energy LINAC, a single accumulator ring and its transfer lines, and the target. The alternative accelerator complex consists of similar source, front end, and target, but a shortened LINAC and a pair of rapid-cycling synchrotrons. On April 9, 1999, the SNS management defined the boundary condition for this alternative complex to consist of a 400 MeV LINAC injecting into

two synchrotrons, each accelerating beam pulses of 1.04×10^{14} protons at a repetition rate of 30 Hz from 400 MeV to 2 GeV, producing a combined beam power of 2 MW. The two synchrotrons are vertically stacked sharing the same tunnel.

Reliability and maintainability are of primary importance to the SNS facility. Based on operational experience at both LINAC and the AGS Booster, hands-on maintenance demands that the uncontrolled beam loss be limited to about 1 W of beam power per tunnel meter, For two synchrotrons, each with circumference near 300 meters, this corresponds to an average uncontrolled beam loss of 4×10^{-4} at 400 MeV beam energy.

Among the existing RCS machines, typical beam loss ranges from several to tens of percent. Major beam loss usually occurs at injection and the initial ramping stage (first 5 ms). These beam losses are typically attributed to a high space change tune shift (0.5 or larger), limited physical and momentum acceptance, and large magnetic field errors.

The SNS synchrotrons are designed with practically achievable large acceptance so that beam space charge tune shift remains about 0.2. The use of programmable ramping moderates the required RF voltage and ramp rate, resulting in a reasonable machine circumference and a tolerable eddy-current induced magnet errors. Lengths of the magnets are chosen to avoid excessive error due to saturation fringe field.

Effective collection of the beam halo is essential for maintaining a low uncontrolled beam loss. To facilitate the momentum cleaning and multi-stage collimation systems, a wide momentum acceptance (full beam plus $\pm2\%$ in $\Delta p/p$) is chosen. This allows cleaning of the momentum halo using a multi-turn beam gap kicker system. With the collimation system designed to be more than 90% efficient, the total allowed beam loss is at 1% level.

Flexibility is another important aspect considered in the design. A matched FODO/doublet hybrid lattice is chosen so that chromatic and resonance correction can be done mainly in the FODO arcs, while long uninterrupted doublet straight sections allow flexible modular operation (injection painting independent of lattice tuning, long uninterrupted straight section, balanced RF cavity arrangement, possible collimation "dog leg", etc.). Since the FODO arc and doublet straight section are optically matched, a low amplitude (β_{max}) is achieved for the given cell length, thus confining the beam size.

To address the issue of engineering reliability, the collimator and shielding hardware are designed to withstand an average of 10^{-2} beam power. In addition, the machine is designed to withstand a couple of full beam pulses during commissioning and in case of emergency.

In summary, in order to build a RCS machine that will perform to the stringent beam loss limit required by the high-intensity, high power operational scenario, we must meet the following challenges:

- cleaning of ramping and RF capture beam loss
- development of programmable magnet power supply
- construction of large-bore magnets with laminated coils
- construction of large-aperture vacuum chambers with RF shielding
- control of magnetic field errors due to ramping eddy current and saturation
- need for separate quadrupole magnets for eddy current mismatch compensation
- instabilities (head-tail, e-p like (PSR), etc.)
- achievement of desired beam distribution at the target (may require octupole manipulation in RTBT)

4.3.2 Beam-loss driven design optimization

After reaching the conclusion that an RCS design for a 2 MW Spallation Neutron Source is less cost-effective in comparison with a full energy LINAC-accumulator ring design, our physics group re-focused on design optimization of the present ring. Concern of beam loss is incorporated in the design of the ring and transfer lines (HEBT, RTBT) at three stages: [4] linear machine design (lattice, aperture, injection and extraction, magnet field errors and misalignment, etc.), beam core manipulation (space charge, painting, instabilities, RF requirements, etc.), and beam halo consideration (collimation, beam envelope variation, e-p issues, etc.). As shown in Fig. 4.2, the ring has a

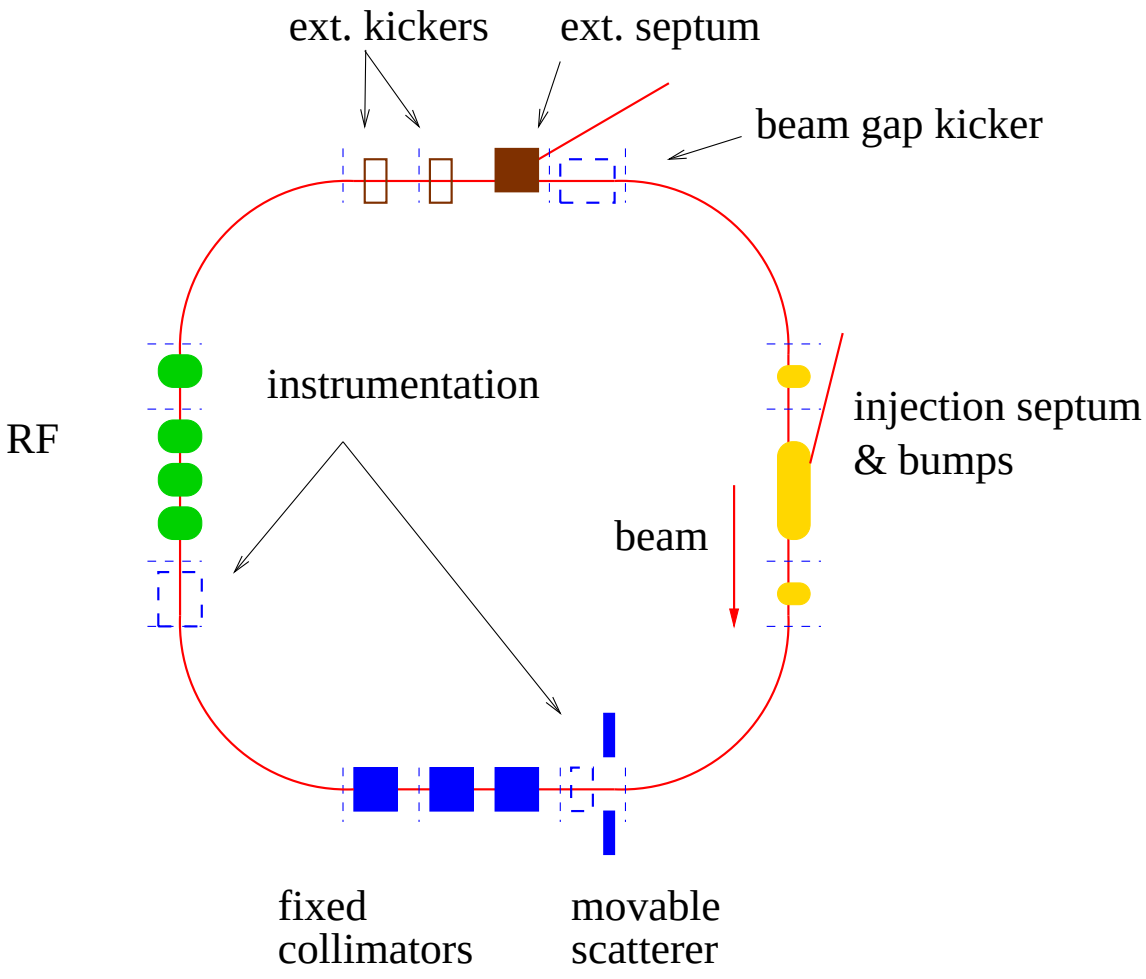

Figure 4.2: Schematic layout of the LINAC-accumulator ring indicating sections for injection, collimation, beam gap cleaning, RF system, instrumentation, and extraction.

four-fold symmetry consisting of four straight sections intended for injection, beam collimation, RF system and beam instrumentation, and extraction. Chopped H^- beams are injected through charge exchange painting process to the ring, accumulated for 1225 turns, and then extracted with fast kickers.

4.3.2.1 FODO/Doublet hybrid lattice

Key issues of the ring lattice design are adequate transverse and momentum acceptance for beam-tail development control and collimation, easiness for chromatic and resonant correction, and flexibility for injection, extraction, and collimation arrangement. We have been studying the benefit of an alternative lattice, the so-called hybrid lattice [5, 4] consisting of FODO structure in the arcs but doublets in the straight sections. The FODO arcs are ideal for chromatic and resonance correction. The long uninterrupted straight sections are flexible to accommodate injection, collimation, and extraction schemes which are essentially independent of lattice tuning, reducing the need for extra-large bore (31 cm inscribed diameter) quadrupoles and sextupoles. As shown in Fig. 4.3, the

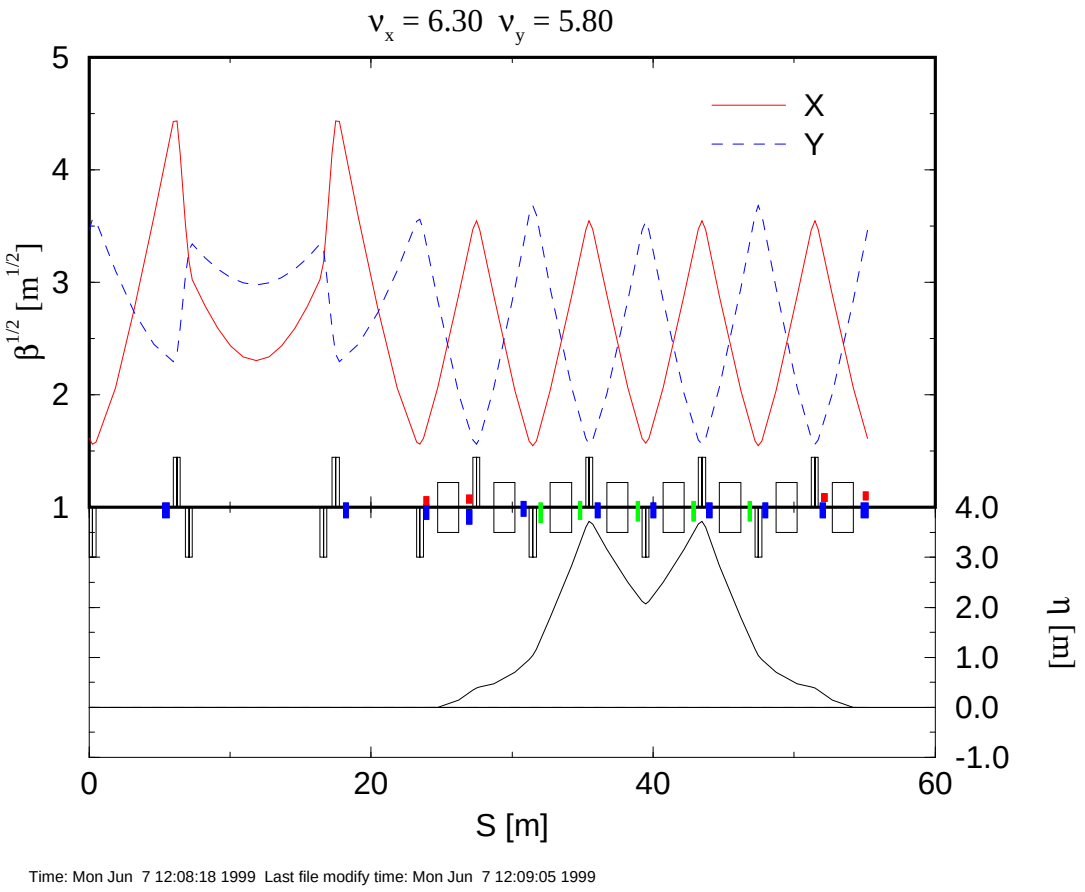

Figure 4.3: An alternative SNS Ring hybrid lattice with FODO arc and doublet straight sections.

arc and straight sections are optically matched, increasing the total ring acceptance from previously about 360 πmm·mr to 480 πmm·mr. Furthermore, the transverse tunes are fully adjustable and are planned to be split to minimize coupling and to reduce the beam envelope variation (i.e. β_{max}/β_{min} ratio). Chromatic sextupoles are introduced to control chromaticity, to minimize off-momentum optics mismatch, and to improve dynamic acceptance and momentum acceptance.

4.3.2.2 Acceptance requirement and collimation efficiency

Hands-on maintenance condition requires an average uncontrolled beam loss of about 1 W per meter, corresponding to about 10^{-4} total beam loss in the ring. In order to achieve this loss level, high beam collimation efficiency is essential. For the SNS, we (N. Catalan-Lasheras, et al) are planning a two-stage collimation combined with beam gap cleaning. [6, 7] As shown in Fig. 4.4, the neces-

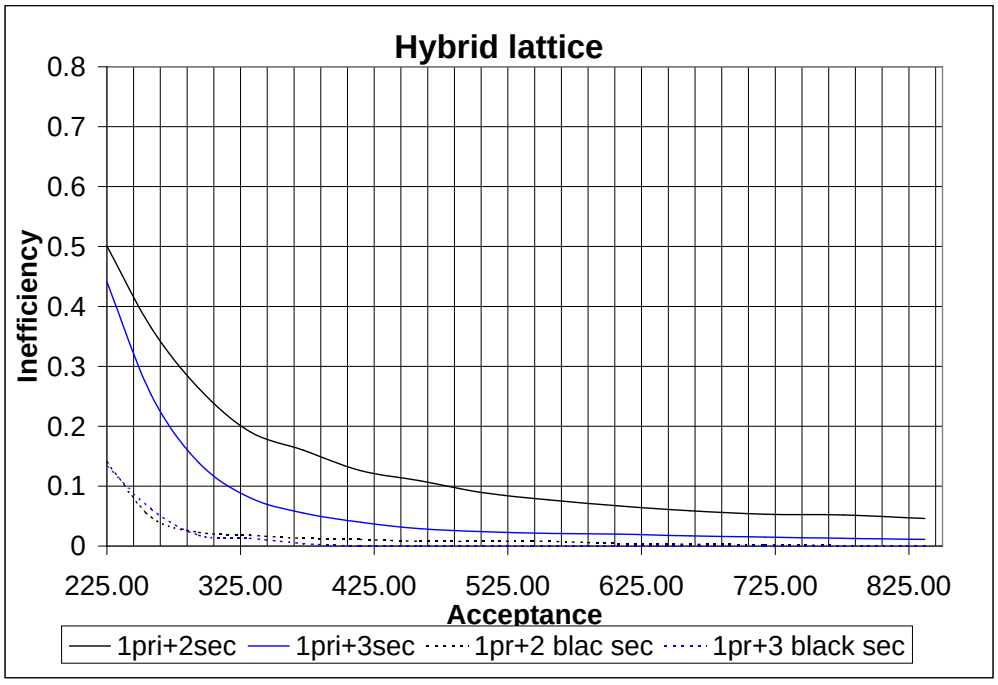

Figure 4.4: Efficiency of ring collimation system as a function of ring physical acceptance with the hybrid lattice.

sary condition for an effective collimation is adequate physical and momentum acceptance. With the hybrid lattice, the efficiency is increased from about 90% to more than 95% due to increased acceptance (from 360 to 480 πmm·mr). Fig. 4.5 (N. Catalan-Lasheras, D. Raparia, et al) shows the expected distribution of controlled and uncontrolled beam loss in HEBT line, Ring, and RTBT line.

4.3.2.3 Other activities

Other accelerator physics activities include:

- analysis of magnet field error and misalignment impact [4]
- analysis of magnet fringe fields [8]
- space charge simulation and codes comparison (SIMPSONS, ORBIT) [9]

- SNS end-to-end simulation (HEBT, Ring, and RTBT) [10]
- development of Unified Accelerator Libraries (UAL) platform to accommodate magnetic errors, misalignments, corrections, space charge effects, injection painting, and collimation [11]
- study of collimator performance [12]
- study of collection schemes for foil stripped electrons [8]
- impedance & instability analysis [13, 14]
- machine studies and experiments (beam grazing and electron production, e-p like instability at the AGS Booster, PSR instability participation, etc.) [15, 4]

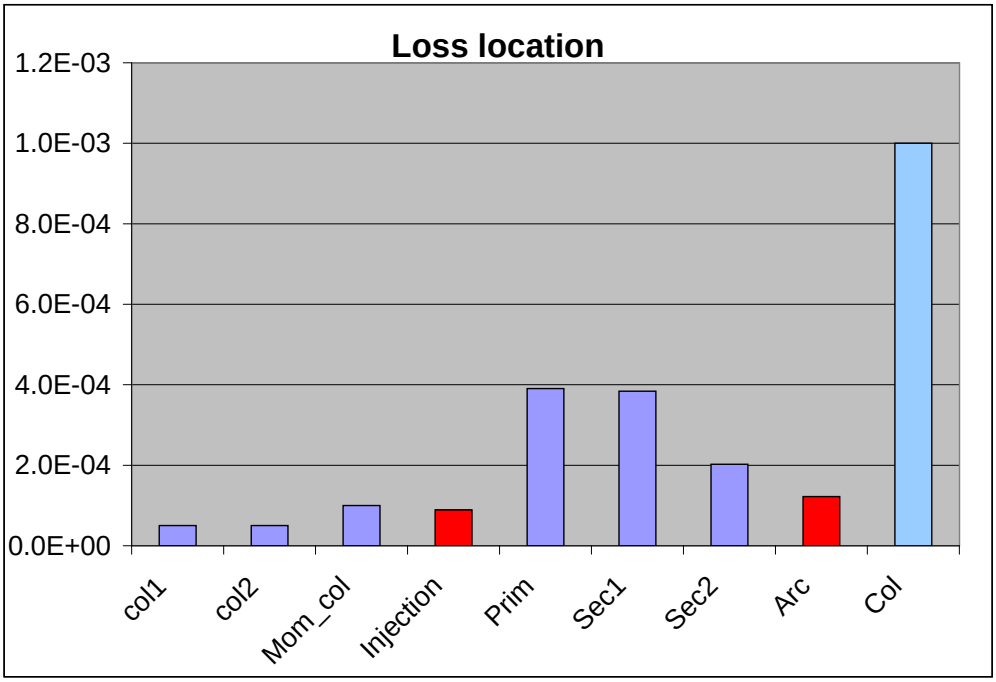

Figure 4.5: Expected controlled and uncontrolled beam loss at various locations of High-Energy-Beam-Transfer (HEBT) line, Ring, and Ring-to-Target-Beam-Transfer (RTBT) line.

References

[1] *SNS/RCS Pre-Conceptual Design*, (Draft) May 1999.

[2] *Spallation Neutron Source Design Manual*, 1998.

[3] J. Wei, et al, ICFA Newsletter No. 19 (April 1999).

[4] J. Wei, et al, *Beam-Loss Driven Design Optimization for the Spallation Neutron Source Ring*, PAC99 (1999) p. 3185.

[5] C. Gardner, et al, *An Alternative Lattice for the Spallation Neutron Source Ring*, PAC99 (1999) p. 3182.

[6] N. Catalan-Lasheras, DOE Review Presentations, July 1999 (to be published).

[7] R. Witkover, et al, *Beam Instrumentation for the Spallation Neutron Source Ring*, PAC99 (1999) p. 2250.

[8] D. Abell, private communications.

[9] SIMPSONS: written by S. Machida; ORBIT: written by J. Galambos et al.

[10] J. Beebe-Wang, et al, *Transverse Phase Space Painting For SNS Accumulator Ring Injection*, PAC99 (1999) p. 1743.

[11] N. Malitsky, et al, *UAL-Based Simulation Environment for Spallation Neutron Source Ring*, PAC99 (1999) p. 2713.

[12] H. Ludewig, et al *Collimator Systems for the SNS Ring*, PAC99 (1999) p. 548.

[13] SNS Ring Technical Notes 33 (1997), 43 (1998), 61 (1999).

[14] M. Blaskiewicz, *Instabilities in the SNS*, PAC99 (1999) p. 1611.

[15] S.Y. Zhang, *Secondary Electron Production at the SNS Storage Ring Collimator*, PAC99 (1999) p. 3297.

4.4 Spallation Neutron Sources in Europe: ISIS and ESS

C.R. Prior C.R.Prior@rl.ac.uk Rutherford Appleton Laboratory
C.M. Warsop C.M.Warsop@rl.ac.uk UK

4.4.1 Introduction

ISIS and ESS represent the two main accelerator-driven sources of pulsed neutrons in Europe, the former an existing and highly successful machine and the latter a proposal aimed at meeting the needs of the next generation of neutron scientists. ISIS is the Spallation Neutron Source at the Rutherford Appleton Laboratory in the UK, and is presently the world's most powerful source, providing a mean beam power of up to 160 kW. ESS is a proposal for a green-field site and would provide up to 5 MW of beam power. Here we give an outline of both machines, concentrating in the case of ISIS on the synchrotron, which has relevance to numerous proposed high intensity proton rings. Recent work is described and future plans in both cases are considered.

4.4.2 ISIS Accelerators and Future Plans

4.4.2.1 The ISIS Accelerators

The ISIS accelerators (Figure 4.6) consist of an H^- Penning ion source, a 665 kV Cockcroft Walton HT set and DC accelerating column, a 70 MeV four tank 202 MHz Alvarez Linac and a high intensity Rapid Cycling Synchrotron (RCS). The design current of 200 μA (mean current on target) has been exceeded, with values above 210 μA being achieved operationally for prolonged periods. Typical operational values are 180-200 μA.

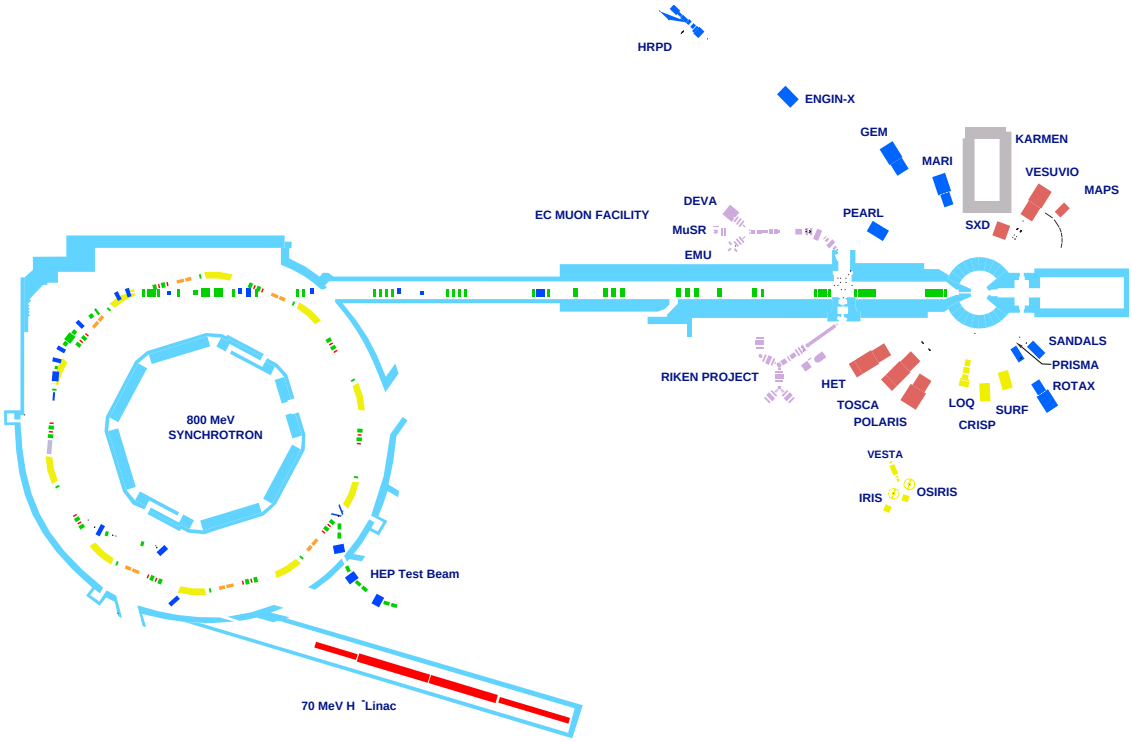

Figure 4.6: Layout of the ISIS Facility

Synchrotron Operation

Typically 2.8×10^{13} protons are accumulated over the 200 μs or 135 turn injection process. The H^- ions are stripped with a 0.3 μm Al_2O_3 foil as they enter the ring acceptance. The injected emittance ($\sim$20 π mm mr) is painted over both transverse collimated acceptances ($\sim$300 π mm mr). In the horizontal plane, the radial movement of the beam due to the falling main magnet field is exploited, to provide a betatron amplitude that increases through injection. In the vertical plane a programmable steering magnet in the injection line allows 'anti-correlated' vertical painting, with betatron amplitudes decreasing through injection. The foil is 120×40 mm, and supported on 1.5 edges. The beam is effectively unbunched during injection. The efficiency of the injection process is 98%, most of which is due to stripping losses. Provision is made for electron and H^0 collection and removal in the injection region. A symmetric four magnet bump moves the circulating beam onto the foil during injection, but is then rapidly removed before acceleration.

Acceleration from 70-800 MeV takes place over the 10 ms sinusoidal field ramp. Non-adiabatic trapping of the unbunched injected beam takes place over the first $\sim$1.0 ms; two bunches are formed by the single harmonic ($h = 2$) RF system. Most beam losses occur during this process, typically 10%, but untrapped beam is of low energy (< 100 MeV), and efficiently intercepted with a momentum collimator at a high dispersion point in the lattice. At highest intensities longitudinal and transverse space charge effects contribute to losses; incoherent space charge tune shifts peak at about -0.4, causing some crossing of the $Q_h = 4$ resonance.

The six double-gapped ferrite-tuned RF cavities run from 1.3-3.1 MHz, and provide a peak total volts per turn of 140 kV. Measures necessary for accelerating full intensity beams include feed for-

Repetition Rate (Hz)	50
Injection Energy (MeV)	70
Injection Type	H^- multi-turn, charge-exchange
Typical Injected Intensity	2.8×10^{13} ppp
Extraction Energy (MeV)	800
Typical Extracted Intensity	2.5×10^{13} ppp
Extraction Type	Fast, single turn
Circumference (m)	163.3
Nominal Betatron Tunes	$Q_h = 4.31$, $Q_v = 3.83$
Superperiods	10
Main Magnet Excitation	50 Hz resonant sinusoidal
Harmonic Number	2
Peak volts per turn (kV)	$\sim$140
RF Cavities	6, ferrite tuned
RF Frequency Sweep (MHz)	1.3-3.1
Typical Efficiencies:Injection, Trapping, Extraction	98%, 90%, $> 99.9\%$

Table 4.1: ISIS Synchrotron Parameters

ward beam loading compensation early in the cycle and reactive beam loading compensation for the last 8 ms. Numerous control loops maintain cavity tune and correct beam dipole, quadrupole and radial errors. Extraction takes place in a single turn with a lumped fast kicker system. There are six push-pull kicker modules, incorporating a central earthing strip so as to present a low impedance to the beam. Kicker rise times of $\sim$200 ns are achieved with a pulse forming network discharging from 40 kV at 5000 A through a thyratron switch.

Notable Features of the Synchrotron

Important features of the synchrotron include

- Ceramic vacuum chambers with profiled RF shields
- Fast, time dependent programming of betatron tune through the machine cycle
- Fast, time dependent closed orbit and gradient error correction
- Incoherent crossing of horizontal integer resonance under space charge
- Linear lattice with no sextupoles or octupoles powered
- Sensitive ionization Beam Loss Monitors distributed along the length of the machine

- Momentum collection of dominant trapping loss

The ceramic vacuum chambers in the fast cycling magnets ensure eddy current effects do not distort magnetic fields, while the RF shields minimize beam impedance. Two sets of 10 independently programmable trim quadrupoles allow (Q_h, Q_v) to be set independently through the machine cycle. Changing Q values, to minimize losses arising from varying beam conditions as the energy ramps, has been essential for achieving highest intensities. Initially tunes are ramped during injection, as the main magnet field falls, to compensate for the natural chromaticity. During trapping when space charge forces peak, Q values are raised to minimize effects of space charge tune depression. Shortly after this, vertical Q is rapidly dropped to avoid a resistive wall head-tail instability. Fine tuning of Q is also essential for good extraction. Varying strengths of trim quadrupoles harmonically around the ring allows for gradient error correction, which is important for optimal running.

Beam loss and associated tolerable activation levels (for hands on maintenance) limit machine operational intensity. Most loss occurs during the trapping process. The fast radial motion of untrapped beam, caused by the quickly ramping field, is exploited by placing a momentum collector at a high dispersion point. Most beam impacts deeply into the collector minimizing out-scatter problems. Collectors are located in one shielded straight, where most loss is localized, which minimizes activation over most of the machine. Detailed knowledge of loss spatial distribution and time dependence is essential and is provided by 40 beam loss monitors distributed around the ring circumference. A complex beam loss detection system warns operators of excessive loss and in certain circumstances will shut off the beam.

4.4.2.2 ISIS Accelerator Improvement and Upgrade Projects

The New ISIS RFQ PreInjector

Work to replace the Cockcroft-Walton HT set, 665 kV high voltage platform and accelerating column, which have caused significant reliability problems in the past, is well under way. The new system will consist of a 35 kV platform for the H^- Penning ion source, a solenoid beam matching and steering system, and a 202 MHz, 665 kV RFQ, which then injects into the existing Alvarez Linac.

Design of the system is complete and much of the hardware is in place. A test stand is under construction, where the new RFQ operation will be thoroughly tested before installation on the operational machine. The RFQ test program is expected to start later this year. The RFQ test facilities will also be utilized for studying the ESS RFQ and pre injector systems.

The Synchrotron Dual Harmonic RF Upgrade

Studies have shown the dominant trapping losses on the ring can be halved by addition of a higher harmonic ($h = 4$) to the RF system. Simulations indicate that with careful control of relative phases and voltage of the $h = 2$ and $h = 4$ RF, beam currents of about 300 μA should be possible with THE same or less absolute beam power loss. The required RF volts at $h = 4$ is provided by four additional RF cavities.

A higher harmonic cavity has been designed and is under construction. The design and production of associated control, low and high power electronics is also well under way. Tests will start

shortly. Collaborations with Argonne National Laboratory (USA) and KEK (Japan) have been extremely useful in studying best options for the high power RF drive. Design of mechanical modifications to the ISIS ring to allow installation of the new cavities is in hand. Full funding to allow construction of all cavities and associated RF drive is expected soon.

General Accelerator Developments

A substantial obsolescence program is underway, replacing old equipment and upgrading where possible. RF drive systems to the linac cavities are being modernized, and power supplies for tank quads being replaced. Improvements to collector systems and the extraction septum are being studied and designed. There are also plans for power supplies to many ring magnets to be upgraded. An on-going beam control and study program, utilizing upgraded instrumentation and computers, is providing more detailed knowledge and control of the machine.

Proposals and Studies for Major Facility Upgrades

Proposals and designs for a second low rep rate neutron target station are at an advanced stage, and would allow substantial expansion and optimization of the user science program. Similarly the Sirius project, a proposed radioactive ion beam facility, is generating much interest in the nuclear physics community. Studies looking at major upgrades to the ISIS Facility, providing beam powers of $\sim$1 MW, are also underway.

4.4.3 The European Spallation Source (ESS)

With the success of ISIS and growing demand for neutrons from the European physics community, studies have been undertaken by a consortium of laboratories into the feasibility of a new 5 MW pulsed neutron source. Known as ESS, this is a Europe-wide initiative, relying on experience gained at ISIS but regarded as an entirely separate, green-field project. Phase 1 of the design study was completed with publication of a report to the European Commission[1] in November 1996. Since then work has continued to tackle the problems identified, to rectify weak links in the original design and to consider alternative ideas.

4.4.3.1 The ESS Reference Design

The reference design for the ESS (Figure 4.7) is for a 5 MW pulsed neutron source with a repetition rate of 50 Hz and a pulse length of 1 μsec. Facilities would be provided for users via two targets, one at 5 MW and 50 Hz for high intensity applications, and a second, using every fifth pulse, at 1 MW and 10 Hz for high resolution and long wavelength instruments. The guiding principles in the design have been the need for operational reliability, low beam loss and relatively low cost.

The original proposal envisages a 1.334 GeV linac, producing pulses of H^- ions at a mean current of 65 mA. These are transported and injected sequentially, via charge exchange foil stripping, into two compressor rings. During an injection period of 0.6 msec (1000 turns), each ring accumulates 2.34×10^{14} protons in a single 400 nsec bunch. Pulses of $\sim$1 μsec are achieved by extracting

[1] G. Bauer, T. Broome, D. Filges, H. Jones, H. Lengeler, A. Letchford, G. Rees, H. Stechemesser, G. Thomas (eds): *ESS: A Next Generation Neutron Source for Europe. Vol III: The ESS Technical Study.*, November 1996.

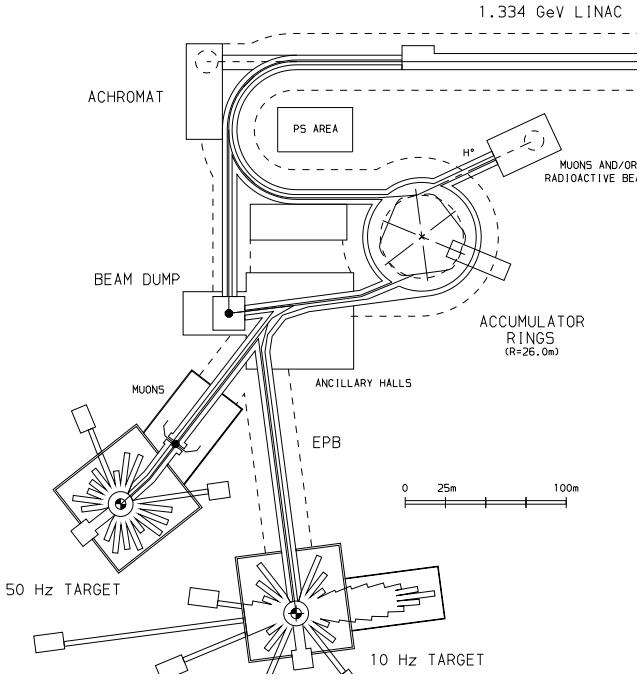

Figure 4.7: Layout of the ESS Reference Design.

the bunches from one ring immediately after the other giving 100 kJ per pulse at 50 Hz. The targets chosen for the reference design are liquid mercury, but the possibility of using solid targets has not been ruled out.

At the low energy end of the structure, H^- ion sources of the Penning or volume type generate 70 mA pulses with normalized rms emittances 0.1 π μrad m. These are matched at 50 keV into the first of two RF quadrupole linacs which operate at 175 MHz. The first increases the energy to 2 MeV, when a fast chopper chops the pulses with a 60% duty factor at the ring revolution frequency (1.67 MHz). The second RFQ then accelerates the beam to 5 MeV. Two arms of this structure are planned, and the bunches will be merged together by a funneling mechanism so as to increase the current to 107 mA (see Figure 4.8). The funnel is effectively a two-beam RFQ with a resonator-driven deflector. Subsequent acceleration is carried out in a 350 MHz drift tube linac to 70 MeV, and then to the design energy of 1.334 GeV by a cavity coupled linac at 700 MHz, 663 m long.

The two accumulator rings are designed for hands-on maintenance with losses contained to within 0.02%. The main purpose of the transfer line from the linac to the rings is to facilitate this by preparing the beam for injection using a series of transverse and momentum collimators. Horizontal phase space painting requires the momentum to be ramped immediately after the linac. When the beam has partly debunched, a bunch rotation cavity reduces the momentum spread by a factor 3. The beam then passes through a 180° achromatic bending section of mean radius 42.5 m. Here, combined function magnets provide both a high normalized dispersion for momentum collimation and, at the same time, sufficiently low fields that the H^- ions do not strip prematurely. Stripping foils at various points in the achromat are used for the collimation. Further debunching and subsequent transport to the two accumulator rings, stacked one above the other, is via two matching

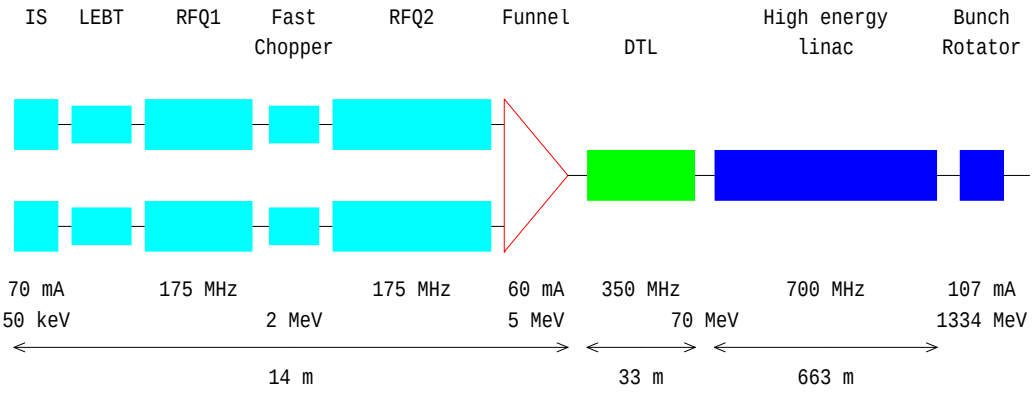

Figure 4.8: Reference Design of the ESS Linac

sections separated vertically by 2 m. Switching between the two as filling proceeds is by means of a pulsed dipole.

The rings have a mean radius of 26 m. Each comprises three superperiods of 15 cells forming first order achromats around long low field dipoles, one of which is used for injection. A study of the atomic physics of Stark lifetimes of H^0 excited states has led to the combination of an injection energy of 1.334 GeV and dipole fields of 0.177 T. The latter is chosen to give negligible pre-stripping of H^- ions ahead of the foil, minimize delayed stripping of H^0 atoms in the ring and bend stripped electrons directly to a collector.

A major problem is the heating of the foil, which is expected to be of graphite with thickness 545 μg cm^{-2}. Mismatching the linac beam into the ring helps to reduce subsequent traversals by recirculating protons. This is achieved by creating zero dispersion and betatron waists in the transport line at the foil but a normalized dispersion, $\alpha_p/\sqrt{\beta_h}$, of 2.0 m$^{1/2}$ and larger β-values in the ring. The non-zero ring dispersion is used to advantage in the method of phase space painting adopted in the design. Longitudinal painting depends on ramping the beam momentum from $[0 \rightarrow 2] \times 10^{-3}$ to $[2 \rightarrow 4] \times 10^{-3}$ linearly over the 1000 turns of the injection and steering the RF bucket by varying the RF frequency. This correlates into the transverse plane via the dispersion, giving large initial betatron oscillations which diminish as injection proceeds. Vertical painting is achieved by means of four vertical orbit bump magnets set for inversely correlated oscillations, small to large, as the ring fills. Studies have shown that, for dispersion painting of this kind, anti-correlated oscillations provide the best chance of avoiding subsequent foil traversals and help to minimize the effects of space charge in the final beam distribution.

The optimal RF voltages and the vertical orbit bump program necessary to keep the foil traversals to a minimum have been obtained from computer simulations. With a predicted average of between six and seven foil interactions per particle[2], total ring losses from delayed stripping, inelastic collisions, scattering and momentum variations should be within the design requirements of 0.02%. Nevertheless, the peak foil temperature is estimated to be near 2500°K. Modeling shows that longitudinally the bunches are well-confined, with no particles straying into the extraction gaps.

Fast extraction is single turn from a dispersion-free region in the horizontal plane, and kickers and septum extraction magnets are positioned so that the bunches from each ring are spaced closely together during transport to the targets. Bunch and pulse durations are 0.4 and 1.0 μsec respectively.

[2]Foil interactions have been reduced to three in a new model with larger ring radius.

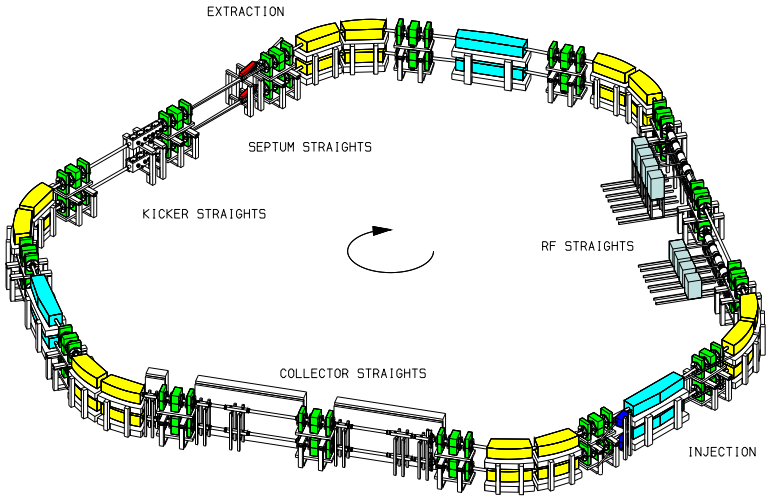

Figure 4.9: The ESS Accumulator Rings.

Transport to the targets is via beam lines based on 90° and 60° FODO cells, allowing the use of several magnets of the same type and providing easy dispersion matching where appropriate. In normal mode of operation, 1 MW of beam power passes from the rings to the 10 Hz target and 4 MW to the 50 Hz target. The full 5 MW can be exploited at the 50 Hz target when the other is out of service. A muon transmission target is envisaged in the 50 Hz line.

4.4.3.2 Recent Developments

Since publication of the reference design, R&D work has been undertaken on the ion source, the RF quadrupole linacs and some beam diagnostic techniques. Inconsistencies in the linac parameters have prompted study of an alternative layout, including design of a 20 MeV funneling system and a 2.5 MeV chopper line. The superconducting option is under active consideration. The projected foil temperatures of 2500°K are too high and one possibility of achieving lower values is to chop at 70% and inject less turns. Another is larger accumulator rings and both of these options are under study. More recently, a resonant laser optical system has been suggested for H^- stripping. Preliminary studies show some promise and a collaboration has been set up jointly by JAERI, LANL and RAL. The scheme would avoid the over-heating problems, and there would be less chance of particle loss and emittance growth at injection. A superconducting linac option could also be adopted. Unfortunately, difficulties have since emerged in the control of the beam divergence in the laser stripping scheme though study continues.

The University of Frankfurt is looking into the design of a volume source driven by arc discharge to produce the necessary 70 mA of H^- ions in 1.2 msec pulses. 140 mA have in fact been achieved through the use of pulsed caesium, with less than 3% of residual electrons, and continuous operation demonstrated for several days. The LEBT has already been constructed. Other work at Frankfurt has been directed towards the RFQs, particularly in connection with the design being built at RAL for ISIS, studies of which are hoped eventually to lead to full development of a unit for ESS.

A new RFQ computer code is being written to include more sophisticated geometries, realistic 3D space charge calculations and take account of neighboring bunches. The aim is a full 3D simulation of the beam through the entire linac structure, RFQ, DTL and CCL. Halo growth needs

to be understood and controlled, and simulations are already giving some insight into radial-axial coupling for halo particles in the CCL and the general effect of halo production by mismatching in bunched beams.

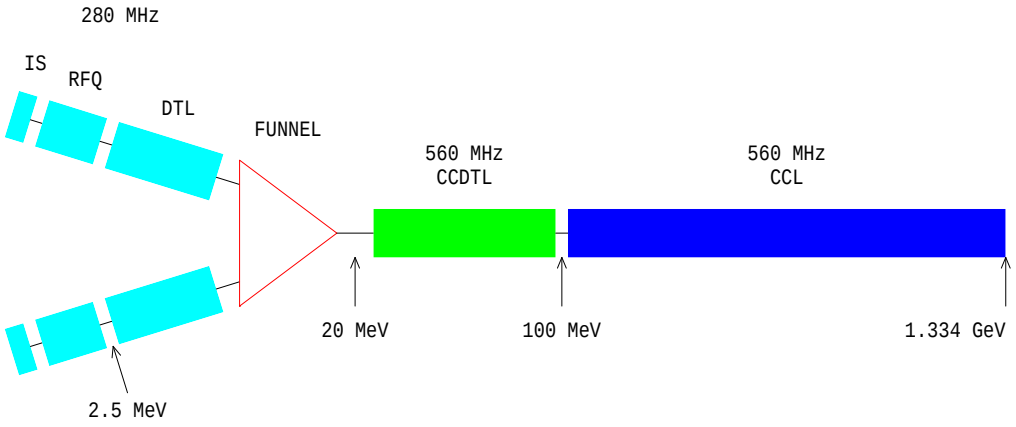

Figure 4.10: A Possible Alternative Design for the ESS Linac

Some encouraging preliminary work has also been carried out on an alternative (room temperature) linac. It appears that there might be advantages, in terms of size and efficiency, in using inductive output tubes (IOTs) operating at frequencies of 280 and 560 MHz, instead of klystrons. A possible layout might then comprise an RFQ-DTL system funneled at 20 MeV, followed by CCDTL and CCL accelerating systems to the design energy. The lower space charge levels make this a particularly attractive option for funneling. In addition, the sequence of focusing transitions ($2\beta\lambda$ (RFQ) $\rightarrow$ $4\beta\lambda$ (DTL) $\rightarrow$ $9\beta\lambda$ (Funnel) $\rightarrow$ $10\beta\lambda$ (CCDTL) $\rightarrow$ $11\beta\lambda \rightarrow 12\beta\lambda$ (CCL) per cell) in this design should be smoother than in the reference proposals. Specific study has focused on a long 2.5 MeV RFQ at 280 MHz which gives high transmission efficiency and low emittance growth as well as minimal longitudinal filamentation. The beam can be well matched into the regular focusing of the DTL, despite the relatively low energy. A possible design for the funneling mechanism has been completed, based on an achromatic set of FODO cells and RF buncher cavities, mainly at harmonic number 3 (840 MHz). Bunches in the two arms are merged via an arrangement of 10° and 2° septum magnets, and an electrostatic deflector. By carefully controlling betatron oscillations and the longitudinal bunch motion, emittance growth has been minimized and simulations show the likely increase to be less than 2%.

4.4.3.3 Future Plans

Funding for the ESS R&D program currently relies on support from individual institutions, with some money available from the European Union for target studies. FZJ (Jülich) has an accelerator and target program (including code development) based around a 500 MHz superconducting cavity with two input coupling ports for studying pulsed behaviour under power splitting. At the University of Frankfurt and at RAL, H^- ion source and RFQ development continue in close collaboration. A test-stand has been constructed at RAL to test the ion source and an RFQ intended for ISIS; this will be followed by the ESS RFQ design. Later a beam chopper will be incorporated followed by

one arm of the funnel. It is hoped to build and test the second leg and the complete funnel by the year 2003. Of the other European countries, CEA Saclay (France) is now involved with the superconducting linac design; work is being carried out in Sweden on instruments for linac longitudinal emittance measurements; the Netherlands, Denmark and Italy are involved on the instrumentation side; and Spain and Switzerland are also contributing to the study. It is hoped that the strong neutron users' community in Europe can exert influence to ensure the R&D program receives adequate central financial support.

4.5 Los Alamos Proton Storage Ring (PSR) Parameter List

Robert J. Macek macek@lanl.gov Los Alamos National Lab
T-S. Wang twang@lanl.gov USA

PSR Parameter List

Beam Kinetic Energy	T	797 MeV
Betatron Tunes	ν_x, ν_y	3.16, 3.14
Inc. Tune Shifts at 70 μA	$\Delta\nu_x$, $\Delta\nu_y$	-0.110, -0.094 (calc.)
Chromaticities (normalized)	ξ_x	-1.22 $\pm$ .07 (meas.), -0.8 (calc.)
	ξ_y	-1.14 $\pm$ .06 (meas.), -1.3 (calc.)
Transition γ	γ_t	3.1
Phase Slip Factor	η	-0.19
Max. rf Voltage	V_{rf}	12 kV
Synchrotron Tune (10 kV)	ν_0	0.00042
Buncher Harmonic, Freq.	h, f	1, 2.795 MHz
Mean Pipe Radius	b	0.05 m
Circumference	$C = 2\pi R$	90.2 m

4.6 High Intensity Performance and Operation at the Brookhaven AGS

Thomas Roser roser@bnl,gov AGS Department
Brookhaven National Laboratory

Fig. 4.11 shows the present layout of the AGS-RHIC accelerator complex. The high intensity proton beam of the AGS is used both for the slow-extracted-beam (SEB) area with many target station to produce secondary beams and the fast-extracted-beam (FEB) line used for the production of muons for the g-2 experiment and for high intensity target testing for the spallation neutron sources and muon production targets for the muon collider. The same FEB line will also be used for the transfer of beam to RHIC.

The proton beam intensity in the AGS has increased steadily over the 40 year existence of the AGS, but the most dramatic increase occurred over the last few years with the addition of the new

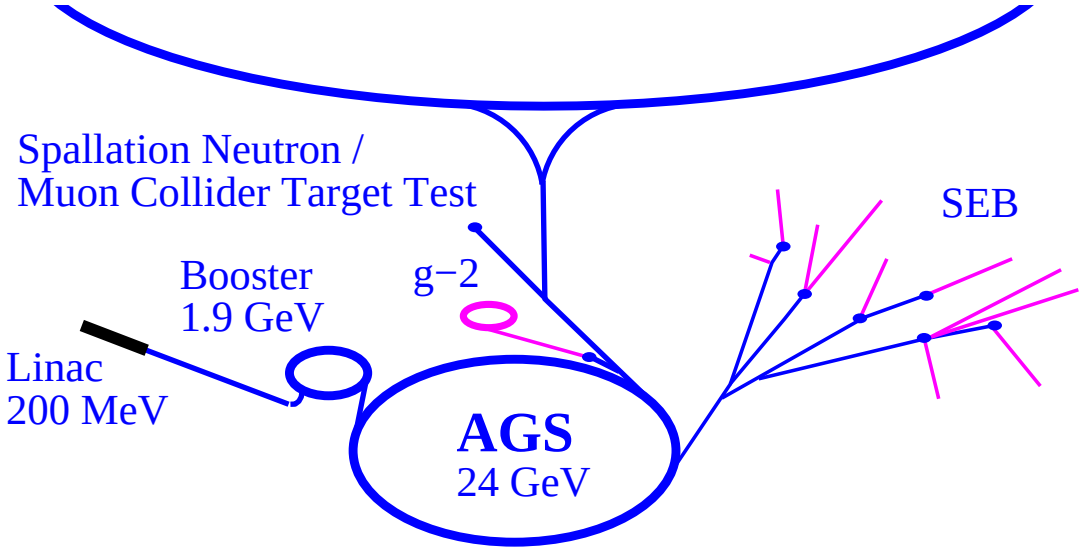

Figure 4.11: The AGS-RHIC accelerator complex.

AGS Booster. In Fig. 4.12 the history of the AGS intensity improvements is shown and the major upgrades are indicated. The AGS Booster has one quarter the circumference of the AGS and therefore allows four Booster beam pulses to be stacked in the AGS at an injection energy of $1.5 - 1.9\,GeV$. At this increased energy, space charge forces are much reduced and this in turn allows for the dramatic increase in the AGS beam intensity.

The 200 MeV LINAC is being used both for the injection into the Booster as well as an isotope production facility. A recent upgrade of the LINAC rf system made it possible to operated at an average H^- current of $150\ \mu A$ and a maximum of 12×10^{13} H^- per $500\ \mu s$ LINAC pulse for the isotope production target. Typical beam currents during the $500\ \mu s$ pulse are about $80\ mA$ at the source, $60\ mA$ after the $750\ keV$ RFQ, $38\ mA$ after the first LINAC tank ($10\ MeV$), and $37\ mA$ at end of the LINAC at $200\ MeV$. The normalized beam emittance is about $2\ \pi\ mm\ mrad$ for 95 % of the beam and the beam energy spread is about $\pm 1.2\ MeV$. A magnetic fast chopper installed at $750\ keV$ allows the shaping of the beam injected into the Booster to avoid excessive beam loss.

The achieved beam intensity in the Booster surpassed the design goal of 1.5×10^{13} protons per pulse and reached a peak value of 2.3×10^{13} protons per pulse. This was achieved by very carefully correcting all the important nonlinear orbit resonances especially at the injection energy of $200\,MeV$ and by using the extra set of rf cavities that were installed for heavy ion operation as a second harmonic rf system. The second harmonic rf system allows for the creation of a flattened rf bucket which gives longer bunches with lower space charge forces. The fundamental rf system operated with $90\ kV$ and the secondary harmonic with $30\ kV$. The typical bunch area was about $1.5\,eVs$. Even with the second harmonic rf system the incoherent space charge tune shift can reach one unit right at injection (3×10^{13} protons, norm. 95 % emittance: $50\ \pi\ mm\ mrad$, bunching factor: 0.5). Of course, such a large tune shift is not sustainable, but the beam emittance growth and beam loss can be minimized by accelerating rapidly during and after injection. Best conditions are achieved by ramping the main field during injection with 3 T/s increasing to 9 T/s after about 10 ms. The quite large non-linear fields from eddy currents in the Inconel vacuum chamber of the

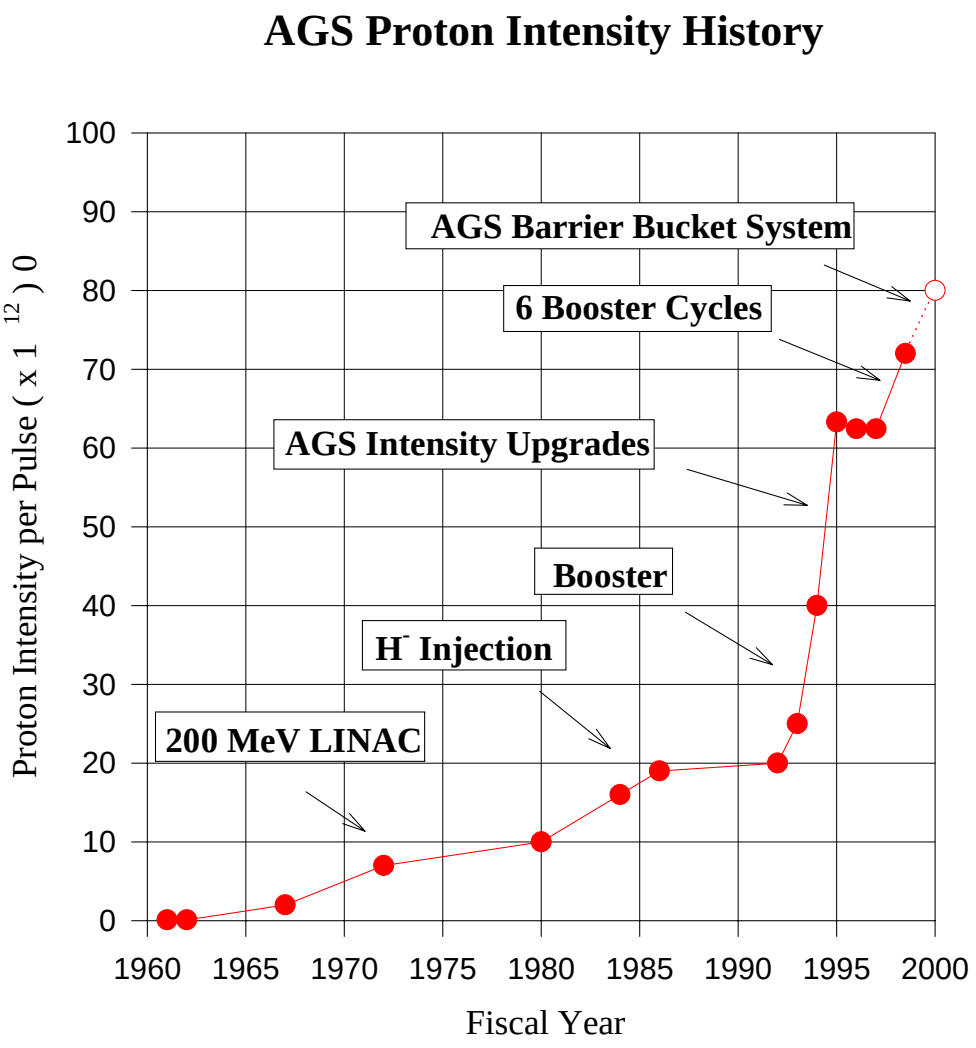

Figure 4.12: The history of the evolution of the proton beam intensity in the Brookhaven AGS.

Booster are passively corrected using correction windings on the vacuum chamber that are driven by backleg windings.

Recently the Booster rf system was modified to allow for the acceleration of a single bunch. At this lower frequency 45 kV was available for the first harmonic and 22 kV for the second harmonic. This results in the same available total bucket area. With only one bunch in the Booster a peak intensity of about 1.8×10^{13} was reached. Single bunch operation in the Booster allowed for the transfer of six Booster loads into the AGS reducing the need for very high intensity in the Booster. Nevertheless, the lower peak intensity was a surprise which was eventually traced to the factor of two lower synchrotron frequency. During the approximately $250\mu s$ long H^- injection period the synchrotron motion is now not providing enough dilution and high peak line densities are developing. More elaborate longitudinal painting schemes were studied which may eventually result in higher intensity even with single bunch operation.

The AGS itself also had to be upgraded to be able to cope with the higher beam intensity. During beam injection from the Booster, which cycles with a repetition rate of $7.5\ Hz$, the AGS needs to store the already transferred beam bunches for about 0.4 seconds. During this time the beam is exposed to the strong image forces from the vacuum chamber which causes beam loss from resistive wall coupled bunch beam instabilities within as short a time as a few hundred revolutions. A very powerful feedback system was installed that senses any transverse movement of the beam and compensates with a correcting kick. This transverse damper can deliver $\pm 160\ V$ to a pair of $50\ \Omega$, one-meter-long strip-lines. A recursive digital notch filter is used in the feed-back circuit to allow for accurate determination of the average beam position and increased sensitivity to the unstable coherent beam motion. This filter design is particular important for the betatron tune setting of about 8.9 which is required to avoid non-linear octupole stopband resonance at 8.75. With an incoherent tune shift at the AGS injection energy of 0.1 to 0.2 it is still necessary, however, to correct the octupole stopband resonances to avoid excessive beam loss.

To reduce the space charge forces further the beam bunches in the AGS are lengthened by purposely mismatching the bunch-to-bucket transfer from the Booster and then smooth the bunch distribution using a high frequency $100\ MHz$ dilution cavity. The resulting reduction of the peak current helps both with coupled bunch instabilities and stopband beam losses.

A large part of the injection losses at the AGS are due to a relative slow loss during the first millisecond the transferred bunches circulate in the AGS. No direct cause for this loss could be identified but it is correlated with a sustained transverse coherent beam oscillation shown in Fig. 4.13. The coherent oscillations result from miss-matched beam injection to blow-up the transverse emittance and therefore reduce the space charge tune shift. Although the coherence persists over a whole millisecond the middle part of the beam bunch has a coherent space charge tune shift of about 0.1 and therefore very high frequency vertical modulations appear. The bunch intensity is about 1.3×10^{13} protons.

At bunch intensities above 1.3×10^{13} protons a single bunch vertical head-tail instability develops. Fig. 4.14 shows both the bunch shape as well as the vertical modulation. The modulation develops towards the tail of the bunch and is very asymmetric. The instability can be cured by changing the vertical tune.

The large space charge forces during AGS injection can be mitigated by maintaining a practically debunched beam during the AGS injection process. To accomplish this, cavities that produces isolated rf buckets can be used to maintain an empty gap for injection of additional Booster beam pulses. Isolated bucket cavities, also called Barrier Bucket cavities, have been used elsewhere.

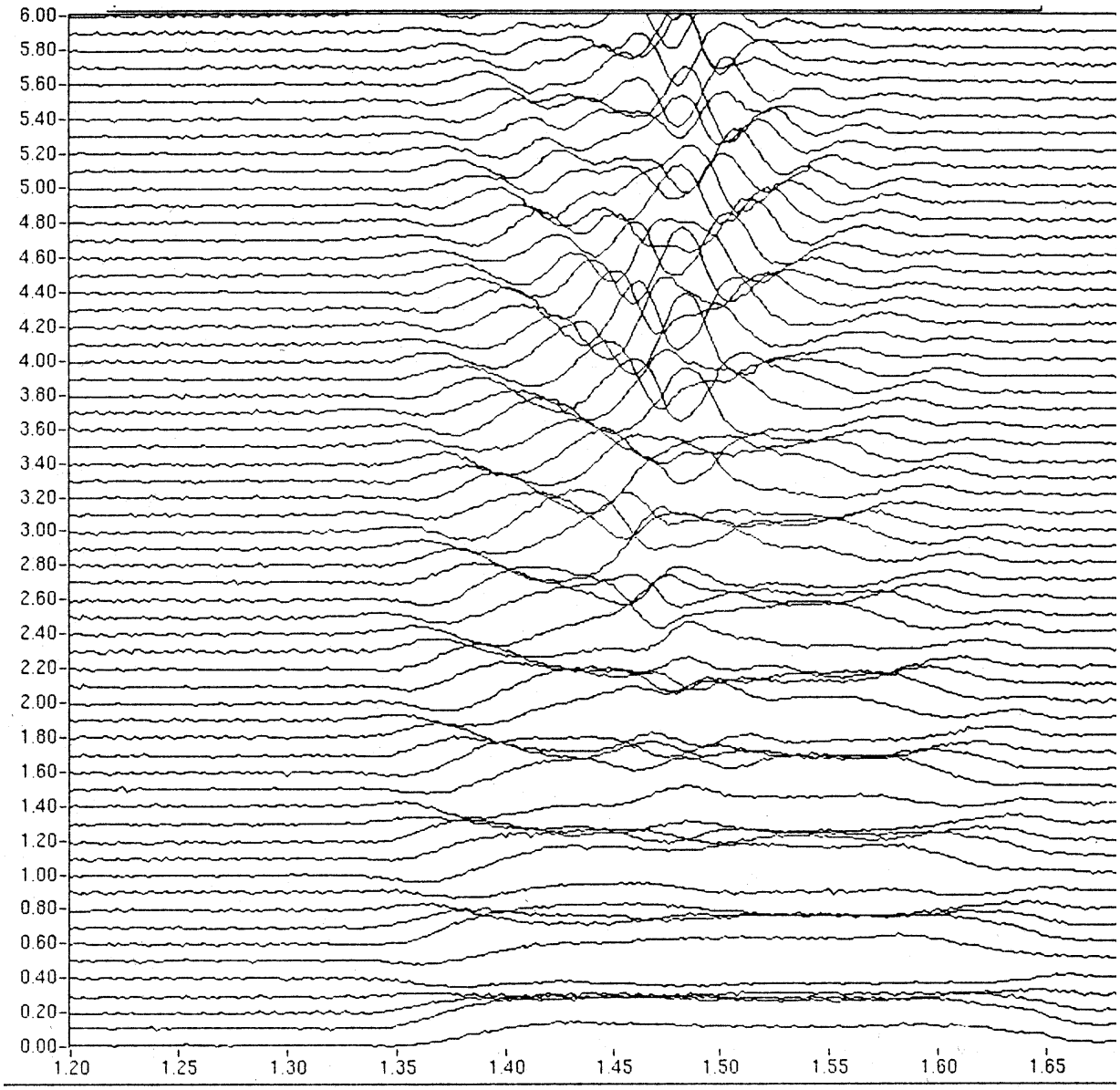

Figure 4.13: Evolution of the vertical miss-match at AGS injection. The traces show the vertical displacement of the same bunch every revolution. The horizontal scale is in microseconds.

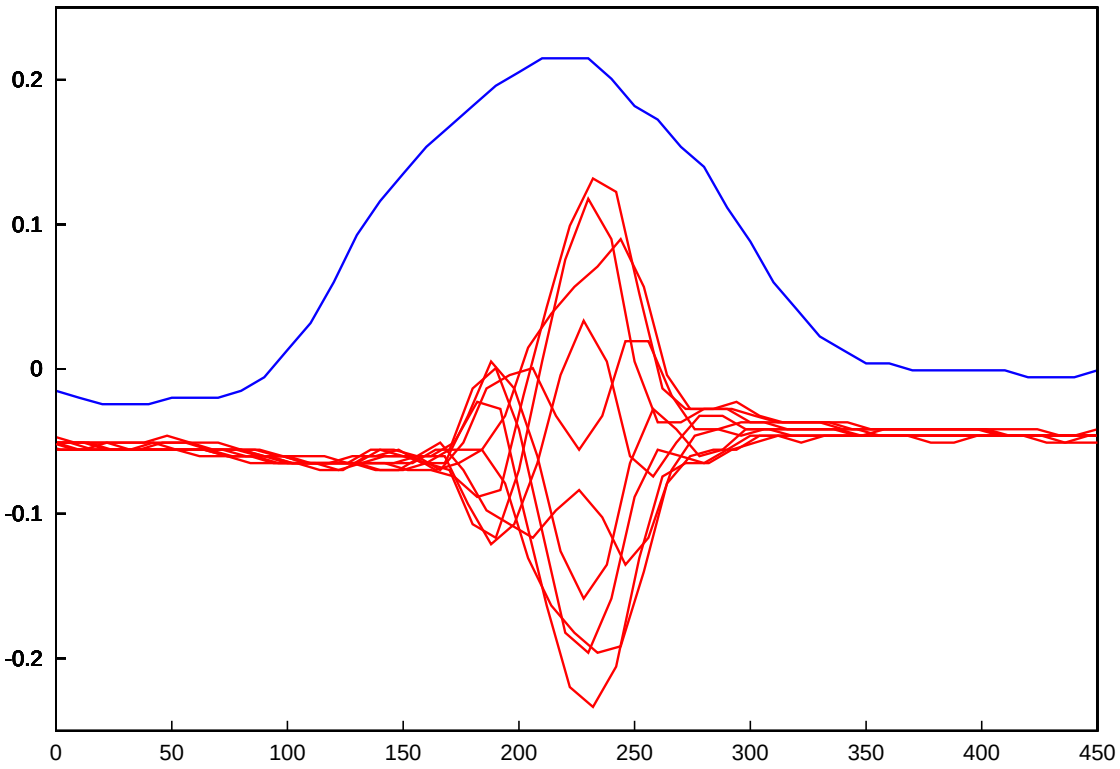

Figure 4.14: Bunch shape (top) and vertical modulation of a high intensity bunch at AGS injection energy of 1.9 GeV during a single bunch head-tail instability. The vertical scale is in arbitrary units and the horizontal scale is in ns.

However, for this stacking scheme, a high rf voltage will be needed to contain the large bunch area of the high intensity beam. A successful test of this scheme has recently been completed using two 40 kV Barrier cavities.

During acceleration the AGS beam has to pass through the transition energy after which the revolution time of higher energy protons becomes longer than for the lower energy protons. This potentially unstable point during the acceleration cycle was crossed very quickly with a new powerful transition energy jump system with only minimal losses even at the highest intensities. The large lattice distortions introduced by the jump system prior to the transition crossing severely limits the available aperture of the AGS in particular for momentum spread. Efforts to correct the distortions using sextupoles have been partially successful. After the transition energy, a very rapid, high frequency instability developed which could only be avoided by purposely further increasing the bunch length using again the high frequency dilution cavity.

The peak beam intensity reached at the AGS extraction energy of $24\,GeV$ was 7.2×10^{13} protons per pulse also exceeding the design goal for this latest round of intensity upgrades. It also represents a world record beam intensity for a proton synchrotron. Individual bunches with an intensity of 1.2×10^{13} had a bunch area of about 3 eVs at AGS injection but were diluted to about 10 eVs during acceleration.

At maximum beam intensity about 30 percent of the beam is lost at Booster injection ($200\,MeV$), 20 percent at injection into the AGS ($1.9\,GeV$), which includes losses during the 0.4 second storage time in the AGS, and about 3 percent is lost at transition ($8\,GeV$).Although activation levels are quite high all machines can still be manually maintained and repaired in a safe manner.

4.7 Beam Dynamics Activities at the CERN PSB-PS

4.7.1 Beam performance in the longitudinal phase plane in the CERN PSB and PS

R. Garoby Roland.Garoby@cern.ch CERN

The RF systems which are necessary for the generation of the nominal proton beam for the LHC in the PS Complex have been installed in the PSB and in the PS during the shut-down 97-98 [1]. Table 4.2 lists the RF equipment presently available in both machines:

Table 4.2: RF systems in the PSB and in the PS.

Machine - System	Nb. of cavities	Frequency (MHz)	Vpeak[a] (kV)	HF feedback gain (dB)	Impedance[a] (kOhm)
PSB - C02[c]	1 per ring	0.6 - 1.8	8	20	0.3
PSB - C04[c]	1 per ring	1.2 - 3.9	8	20 - 26	0.9 (+ S.C.)
PSB - C16[b]	1 per ring	6 - 17	6	13 - 26	1.5 (+ S.C.)
PS - C10[b]	11	2.7 - 10	20	20	0.7 (+ S.C.)
PS - C40[c]	1 (+1[d])	40.05	300	43	2.4 (+ S.C.)
PS - C80[c]	2 (+1[d])	80.1	300	44	5.7 (+ S.C.)
PS - C114[b]	2	114.511	500	-	3000 (+ S.C.)
PS - C200[b]	8	199.950	30	-	7 (+ damper)

[a] Per cavity
[b] Unchanged systems
[c] Systems installed for the start-up 1998
[d] Systems installed for the start-up 1999

New capabilities result from the modifications:

- the PSB can accelerate one bunch per ring, permitting exotic harmonic numbers in the PS (h=8, 10, 16 and 7 have been used yet),
- controlled longitudinal blow-up is possible in the PSB,
- double batch filling of the PS is possible,
- the 40 and 80 MHz RF systems in the PS are used to deliver proton beams approaching the performance required for LHC.

The longitudinal characteristics of the various beams and the RF gymnastics used to generate them have been completely changed to make the best use of the new hardware. The following beam gymnastics are routinely performed:

- dual harmonic acceleration in the PSB with harmonics 1 and 2,
- bunch splitting in two, both in the PSB and in the PS and up to the highest intensity,
- controlled longitudinal blow-up in the PSB and in the PS, helping optimize longitudinal emittance at all energies,
- debunching (h=16) / rebunching (h=84) at 26 GeV/c in the PS.

4.7.1.1 Longitudinal beam characteristics

In the PSB an important basic improvement has come from the disappearance of the longitudinal coupled bunch instabilities which required tedious and delicate adjustments of feedbacks. The other

improvements result from the fact that the RF systems have been designed to operate "comfortably" at the highest beam intensities, and from the new beam control electronics. Dual harmonic acceleration, in particular, is now much more reliable. The only unexpected problems were caused by the higher impedance of the RF by-passes between vacuum chambers at the new operating RF frequency. A new design is being implemented as a cure. As a result of these changes a record intensity of 3.6×10^{13} protons has recently been accelerated at 1.4 GeV.

In the PS the major changes involved the beam controls which were fully rebuilt according to the needs of the new modes of operation. A feedback had to be installed to damp a longitudinal coupled bunch instability at 3.5 GeV/c (mode n=6) which disturbed the splitting process. The various proton and ion beams required for physics were delivered as planned and a record number of protons on the SPS neutrino target was obtained in 1998.

The proton beam for LHC has also been set-up and ejected to the SPS. As far as longitudinal beam parameters are concerned, the PSB is fully ready. Difficulties remain in the PS to obtain the required longitudinal emittance of 0.35 eVs for the bunches at 40 MHz (Table 4.7.1.1) because of an instability which blows up the beam at the end of debunching. The impedance of the 114 MHz cavities (see Table 4.2) is suspected, but a definitive demonstration will only be made at the end of the year 2000 when these cavities will be removed.

Table 4.3: Longitudinal characteristics of the proton beam for LHC in the PS.

Intensity (protons / bunch)	1×10^{10} (1998)	1×10^{11} (1998)	1×10^{11} nominal
Longitudinal emittance per bunch before debunching (eVs)	0.9	1.2	1.0
Longitudinal emittance per bunch at ejection (eVs)	0.4 ± 0.05	0.5 ± 0.05	0.35 -
Bunch length at ejection (ns)	4.3 ± 0.2	5 ± 0.2	4 -
Total $\Delta p/p$ at ejection	4.3×10^{-3}	4.5×10^{-3}	4.1×10^{-3}

4.7.1.2 Ongoing developments

A new gymnastics has been proposed to attain the required longitudinal emittance for LHC and provide a gap in the bunch train before ejection [2]. Debunching/rebunching is avoided and replaced by splitting bunches in three at 3.57 GeV/c and twice in two at 26 GeV/c. Tests with beam splitting in three are planned during the summer of 1999. Full scale experiments will take place in the year 2000, when a prototype 20 MHz system will be available in the PS.

The generation of hollow distributions in the PSB is being pursued, depositing empty high frequency buckets inside the coasting Linac beam before RF capture [3]. The resulting "flat-topped bunches" could be accelerated on h=1 only and would reduce the Laslett tune-shift at low energy

in the PS. Encouraging results have been obtained, but also beam instabilities have been observed. Longitudinal tomography is routinely used to monitor the behaviour of the beam during these manipulations.

The antiproton production beam is being prepared in the PS for the needs of the Antiproton Decelerator (AD). Based on the principle of "batch compression" previously used for the Antiproton Accumulator and Collector (AA/AC), it will work with harmonic numbers 8, 10, 12, 14, 16, 18, 20 and benefit from the present capability of the PSB to deliver in matched conditions its total intensity inside one half of the PS ring. The operational beam is scheduled for the end of 1999.

4.7.2 Beam performance in the transverse phase plane in the PSB

M. Chanel Michel.Chanel@cern.ch CERN

The PSB machine can deliver up to 3.6×10^{13} protons to the users which means about 9×10^{12} protons per ring. The multi-turn injection and the first 100 ms of acceleration are the most critical part of the cycle as an incoherent tune shift of more than 0.5 is observed even with an improved bunching factor obtained with a dual RF system (h=1 and h=2) and an efficient painting of the phase space helped by skew quadrupoles. The machine tune is set above $Q_V = 5.5$ and the particles are experiencing many second and third order resonances which have to be properly compensated. For the LHC beam a lower beam intensity is needed (only 1.1×10^{12} protons per ring) but with stringent emittance characteristics: $(\epsilon_H + \epsilon_V)/2 < 2\mu\mathrm{m}$ (where the emittances are *rms*, normalized). This implies a good control of emittance blow-up during acceleration and a good recombination of the four rings to minimize misteering and mismatch between bunches coming from different rings.

To ease the adjustment of the beam trajectory, an Automatic Beam Steering (ABS) system is currently implemented in all the transfer lines.

To understand the mismatch between the different rings, careful studies are being made and most probably one or more quadrupoles will have to be added.

An important program to better understand the high-density beam behaviour during the injection process and the beginning of acceleration is actually in progress both by numerical calculations and beam experiments. It is also useful for the next generation of accelerators proposed for protons beam production in muon colliders.

4.7.3 Transverse phase plane performance of the PS beam for LHC

R. Cappi Roberto.Cappi@cern.ch CERN
E. Métral Elias.Metral@cern.ch

Machine studies for the LHC beam production are successfully going on. Since the increase of the PS Booster energy from 1 to 1.4 GeV, many machine development sessions were devoted recently to study the low energy transverse beam behaviour of a single bunch (out of the 8 foreseen for the nominal beam). Finally a bunch of 1×10^{12} protons, 150 ns long with transverse normalized *rms* emittances $\epsilon_H \approx \epsilon_V \approx 2\mu\mathrm{m}$ (measured 10 ms after injection) was circulating on a 1.4 GeV, 600 ms long flat-bottom without undergo any transverse blow-up.

The predicted and observed head-tail transverse instabilities at m=6 where successfully cured by appropriate coupling of horizontal and vertical plane with skew quadrupoles [4]. Also octupoles were useful to damp these instabilities. Note that the relatively large space charge tune spread of about -0.2 in both planes was of no help in stabilizing these higher mode instabilities except if octupoles were also pulsed, confirming predictions [5]. A horizontal tilt (few mm) with respect to the PS closed orbit was discovered on bunches coming from ring 3 of the PSB, as a consequence of an anomalous ripple of about 5% on the PSB extraction kicker. Improvements and modifications of the kicker pulse are under study.

Studies of PSB-PS dispersion matching are also proceeding. In the next months its planned to inject the full nominal beam (2 x 4 bunches) to analyze the precise requirements of a future damper to rectify bunch to bunch differences.

4.7.4 PS-SPS Transfer Line Studies

M. Giovannozzi Massimo.Giovannozzi@cern.ch CERN

The TT2/TT10 beam line is used to transfer from PS to SPS protons and lead ions for fixed-target physics, protons to simulate the future LHC-type beam and positrons for LEP. In recent years, there has been a renewed interest in the optics of this transfer line for two main reasons.

Firstly, the tight emittance budget for the LHC beam. The maximum allowed emittance blow-up in the transfer from PS extraction to SPS extraction is 17 % and only a small fraction of this is assigned to mismatch at injection. Since this beam has a small emittance and a large momentum spread, dispersion mismatch is a major concern.

Secondly, high-intensity proton and lead ion beams are required by the physics community, therefore minimum emittance blow-up is needed to minimize beam losses and thus increase the beam intensity delivered to the experiments.

A measurement campaign was undertaken during the 1998 physics run to define and improve the model of the TT2/TT10 transfer line and to measure the optical parameters α, β, the dispersion D and its derivative D' so that improved optics could be computed and tested in operation [6].

For the different beam types (26 GeV/c fast extracted proton beam, 14 GeV/c continuous transfer proton beam and fast extracted lead ion beam) the same measurement procedure has been applied. Firstly D has been measured in TT2/TT10, then the Twiss parameters have been deduced using the Secondary Emission Monitors (SEMs) in TT2 and TT10. Finally, the optical parameters at the entry point of the transfer line have been obtained by tracking back the values at the SEM locations. The knowledge of the model and of the initial optical parameters has allowed the computation of new transfer line optics with reduced blow-up.

The 26 GeV/c fast extracted proton beam is the so-called LHC beam. The measured values of D_H in TT2/TT10 and the SPS for the initial optics (left) and the matched one (right) are shown in Fig. 4.15. The overall reduction of D_H is clearly visible. The values of the mismatch factors after filamentation for the old and new optics are listed in Table 4.7.4. The improvement is remarkable,

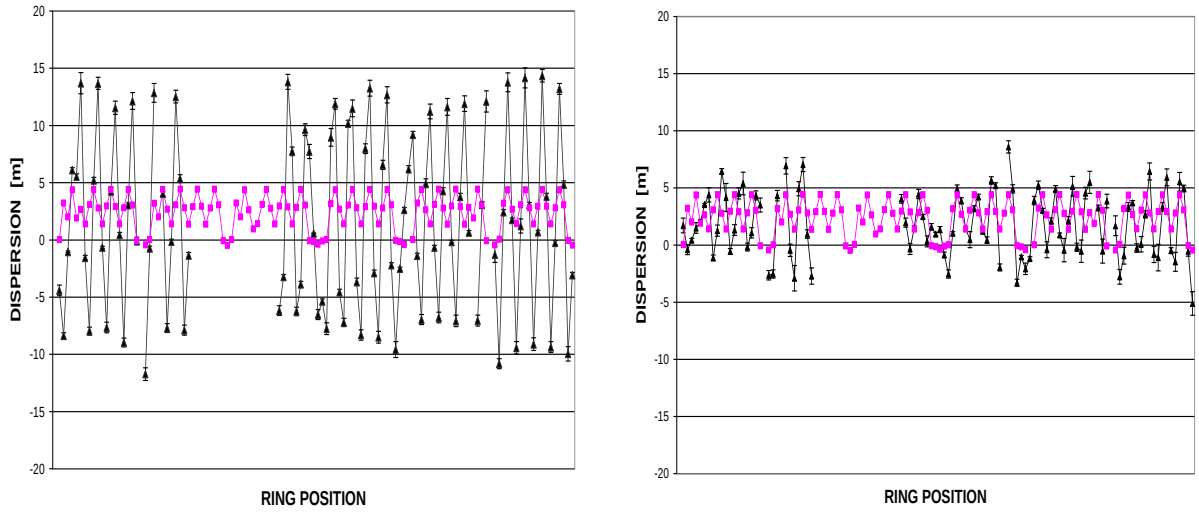

Figure 4.15: Measured (darker triangles) and theoretical (squares) horizontal dispersion in the SPS ring before (left) and after (right) matching the injection line.

Table 4.4: Measured filamented betatron and dispersion blow-up factors for old and new optics.

	Old optics	New optics
H (H-plane)	1.1	1.0
H (V-plane)	1.3	1.0
J (H-plane)	11.6	1.7
J (V-plane)	1.0	1.0

even though the blow-up due to D_H is far from the nominal value imposed by the real LHC emittance budget. Further studies are needed to improve this situation.

The control of the mismatch for the high intensity (about 3×10^{13} protons) 14 GeV/c proton beam for fixed target physics is mandatory in order to reduce beam losses and thus increase the intensity delivered to the targets. For this beam the TT2/TT10 line is set-up with an emittance exchange section to match the beam envelope with the physical aperture of the SPS machine.

A new optics tested in operation allowed the reduction of the injection losses by a factor two and the increase of the transmission efficiency by 2 %, reaching a value of 92 %. Furthermore, the improved knowledge of the optical parameters allowed the elimination of a long-lasting discrepancy between the emittance values measured in TT2 and TT10.

As a result of the betatron matching of the transfer line, the quality of the lead ion beam was highly improved. The transmission through the SPS went up from 75 % to 88 % and the beam intensity delivered to the targets increased accordingly. In Fig. 4.16 the average number of lead ions is shown: the sudden increase in the intensity is due to the new optics in TT2/TT10.

The study will continue during the 1999 run with particular attention to the precise measurement

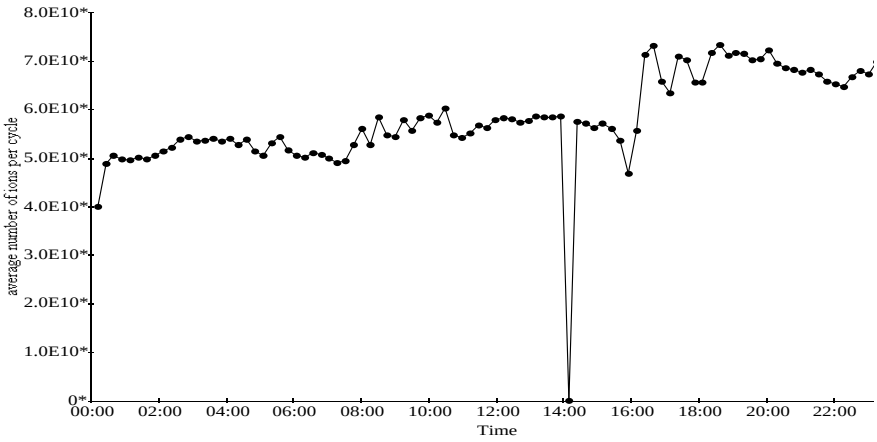

Figure 4.16: Average number of lead ions per cycle over 24 hours. The step function in efficiency is due to the matched optics in TT2/TT10.

of the beam energy and adjustment of its control value accordingly, extension of the error analysis to all measurement stages, measurement of the dependence of mismatch on extraction conditions (energy, extraction trajectory), on-line measurement of optical parameters and matching correction.

4.7.5 Neutron Time Of Flight Facility

R. Cappi Roberto.Cappi@cern.ch CERN
G. Métral Gabriel.Metral@cern.ch

The neutron Time Of Flight (TOF) beam [7], to be used in operation in the year 2000, will require a single bunch of high intensity (about 7×10^{12} protons) and short length (about 7 ns *rms*) at 20-24 GeV/c. The maximum intensity achieved in recent machine studies was 4×10^{12} protons/bunch. The limitations come from fast head-tail vertical instabilities appearing very close to the transition energy of 6 GeV/c. The present chromaticity jump, from negative to positive, at transition will have to be more carefully controlled to allow a further increase of the bunch intensity.

Moreover, to spare a machine cycle in the super-cycle, we have explored the possibility of producing such a beam during one of the 24 GeV/c cycles dedicated to slow-extraction physics. These cycles normally use a single bunch of 10^{11} protons/bunch. The procedure to be put in operation is the following

- to accelerate a high intensity bunch together with a low intensity one,
- to make a bunch compression (by RF phase jump on both bunches),
- to extract the high intensity one,
- to decompress to the initial values (by inverse phase jump) the remaining small bunch,
- to eject the small bunch by using a slow-extraction process.

This operation has been successfully tried for intensities of 2×10^{12} protons/bunch and 2×10^{11} protons/bunch for the intense and small bunch respectively.

References

[1] A. Blas, R. Cappi, R. Garoby, S. Hancock, K. Schindl, J. L. Vallet, (1998). "Beams in the PS Complex after the RF Upgrades for LHC", *CERN PS/***98 022** *(RF)* and Proceedings of the EPAC98 Conference.

[2] R. Garoby, "Status of the Nominal Proton Beam for LHC in the PS", (1999). Proceedings of the Workshop on LEP-SPS Performance - Chamonix IX, *CERN SL/***99 007** *(DI)*, p.94.

[3] A. Blas, S. Hancock, S. Koscielniak, M. Lindroos, F. Pedersen, (1999). "New Technique for Bunch Shape Flattening", *CERN PS/***99 036** *(RF)* and Proceedings of the PAC99 Conference.

[4] E. Metral, (1999). "Theory of Coupled Landau Damping", *Part. Accel.* **62***, 3-4, p.259.*

[5] D. Möhl, (1995). "On Landau Damping of Dipole Modes by Non-linear Space Charge and Octupoles", *Part. Accel.* **50***, 1-3, p.177.*

[6] G. Arduini, M. Giovannozzi, K. Hanke, D. Manglunki, M. Martini, G. Métral, (1999). "Measurement and Optimization of the PS-SPS Transfer Line Optics", *CERN PS/***99 22** *(CA)* and Proceedings of the PAC99 Conference.

[7] S. Andriamonje et al., (1998). "Feasibility Study of a Neutron Time Of Flight Facility at the CERN-PS", *CERN PS/***98 65** *(CA).*

4.8 High Intensity Challenges at the CERN SPS

T. Linnecar T. Linnecar@cern.ch CERN, SL Division
1211 Geneva 23, Switzerland

4.8.1 Maximum intensities up to now

The maximum total intensity achieved in the SPS up to now is 4.84×10^{13} protons, obtained in fixed target physics and with a beam more or less equally distributed around the circumference, each of the 4200 bunches having $\sim 10^{10}$ protons. In normal operation with this beam there is a longitudinal emittance blow-up to about 2 eVs during the cycle. This increase, by one order of magnitude, mostly occurs between transition and top energy, 450 GeV, and is caused by coupled bunch instabilities. Injection is at 14 GeV, below transition, ($\gamma_{tr} = 23.4$).

The maximum bunch intensity that has been obtained was in ppbar operation (proton-antiproton), where it reached $\sim 2 \times 10^{11}$ but with only six of these bunches in the machine. Injection energy for this mode of operation had to be increased to 26 GeV, to be above transition. Crossing transition with intense bunches was limited to maximum bunch intensities of $\sim 2 \times 10^{10}$ due to the longitudinal negative mass instability and the transverse strong head-tail instability. Following this change of injection energy the major limitation was the microwave instability at injection, which

was solved by injecting long bunches of large emittance. (A new RF system at half the frequency of the main system was installed).

4.8.2 Future high intensity requirements

The future high intensity requirements for the SPS machine are given by two projects: one as injector for the Large Hadron Collider, LHC, at present under construction, and the second as a proton source for neutrino physics. Table 4.5 gives the main parameters for the existing and future operational modes.

As injector for LHC [1], the SPS must accelerate 243 bunches of the same intensity as for ppbar and concentrated in 3/11 of the circumference. This combines both the single bunch and multi-bunch problems. The beam parameters required at extraction to the LHC are stringent in both the longitudinal and transverse planes. The longitudinal emittance must be below 0.6 eVs at extraction while at injection it will be 0.35 eVs, limited by the total RF voltage available in the injector. The emittance at extraction can be allowed to increase to 1.0 eVs but at the expense of a new 200 MHz RF system for capture in the LHC, which has a main accelerating RF system working at 400 MHz.

The transverse emittance must not increase by more than a factor 15% from 3.0 μm (rms, normalized) in the two planes at injection in the SPS.

The high local intensities cause considerable beam-loading problems in the 200 MHz traveling wave cavities, the main acceleration system in the SPS. These cavities have short filling times of the order of 500 ns. Phase modulation of the bunches during this transient period can cause emittance increase at injection and difficulties with the transfer to LHC which must be loss free.

For the possible future neutrino program [2], with desirable total intensities $\geq 7 \times 10^{13}$, the main problem will be to keep losses as low as possible, both micro losses during acceleration and losses in the extraction area. This implies the control of possible multi-bunch instabilities in both planes to keep the emittances as low as possible.

A program of experimental and theoretical studies to address these challenges has started. Recently two days at a workshop in Chamonix [3] were devoted to the future requirements for the SPS. In addition a working group has been formed to specifically study the implications of going to much higher intensities.

4.8.3 Present studies and hardware upgrades

4.8.3.1 Single bunch phenomena

For the single bunch microwave instability the primary sources of impedance in the machine have been identified using a technique based on the observation of growing modes on a single bunch injected into the machine above threshold [4]. As a result of these measurements a campaign is underway to shield the 16 magnetic septa and 800 pumping ports which have been found to be responsible. In the last long shutdown , 1998/1999, RF shields were placed in half the magnetic septa. The rest will be shielded in the next shutdown, 1999/2000. The shielding of the pumping ports is a delicate problem. These ports are found mainly between the magnets. The vacuum chambers from the two adjacent magnets enter this cylindrical cavity which is made in two pieces connected by

Operating mode	E_{max} (GeV)	N_{tot} (10^{12})	N_b (10^{12})	A_b (eVs)	ϵ^H_{rms} (μm)	ϵ^V_{rms} (μm)
SPS ppbar protons. (past)	315	1.2	0.2	$\sim$ 1.0	$\sim$2.75	$\sim$2.75
SPS fixed target (present)	450	48.4	0.012	$\sim$ 2.0	10	7
SPS for LHC (project)	450	24 (3/11 ring)	0.11	0.6 - 1.0	3.5	3.5
SPS for Gran Sasso (study)	350	$\geq$70	0.014	$\leq$ 2.0	10	10

Table 4.5: Present and future SPS parameters

a vacuum joint to allow separation when a magnet must be removed. The shield will be inserted in this cylinder to ensure a smooth electrical connection between the two vacuum chambers. The problems lie in providing good RF contacts at the end joints and also in the middle where they must be sliding contacts with a mechanism to move them to one side when removing magnets. A solution must be found which will ease mounting in the ring - half the existing magnets must be removed and then put back during the initial installation process. A final design is nearly achieved and prototypes will be placed in test areas in the SPS ring in the near future. The idea is to install up to one third of the shields in the next shutdown, the rest being installed during the very long shutdown associated with the closure of LEP in 2000/2001.

Other techniques to raise the threshold of the microwave instability, such as increasing the momentum spread or lowering the transition energy, either with dedicated quadrupole families or by lowering significantly the machine tune, have been studied but are kept in reserve. In one particular experiment the transition energy was lowered by operating the machine at tune values near a resonance of the machine super-periodicity. Using the technique cited above to measure the unstable bunch spectrum it was possible to show the effect of this change on the microwave instability. In itself this method of lowering the transition energy cannot be used due to the large beta values and poor lattice characteristics at the injection point.

4.8.3.2 Multi-bunch phenomena - longitudinal

For the multi-bunch phenomena in the longitudinal plane attacks are being made on several fronts:

• Optimization of the use of the existing 800 MHz Landau damping system which consists of two traveling wave cavities. Theoretical analysis has shown [5] that the bunch lengthening mode of operation is only advantageous for very small emittance bunches and to get this advantage extremely accurate programming of the phase shift between the two RF systems is required. In general the bunch shortening (BS) mode of operation is more efficient and much easier to handle. This explains experimental experience at both the SPS and HERA where the BS mode is preferred.

• Analysis of the unstable bunch spectra in the hope that impedance sources can be identified and subsequently damped

• Upgrade of the single turn RF feedback and introduction of a feedforward system for the main accelerating cavities. This is not only important for impedance reduction but is also essential for

reducing the phase modulation in the transient period of the cavity rise-time, (see above).

• Introduction of a longitudinal feedback system. Our intention is to use part of the existing 200 MHz lepton acceleration system which uses standing wave cavities and which will become available in 2001. However the bandwidth of the system must be increased to $\pm$ 20 MHz to cover all possible modes. Present activities concentrate on the amplifier to cavity connection which due to reflections in the short transmission lines is delicate for this bunch by bunch feedback (25ns bunch spacing).

• Removal of all equipment at present solely used for lepton acceleration. This will be possible from 2001 when LEP closes.

4.8.3.3 Transverse phenomena

In the transverse plane the small transverse emittance budget for the LHC implies strong efforts in several areas.

• The power bandwidth of the transverse damper must be increased to 5 MHz to cope with injection kicker ripples with significant gain being maintained to 20 MHz to damp all possible coupled bunch modes. This work is under way, the power part having been installed on half the system, the remainder foreseen for the year 2000.

• Accurate control of the chromaticity is required to kill the first head-tail mode while not introducing too much tune spread. Landau damping is assumed sufficient for the higher modes. Similarly the tune must be carefully adjusted; the footprint is of the order of 0.03 in both planes.

• Very careful matching of the injection and extraction optics. In this are included dipole, dispersion and betatron mismatch effects.

4.8.4 Conclusions

For the future LHC needs, production of beams with the required characteristics are expected in 2001. The high intensity neutrino beams are further away in time, but knowledge of the high intensity limitations in the SPS is required this year. We have a very busy program.

References

[1] The SPS as Injector for LHC. Conceptual Design, P. Collier, editor. CERN-SL-97-07 DI.

[2] E. Weisse, The CERN Neutrino beam to Gran Sasso (NGS). Proc. of the workshop on LEP-SPS Performance - Chamonix IX, CERN-SL-99-007 DI.

[3] Proceedings of the workshop on LEP-SPS Performance - Chamonix IX, J. Poole, Editor. January 1999, CERN-SL-99-007 DI.

[4] T.Bohl, T.P.R. Linnecar and E. Shaposhnikova, Measuring the Resonance Structure of Accelerator Impedance with Single Bunches. Phys. Rev. Letts. Vol. 78, Number 16, 21 April 1997.

[5] T. Bohl, T. Linnecar, E. Shaposhnikova and J. Tuckmantel, Study of Different Operating Modes of the 4^th RF Harmonic Landau Damping System in the CERN SPS. EPAC-98, Stockholm, June 1998. also CERN SL-98-026 RF.

4.9 Fermilab Main Injector

S. Pruss pruss@fnal.gov Fermilab

Status After about 6 years of construction and 6 months of intermittent commissioning, the Fermilab Main Injector[1] is now operating for Tevatron fixed target physics. All of the milestones established by DOE[2] have been fulfilled. The following table lists the design parameters of this machine.

This machine replaces the original Fermilab Main Ring. The maximum intensity achieved so far is only 2×10^{13}. While it is expected increasing this to the design goal will require additional operating experience, the physics users of the machine are not requesting high intensity at this time. It is expected that this goal will be exceeded soon after the users request it. The 1.5 second minimum cycle time has not yet been achieved because of late delivery of a large power transformer. A cycle time of 2 seconds has been achieved and the transformer is expected within a few months, before needed for the physics program. The overall efficiency of beam transmission from the injection line to the extraction line is typically above 90%, but may drift somewhat lower if problems elsewhere distract the operators.

Main Injector Parameter List

Circumference	3319.419 m
Injection Momentum	8.9 GeV/c
Peak Momentum	150 GeV/c
Minimum Cycle Time (120 GeV)	1.5 s
Minimum Cycle Time (150 GeV)	2.4 s
Number of Protons	$3 \times x10^{13}$
Number of Bunches	498
Protons/Bunch	6×10^{10}
Maximum Courant-Snyder Beta Function	57 m
Maximum Dispersion Function	1.9 m
Phase Advance per Cell	90°
Nominal Horizontal Tune	26.425
Nominal Vertical Tune	25.415
Transverse Admittance (8.9 GeV)	> 40 mm-mrad
Longitudinal Admittance	> 0.5 eV-s
Transverse Emittance (Normalized)	12 mm-mrad
Longitudinal Emittance	0.2 eV-s
Harmonic Number	588
RF Frequency (Injection)	52.8 MHz
RF Frequency (Extraction)	53.1 MHz
RF Voltage	4 MV
Transition Gamma	21.8
Number of Dipoles	216/128
Dipole Lengths	6.1/4.1 m

Dipole Field (150 GeV)	17.2 kG
Dipole Field (8.9 GeV)	1.0 kG
Number of Quadrupoles	128/32/48
Quadrupole Lengths	2.13/2.54/2.95 m
Quadrupole Gradient at 150 GeV	200 kG/m

Other Achievements The control system is mature and made commissioning easier than previous Fermilab machines. The Beam Position Monitor system and the ramped correction dipoles worked well and made possible precise orbit control during the acceleration, a great improvement from the Main Ring. The large acceptance made high efficiency easy to achieve, this is another great improvement from the Main Ring. Extensive magnetic measurements of all the ring magnets made modeling and tune control during acceleration for both cycles of 120 GeV/c and 150 GeV/c much more accurate than the Main Ring.

Challenges, Yet to complete, Yet to attempt Although the Main Injector has met the DOE milestones for project completion and has been declared operational as the injector for Tevatron fixed target physics, many challenges lie ahead.

Run 2 of the Tevatron Collider will require the use of several subsystems that have not been tested yet. These include: 1) Coalescing of multiple proton bunches and their transfer to the Tevatron, 2) injection of pbars, their acceleration, coalescing and transfer to the Tevatron, 3) injection of 150 GeV/c pbars coming back from the Tevatron at the end of stores and their deceleration, debunching and transfer to the Recycler. All of the subsystems for these functions have been specified, designed, and installed as part of the Main Injector project and they are expected to work, but much remains to be commissioned yet.

The 120 GeV/c fixed target program of the Main Injector will have a different set of challenges than Run 2 of the Tevatron Collider. This will require rapid cycle operation with high intensity slow resonant extraction. The highest intensity request is from the NuMI experiment, which needs in excess of 1×10^{18} protons per day. Calculations indicate the losses associated with the slow extraction electrostatic septum would lead to residual radioactivation levels of many R/hour. This, in turn, would make maintenance of those regions of the accelerator more difficult.

The Main Injector Department of Fermilab maintains an extensive web site [3] with many photographs, drawings technical design notes and current news.

References

[1] S. D. Holmes, Proc. of PAC97.

[2] P. S. Martin et al., Proc. of PAC99.

[3] http://www-fmi.fnal.gov/

4.10 Proton Driver Study at Fermilab

W. Chou chou@fnal.gov Fermilab

4.10.1 Introduction

The proton driver is a high intensity rapid cycling proton synchrotron. Its primary function is to deliver intense short proton bunches to the target for muon production. These muons will be captured, phase rotated, cooled, accelerated and finally, injected into either a storage ring for neutrino experiment (a ν-Factory) or a collider for $\mu\mu$ collision. In this sense, the proton driver is *the front end* of a muon facility.

There are two primary requirements of the proton driver:

1. High beam power: $P_{\rm beam} = 4$ MW.
   This requirement is similar to other high intensity proton machines that are presently under design, *e.g.,* the SNS, ESS and JHF.

2. Short bunch length at exit: $\sigma_b =$ 1-2 ns.
   This requirement is *unique* for the proton driver. It brings up a number of interesting and challenging beam physics issues that we will discuss in this paper. The bunch length is related to the longitudinal emittance ϵ_L and momentum spread Δp by:

$$\sigma_b \propto \frac{\epsilon_L}{\Delta p}$$

   In order to get short bunch length, it is essential to have:

   - longitudinal emittance preservation (no intentional blow-up);
   - large momentum acceptance (in both rf and lattice);
   - bunch rotation at the end of the cycle.

It is interesting to compare the proton driver with the former SSC. The SSC required proton beams very bright in the transverse plane. In order to reach the design luminosity, the design value of the transverse emittance ϵ_T was 1 μm, which was several times smaller than that in any existing high energy proton machines. In the longitudinal plane, however, ϵ_L would be blown up by two orders of magnitude in the injector chain in order to avoid instability and intrabeam scattering problem. The proton driver, on the contrary, requires high brightness in the longitudinal plane because of short bunch length, whereas ϵ_T would be diluted by painting during the injection from the linac to the ring in order to reduce the space charge effect.

4.10.2 Choice of the primary parameters

The beam energy is the product of three parameters: proton energy E_p, number of protons per cycle N_p and the repetition rate (rep rate) $f_{\rm rep}$:

$$P_{\rm beam} = f_{\rm rep} \times E_p \times N_p$$

The rep rate is chosen to be 15 Hz. There are two reasons: (1) Muons decay quickly. So the collider needs to get re-fill quickly. The life time of a 2 TeV muon is about 40 ms. The rep rate

should be comparable to the muon decay rate. (2) Fermilab is experienced in operating 15 Hz linac and booster.

Given the beam power and rep rate, the product $E_p \times N_p$ is determined. At this time, we choose 16 GeV and 1×10^{14} protons per pulse (ppp). This is based on the following trade-off considerations: (1) Higher E_p would give lower longitudinal phase space density N_b/ϵ_L, lower space charge tune shift ΔQ at top energy, and would give smaller momentum spread $\frac{\Delta p}{p}$. (2) However, higher E_p would also mean higher cost (*e.g.*, $V_{rf} \propto E_p^2$) and higher radiation power to the environment. The choice of 16 GeV is a reasonable compromise. There are two other important issues related to the choice of E_p:

- The muon yield per proton N_μ/N_p at the beginning of the decay channel is believed to be proportional to E_p. However, the effective muon yield (*i.e.*, N_μ/N_p at the exit of the decay channel) as a function of E_p is yet to be studied.

- For given $P_{\rm beam}$, the total energy deposition on the target is a constant (about 10%) in the range of E_p from 8 GeV to 30 GeV. However, the deposited energy is not distributed uniformly. A crucial parameter in the target design is the maximum density of energy deposition on the target. It needs to be simulated as a function of E_p.

Table 4.6 is a comparison of these parameters in high beam power proton machines.

Table 4.6: High Beam Power Proton Machines

Machine	Protons per Cycle	Repetition Rate (Hz)	Protons per Second	Beam Energy (GeV)	Beam Power (MW)
Existing:					
BNL AGS	8×10^{13}	0.5	4×10^{13}	30	0.2
FNAL Booster	5×10^{12}	15	7.5×10^{13}	8	0.1
RAL ISIS	2.5×10^{13}	50	1.25×10^{15}	0.8	0.16
LANL PSR	2.5×10^{13}	20	5×10^{14}	0.8	0.064
Planned:					
Proton Driver	1×10^{14}	15	1.5×10^{15}	16	4
Japan JHF	2×10^{14}	0.3	0.6×10^{14}	50	0.5
ORNL SNS	1×10^{14}	60	6×10^{15}	1	1
Europe ESS	2.34×10^{14}	50	1.2×10^{16}	1.334	2.5

4.10.3 Staged implementation

The proton driver consists of three accelerators: a 1 GeV linac, a 3 GeV pre-booster and a 16 GeV booster. At present, Fermilab has a 400 MeV linac and a 8 GeV booster. The proton driver would increase the beam intensity by a factor of 20 and beam power a factor of 40.

The proton driver would be built in two phases. In Phase I, a 16 GeV new booster will be built in a new tunnel, using the present 400 MeV linac as its injector. The beam intensity will be increased

by a factor of 5. In Phase II, a 1 GeV linac and a 3 GeV pre-booster will be added, bringing up the beam intensity by another factor of 4. The parameters in these stages are listed in Table 4.7.

Table 4.7: Parameters of Present, Phase I and Phase II

	Present	Phase I	Phase II
Linac (operating at 15 Hz)			
Kinetic energy (MeV)	400	400	1000
Peak current (mA)	40	45	80
Pulse length (μs)	25	90	200
H^- per pulse	6.3×10^{12}	2.5×10^{13}	1×10^{14}
Pre-booster (operating at 15 Hz)			
Extraction kinetic energy (GeV)			3
Protons per bunch			2.5×10^{13}
Number of bunches			4
Total number of protons			1×10^{14}
Norm. transverse emittance (mm-mrad)			200π
Longitudinal emittance (eV-s)			2
RF frequency (MHz)			7.5
Booster (operating at 15 Hz)			
Extraction kinetic energy (GeV)	8	16	16
Protons per bunch	6×10^{10}	3×10^{11}	2.5×10^{13}
Number of bunches	84	84	4
Total number of protons	5×10^{12}	2.5×10^{13}	1×10^{14}
Norm. transverse emittance (mm-mrad)	15π	50π	200π
Longitudinal emittance (eV-s)	0.1	0.1	2
RF frequency (MHz)	53	53	7.5
Extracted bunch length σ_t (ns)	0.2	0.2	1
Target beam power (MW)	0.1	1	4

4.10.4 Longitudinal beam dynamics

1. High longitudinal phase space density – Keep ϵ_L small:
   Table 4.8 is a comparison of the longitudinal brightness N_b/ϵ_L in existing as well as planned proton machines. The proton driver requires 12.5×10^{12} particles per eV-s, which is almost an order of magnitude (or more) higher than most of the existing machines except the PSR and ISIS, which are low energy (800 MeV) machines.

   In order to achieve such a high brightness, one has to preserve ϵ_L, which is in contrast to the "conventional wisdom" of blowing up ϵ_L to keep beam stable. The following measures are taken for ϵ_L preservation:

Table 4.8: Longitudinal Brightness of Proton Machines

Machine	$E_{\max}$ (GeV)	$N_{\rm tot}$ (10^{12})	N_b (10^{12})	ϵ_L (eV-s)	N_b/ϵ_L (10^{12}/eV-s)
Existing:					
CERN SPS	450	46	0.012	0.5	0.024
FNAL MR	150	20	0.03	0.2	0.15
KEK PS	12	3.6	0.4	2	0.2
FNAL Booster	8	4	0.05	0.1	0.5
PETRA II	40	5	0.08	0.12	0.7
DESY III	7.5	1.2	0.11	0.09	1.2
FNAL Main Inj	150	60	0.12	0.1	1.2
CERN PS	14	25	1.25	0.7	1.8
BNL AGS	24	63	8	4	2
LANL PSR	0.797	23	23	1.25	18
RAL ISIS	0.8	25	12.5	0.6	21
Planned:					
Proton Driver	16	100	25	2	12.5
Japan JHF	50	200	12.5	5	2.5
AGS for RHIC	25	0.4	0.4	0.3	1.3
PS for LHC	26	14	0.9	1.0	0.9
SPS for LHC	450	24	0.1	0.5	0.2

- Avoid transition crossing in the lattice design. This would eliminate a major source of emittance dilution.
- Avoid longitudinal microwave instability by keeping the beam always below transition and keeping the resistive impedance small in the machine design. Experience shows that, below transition, the microwave instability is much less likely to occur when the large capacitive space charge impedance is dominant.
- Avoid coupled bunch instability by using low Q rf cavity.
- Apply inductive insert to compensate the potential well distortion due to the space charge.

2. Bunch rotation:
   A bunch rotation is needed at the end of the cycle in order to shorten the bunch to 1-2 ns. There are three possible ways to do this gymnastics:

   - RF amplitude jump
   - RF phase jump
   - γ_t manipulation

The first two methods have been in use for many years. The third one is a new idea first suggested by J. Norem and has been partially demonstrated at an experiment at the AGS. In either of these methods, the bunch length compression ratio is about 3-4.

Our simulation study is focused on the rf amplitude jump. Although Fermilab has years of experience with this operation, the high bunch intensity poses new problems:

(a) During the debunching process, how low can the rf voltage be?
Lower V_{rf} means lower $\frac{\Delta p}{p}$, which in turn gives larger compression ratio. At a high intensity bunch rotation experiment at the AGS, it was found that the minimum V_{rf} is limited by the beamloading effect rather than beam instabilities.

(b) What is the effect of the higher order terms of the momentum compaction factor α_1 and α_2 in bunch rotation?
In a regular bunch rotation simulation, the momentum compaction is assumed to be a constant α_0. However, the proton driver lattice is nearly isochronous ($\alpha_0 \approx 0$). The higher order terms become important. In other words, particles with different $\frac{\Delta p}{p}$ would have different path length ΔL. We are still in the process to understand this effect. Preliminary simulations show that, if α_1 is not properly chosen, the bunch rotation could fail.

(c) What is the effect of the transverse tune shift in bunch rotation?
This is an effect similar to the above but from the transverse plane. Due to short bunch length, the tune shift ΔQ from direct space charge and image charge remains large even at 16 GeV. This ΔQ also gives different path length ΔL, which would affect bunch rotation. In other words, the path length of each particle depends not only on its longitudinal position but also on its transverse amplitude. One difficulty in studying this problem is how to mimic this space charge effect. Is it conceptually correct simply changing the lattice quad strength to estimate ΔL? Is a 6D simulation necessary to study this complicated transverse-longitudinal coupling problem? It will take a while for us to fully understand this problem.

At a recent workshop at the BNL, it was proposed to have a 5-lab "contest." Namely, five machines – BNL-AGS, FNAL-MI, KEK-PS, CERN-PS and Indiana University-IUCF – will carry out two experiments: (1) bunch rotation, and (2) longitudinal microwave instability below transition. The competing items are: i. maximum peak current $I_{\rm peak}$, ii. maximum longitudinal phase space density N_b/ϵ_L, and iii. maximum compression ratio.

4.10.5 Space charge and instabilities

As in all other high intensity machines, the following measures are taken to reduce the Laslett tune shift ΔQ at injection: high injection energy (3 GeV), large transverse emittance (200π mm-mrad, normalized), painting and a 2nd harmonic rf.

In addition to these, it is also planned to use inductive inserts to reduce the potential well distortion from the space charge. Although this idea was proposed many years ago, nobody ever tried it on a real machine until recently. There are two on-going experiments: one at the LANL-PSR using ferrite inserts, another at the KEK-PS using Finemet inserts. The data are being analyzed.

Simulations show that inductive compensation helps during injection, acceleration and bunch rotation. However, because these inserts also introduce additional resistive impedance, one needs to be careful so that it would not cause any instability problem.

The "conventional" type of instabilities, namely, those we have studied for decades, include the impedance budget, resistive wall, slow head-tail, Robinson, coupled bunch, *etc*. These are by no means trivial. However, it is believed that one knows how to deal with them.

More difficult is another type of problems, the "non-conventional" ones, which become important because of the special requirements of the proton driver. They are yet to be understood.

- Longitudinal microwave instability below transition:
  Below transition, the validity of the Keil-Schnell criterion is questionable. There are a number of cases in which this criterion is violated. For example, the beam intensity in the RAL-ISIS is 10 times higher than the calculated threshold.

  In fact, there is no report on observation of microwave instability in any existing proton machines when they operate below transition. Only in some special machine experiments, which introduce large resistive impedance on purpose, self-bunching and perhaps also instability were seen in a coasting beam.

  More theoretical, simulation and experimental studies are needed on this subject.

- Fast head-tail (transverse mode-coupling) in the presence of strong space charge:
  This type of instability is clearly observed in electron machines. Moreover, the calculated threshold and growth rate agree well with the measurements. However, it has never been observed in any proton machine. There are two possible explanations:

  1. If the betatron tune spread ΔQ_β in a proton machine is many times larger than the synchrotron tune Q_s, then the mode lines ($m = 0, \pm 1$, ...) would get smeared and there won't be any coupling.

  2. In low- and medium-energy proton machines, the space charge force is significant. It would shift $m = -1$ mode downward as the beam intensity increases. Meanwhile, the inductive broadband wall impedance would shift this mode upward. Thus, they intend to cancel each other. This makes the coupling between the mode $m = 0$ and $m = -1$ more difficult.

  These claims need support from more careful analytical and numerical study.

- Synchro-betatron resonance due to dispersion in rf section:
  Due to the compact size of the proton driver, some rf cavities may have to be installed in the dispersion region. Would this be a problem? The concern is about the synchro-betatron resonance $kQ_\beta \pm mQ_s = n$. In previous studies, the case $k = 1$ has been fully analyzed. However, the cases of $k = 2, 3, ...$ remain open. It is not clear at this moment if this would be a problem, although experiences tell us that betatron resonances up to the 3rd order could still be important even in a rapid cycling synchrotron.

4.10.6 Particle loss, collimation and shielding

The tolerable particle loss is an important issue in high intensity proton machine design. One main concern is the hands-on maintenance, which requires the residual dose below certain level before one may proceed to do any repair work. Using the preliminary lattice and magnet design of the proton driver, Monte Carlo simulations using the code MARS show that, at an average particle loss rate of 13 W/m, the residual dose after 30 days irradiation and 24 hours cooldown would be about 10 mrem/hr. However, there is significant difference between these simulation results and those measured and calculated at the LANL. Communication between Fermilab and LANL is under way to try to understand the source of this discrepancy.

In the meantime, a collimation system has been incorporated into the lattice. Even with an assumed 10% loss at 3 GeV (which gives 72 kW), simulation shows that this system would confine more than 99% of the losses in a local section, leaving most of the ring (the so-called "quiet" area) below 10 W/m.

The MARS code was also used for radiation shielding calculation. The needed dirt thickness for shielding 1-hour accidental full beam loss is 29 feet. It is close to the result obtained from the simplified scaling formula (the Dugan criterion), which gives 32 feet.

4.10.7 Transient beamloading

This problem is crucial to the intense short bunch operation. The single bunch intensity (2.5×10^{13}) gives a charge $q = 4$ μC. For a 20 kV cavity and a gap capacitance $C = 400$ pF, the single pass beamloading voltage q/C would reach 10 kV, which has to be compensated. However, because the bunch is very short (σ_b = 1-2 ns), how to inject a short current pulse to do the compensation is challenging. This is a high priority item in the proton driver study.

To make the problem even more difficult, the multi-pass beamloading voltage has a rich Fourier spectrum when a low Q cavity is used. An rf feedback system would have to provide several harmonics for sufficient compensation.

4.10.8 Lattice

The constraints and requirements of the lattice design are:

- $B_{max} \leq 1.5$ Tesla
- No transition crossing (which excludes the FODO lattice)
- Large dynamics aperture ($\epsilon_N = 200\pi$ mm-mrad)
- Large momentum acceptance: $\frac{\Delta p}{p} = \pm 2.5\%$
- Dispersion free straight sections for rf, injection and extraction
- Suitable locations for a collimation system

There are two FMC (flexible momentum compaction) lattice candidates, one is triangular, another racetrack. Both give large or imaginary γ_t and use sextupoles to increase the momentum acceptance. The same sextupoles can also be used to control the slope (α_1) of the momentum compaction factor if a compromise in chromaticity control is acceptable.

It turns out to be impractical to design a 16 GeV lattice that meets all the above requirements while keeps the same size (474 m) of the present booster. The new booster would be larger.

4.10.9 Technical systems

RF The required rf voltage is about 1.2 MV. Due to small size of the machine, the cavity needs to have high gradient (> 20 kV/m). A new type of magnetic alloy called the Finemet will be used. Thanks to the US-Japan collaboration, a 7.5 MHz, 20 kV prototype cavity is under construction. After high power bench test, it will be installed in the Main Injector for beam test.

Magnets These are big magnets. The dipole has an aperture of 5" $\times$ 13" and weighs about 10 tons per meter. The peak field is 1.5 Tesla. Simulation shows the field quality is good: $\frac{\Delta B}{B} < 10^{-3}$ within $\pm$4". One important parameter is the ac loss of these magnets. The data from vendors' catalogs are not applicable, because they are measured at 60 Hz and without dc bias. Our measurement shows that, at 15 Hz and with dc bias current, the as loss is about 1/15 of that in the catalog.

Power supply There are two proposals. One is a programmable power supply using fast switching IGBT (10 kHz or above). The reactive power will be stored in a capacitor bank. Another is a resonant power supply. The latter has three variations: (1) single 15 Hz resonance circuit (as in the present booster), (2) dual-resonance circuit (15 Hz plus 12.5% 30 Hz component), and (3) dual-frequency circuit (up-ramp 10 Hz, down-ramp 30 Hz, using IGBT to switch the frequency). Both (2) and (3) can save significant rf power and rf voltage. One concern about (3) is the ripple effect during injection.

An attractive feature of the programmable power supply is its feasibility, namely, to allow different ramp rate, a flat top and a flat bottom. But it is at least 50% more expensive than the resonant one.

Vacuum pipe The present design is a thin Inconel pipe (5" $\times$ 9" $\times$ 50 mils) with water cooling. Compared with stainless steel, Inconel has high strength and high electric resistivity. Its eddy current is 4 times smaller than that in stainless steel. Compared with the ceramic pipe (as used in the ISIS), Inconel reduces the vertical magnet aperture by 1.5-2 inches. The main concerns about an Inconel pipe are:

- Large deflection under vacuum: $\Delta y = -1$", $\Delta x = -0.7$"
- Eddy current heating: ~ 3 kW/m
- Eddy current induced error field: At $\dot{B}_{max}$, 1" reference point, the harmonic components are b_1 = 93 unit, b_3 = 2.6 unit.

Several pieces of prototype pipes are being fabricated. The water cooling tubes are glued to the beam pipe by some special epoxy. The pipes will undergo vacuum and heating tests.

RF chopper A new type of chopper, which is a pulsed beam transformer using Finemet and will be placed in front of the RFQ in the linac, has been designed and built in collaboration with the KEK. The beam test will be performed at the HIMAC in Japan.

4.11 A High-Power Heavy-Ion Driver Accelerator at the ANL

P.N. Ostroumov, K.W. Shepard, J.A. Nolen, R.C. Pardo

Physics Division
Argonne National Lab
Argonne, IL 60439

The Department of Energy in the United States has charged the Nuclear Science Advisory Committee (NSAC) to evaluate options for the construction of an advanced radioactive beam facility of the isotope separator on-line (ISOL) type. The preliminary conclusion of the NSAC Task Force is that the facility should utilize a multi-beam heavy ion driver capable of delivering beams of a wide variety of ions up to uranium at energies $\sim$400 MeV/u with $\geq$100 kW of beam power. The driver will produce large quantities of short-lived exotic isotopes via a variety of nuclear physics reaction mechanisms including fragmentation of heavy beams on light targets, in-flight fission of uranium beams, and spallation of heavy targets with light-ion beams. A post accelerator will efficiently accelerate the radionuclides so produced and deliver high quality beams of these short-lived isotopes for basic research in nuclear physics. A sub-panel of the NSAC Task Force is currently evaluating technical options for the implementation of such an accelerator complex, tentatively designated the Rare Isotope Accelerator (RIA) Facility. At Argonne National Laboratory the Physics Division has been engaged in R&D for such a facility based on using the existing superconducting linac ATLAS as the post accelerator [1]. In this newsletter we summarize the status of the Argonne design of a CW superconducting high-power heavy-ion driver linac.

The driver accelerator must deliver $\sim$100 kW (upgradable up to higher power) uranium and other heavy ion beams at energies $\sim$400 MeV/u to multiple target stations for the production of radionuclides. The same machine must accelerate light ions up to $\sim$500 MeV/u. For the heaviest ions, such as uranium, the beam currents and corresponding powers may be limited by present-day ion source performance. For these beams the beam power achieved can be increased by acceleration of more than one charge-state through various sections of the linac. For light ions the ion source will not be the power-limiting device; powers to several hundred kilowatts would be available, limited by the RF power only. The Argonne proposal is based on a superconducting CW linear accelerator. Superconducting (SC) structures have found wide application for ion beam acceleration at very low velocities [2] and for acceleration of electrons at $\beta = 1$. However, to date such structures have not been used in the velocity range $0.2 < \beta < 1$. Recently several laboratories demonstrated successful operation of new accelerating structures in this range. At ANL spoke cavities operating at 350 MHz have been designed for $\beta_G = 0.29$ and $\beta_G = 0.40$ and prototypes have been successfully tested [3]. At Saclay 700 MHz single-cell "elliptical" cavities with geometrical $\beta_G = 0.65$ operating at 2° K have been operated recently [4], with effective accelerating gradients (E_0T) as high as 25 MV/m.

An advantage of a SC driver linac is the ability to operate CW mode. This allows us to take maximum advantage of existing ion-source technology and performance. Furthermore, the lower peak currents in CW mode reduce space-charge effects. This keeps both longitudinal and transverse beam emittances very small relative to the linac acceptances. The reduction of space charge forces along the whole linac will reduce beam halo.

The proposed "pre-stripper" section of the driver linac consists of two ECR ion sources followed by mass-separators, room temperature (RT) RFQ, RT IH structures up to $\sim$0.8 MeV/u, SC linac structures similar to ATLAS up to the first stripper at $\sim$10 MeV/u. The rest of the linac is based on the new SC accelerating structures. For the heavy ions that are not fully stripped at the first stripper, there will be additional stripping at $\sim$100 MeV/u. The resonator configuration for the

Table 4.9: ANL driver linac resonator configuration (poststripper part)

β_G	Type	f, MHz	E_0T, MV/m	V, MV	Number of Cavities
0.19	2 drift tubes	175.0	5.0	1.56	72
0.38	2 spoke	350.0	5.0	1.56	96
0.5	6 cell	700.0	8.0	4.33	58
0.6	6 cell	700.0	10.0	6.5	118

Table 4.10: Typical beams available from the driver linac

Ion	Mass	Intensity, Particle μA	Energy, MeV/u	Energy, GeV	Power*, kW
Proton	1	600	657	0.66	$\sim$400
Deuteron	2	400	508	1.0	$\sim$400
Helium	3	200	571	1.7	$\sim$300
Argon	40	10	481	19	$\sim$200
Krypton	84	5	461	38	$\sim$200
Xenon	132	3	448	59	$\sim$200
Uranium	238	2	403	96	$>$100

*power possible with present-day ECR ion sources; actual power may be limited by installed RF power.

poststripper linac (downstream of the first stripper) is shown in Table 4.9. Typical beams available from the driver linac are shown in Table 4.10.

The ANL driver linac parameters are mostly set by the uranium beam requirements. Present-day ECR ion sources, such as the AECR-U source at LBNL, produce up to $\sim$1 pμA of uranium beam per charge state at about 30+. As is shown below, it appears feasible to simultaneously accelerate several charge states through the driver linac. Therefore, the $\sim$100 kW uranium beam power requirement is compatible with present-day ion source performance. The driver linac will produce CW beams of any ion species from hydrogen to uranium. The independently phased SC cavities accelerate the light ions to higher energy (per nucleon) due to their higher charge to mass ratios and the broad velocity acceptance of the resonators.

The pre-stripper linac is similar to the existing ATLAS accelerator except the initial acceleration of the ECR beam is done by a RT RFQ and IH structures. The extraction voltage of the ECR source is a subject for more detailed study in order to produce maximum beam intensity at low emittance. The voltage of the ion source should be kept high for all ion species in order to avoid any

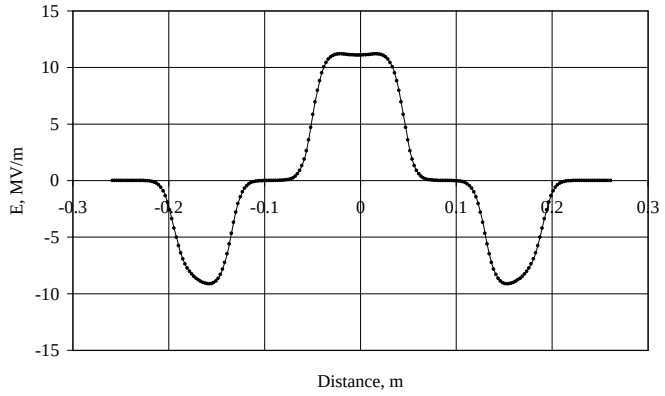

Figure 4.17: Axial electric field distribution in 3-gap spoke cavity, E_0T=5 MV/m, β_G=0.4.

emittance growth between the source and RFQ. Therefore, the RFQ will likely operate on a high voltage platform (about 50 kV) to slow down the lighter ions to the RFQ input velocity.

The CW SC driver linac can produce very high brightness beams (the ratio of average intensity to the square of transverse emittance) due to the available small emittances from the ECR ion source. The CW operation gives low peak beam intensity so that there is no emittance distortion at the front end of the linac including the ion source. The SC linac is ideal for production of very high beam power for both light and heavy ions. For future applications this type of linac could be extended to beam powers well above a megawatt.

For the initial acceleration following the ion source, the choice of a RT RFQ and IH structures is more cost effective than SC structures up to $\sim$1 MeV/u. The operating frequency chosen for the RFQ and IH structures is 87.5 MHz, a regime for which CW RT structures have been demonstrated previously.

As indicated in Table 4.9 the full energy range of the post-stripper linac, from 10 MeV/u to 400 MeV/u, is covered by four types of SC cavities. Typical electric field distribution along the axis of the 3-gap spoke SC cavity with β_G=0.40 operating at 350 MHz is shown in Fig. 4.17.

Synchronous acceleration in a SC ion linac is achieved by independent phasing of the cavities. In the front end of such linac the SC cavities operate at low frequency and at higher energies the operating frequency can be a multiple of the fundamental. At low energies, as at ATLAS, the velocity change in a single SC cavity can be a large percentage so that the beam dynamics calculations must be done numerically. For beam energies above 10 MeV/u the change of velocity inside a cavity is small and the transit time factor (TTF) can be written in the form:

$$T = \frac{\int_{-\frac{L_c}{2}}^{+\frac{L_c}{2}} E_g(z) \cdot \cos\left(\frac{2\pi z}{\beta\lambda}\right) dz}{\int_{-\frac{L_c}{2}}^{+\frac{L_c}{2}} |E_g(z)| dz}, \tag{4.1}$$

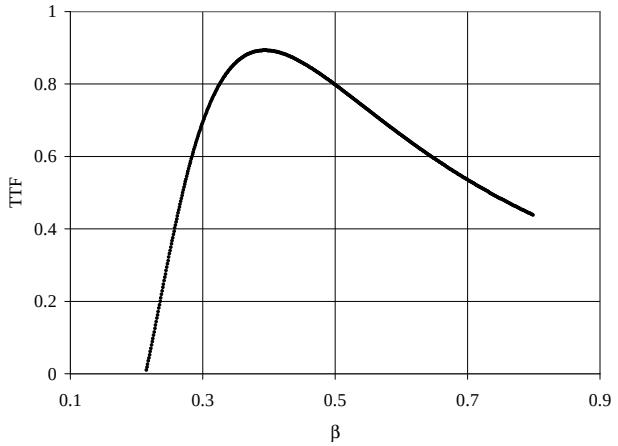

Figure 4.18: Transit time factor for 3-gap spoke cavity as a function of relative beam velocity.

where β is averaged over the cavity length L_c. The cos-like function in TTF is valid for an odd number of cells in the cavity; otherwise this function must be changed to sin-like. The TTF for a 350 MHz 3-gap spoke cavity as a function of the beam velocity is shown in Fig. 4.18. The average effective accelerating gradient along the whole poststripper linac is shown in Fig. 4.19. The averaging is performed over the length that includes the cryostats, the effective length of the cryostats being about twice the cavity length. For transverse focusing we plan to use SC solenoids at low energy (perhaps in prestripper linac) and SC quadrupoles in the post-stripper linac.

The phase setting of the linac is done for charge-state q_0. For uranium beams the charge state is quite high (q_0=75) after stripping at $\sim$10 MeV/u. Multiple charge states after the stripping can be injected and accelerated by the SC linac providing higher intensity of the accelerated beam. In fact, several charge states can be accelerated up to the final energy without significant increase of the longitudinal emittance. Due to the low average current the formation of the longitudinal emittance in RFQ can create the longitudinal emittance as low as 1.0 keV/u $\cdot$ nsec. It will provide the beam acceleration in safe linear region of the separatrix along the whole linac. In fact, it appears that even starting at the RFQ several charge states can be accelerated simultaneously. The details of the beam dynamics in this area have yet to be finalized, but initial calculations have been promising.

Calculations for multiple charge-state acceleration after the first stripping at $\sim$10 MeV/u up to the second stripper at $\sim$100 MeV/u have been carried out to illustrate the feasibility of this concept. Following stripping a neighboring charge state q_0+1 will oscillate with a different synchronous phase

$$\varphi_{s,q_0+1} = a\cos\left[\left(\frac{q_0}{q_0+1}\right)\cdot\cos\varphi_{s,q_0}\right] \tag{4.2}$$

The first stripping at $\sim$10 MeV/ u will produce q_0=75, therefore for $\varphi_{s,q_0} = -30^\circ$ the phase difference for the neighboring charge state is

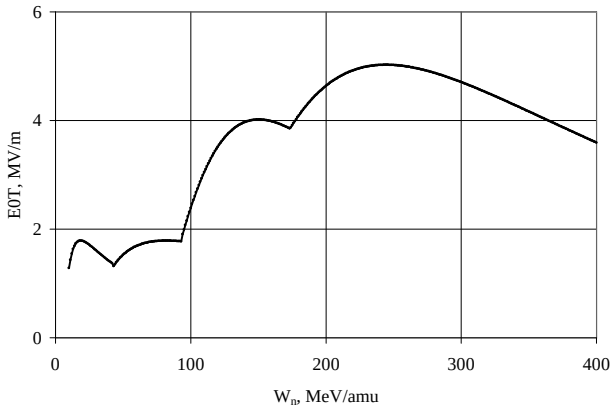

Figure 4.19: Average accelerating gradient as a function of energy along the driver linac

$$\Delta\varphi_s = |\varphi_{s,q_0+1} - \varphi_{s,q_0}| = 1.28^\circ. \tag{4.3}$$

The phase deviation produces average energy oscillation with the amplitude

$$\Delta W_n = m_e c^2 \beta^2 \gamma^3 \frac{\Omega}{\omega} \Delta\varphi_s, \tag{4.4}$$

where m_e is atomic mass unit, $\frac{\Omega}{\omega}$ is the reduced frequency of linear synchrotron oscillations, $\omega = 2\pi f$ is the circular frequency, and γ is the relativistic factor. Calculations show that the acceleration of 5 charge states downstream of the first stripper produces an oscillation of the average kinetic energy of the bunches with respect to the kinetic energy of the equilibrium charge state about 20 times less than the available stability region of the longitudinal phase space. Up to 5-6 charge states can be accelerated to the location of the second stripper. The second stripper at 100 MeV/u will produce q_0=90, and almost all charge states can be accelerated up to the final energy 400 MeV/u. About 80% of beam current initially produced by ECR source at q_0=20 can be accelerated up to the final energy by the SC driver linac. Furthermore, as mentioned above, it also seems possible to accept 2-3 charge states from the ECR ion source for acceleration through the pre-stripper section. The RFQ on the lead injector at CERN has accelerated several charge states of Ta ions from the high charge-state laser ion source [5,6].

Fig. 4.20 shows the average kinetic energy oscillation of multiple charge-state uranium beams in the linac section from 45 MeV/u to 100 MeV/u obtained by Monte Carlo simulations. The amplitude of the energy oscillation is less than 1:1000. The phase space plots of 3 different charge states in the longitudinal phase space at 100 MeV/u is shown in Fig. 4.21.

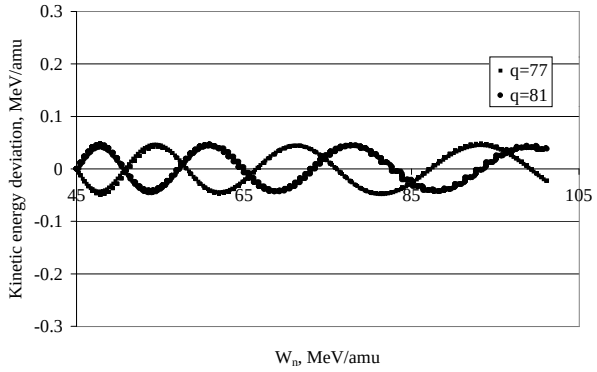

Figure 4.20: Average energy deviation of different charge states with respect to the synchronous particle along the 45-100 MeV/u section of the driver linac

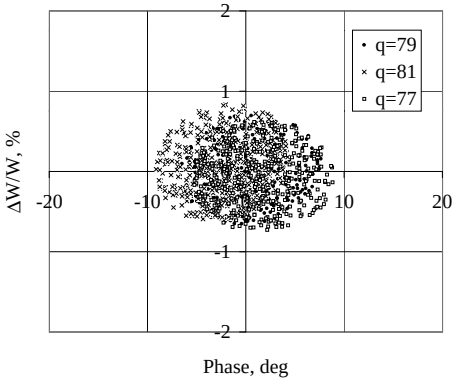

Figure 4.21: Phase space plots of different charge states at 100 MeV/u

References

[1] J. A. Nolen, et al., "An Advanced ISOL Facility Based on ATLAS," Proc. Of the 8^th International Conference on Heavy Ion Accelerator Technology (HIAT98), AIP Conference Proceedings 473, Ed. K. W. Shepard, p. 477, and "Report to Users", ATLAS Facility. ANL-ATLAS-99-1, March 1999.

[2] L. M. Bollinger, "Low-β SC LINACS: Past, Present and Future," LINAC98. http://www.aps.anl.gov/conferences/LINAC98/papers/MO1001.pdf.

[3] K.W. Shepard et al., "Prototype 350 MHz Niobium Spoke-loaded Cavities," PAC99. http://bnlinfo2.bnl.gov/cgi-bin/pac99/displaypaper.cgi?MOP123.

[4] H. Safa. Private Communication. CEA-SACLAY, Gif-Sur-Yvette, 91191, France.

[5] P. Fournier, et al., "CERN PS Laser Ion Source Development," PAC99, see: http://bnlinfo2.bnl.gov/cgi-bin/pac99/displaypaper.cgi?MODR5.

[6] M. Bourgeois, et al., "High Charge-State Ion Beam Production From A Laser Ion Source," Linac96, see: http://www.cern.ch/Linac96/Proceedings/Tuesday/TUP22/Paper.html.

4.12 Nonlinear Beam Dynamics Studies at the PPPL

Ronald C. Davidson rdavidson@pppl.gov Plasma Physics Laboratory
Hong Qin hqin@pppl.gov Princeton University
W. Wei-li Lee wwlee@pppl.gov P.O. Box 451
Sean Strasburg sstrasburg@pppl.gov Princeton, NJ 08543

4.12.1 Introduction

A fundamental understanding of nonlinear space-charge effects on the propagation, acceleration and compression of high-intensity ion beams is essential to the identification of optimal operating regimes in which beam losses and emittance growth are minimized in periodic focusing accelerators and transport systems, with applications ranging from basic scientific research, to spallation neutron sources, to the transmutation of waste, to heavy ion fusion. The theoretical effort on nonlinear beam dynamics at the Princeton Plasma Physics Laboratory (PPPL) focuses on investigations of collective processes in high-intensity ion beams that make use of the nonlinear Vlasov-Maxwell equations and advanced nonlinear perturbative simulation techniques. Recent research has involved collaborations with scientists from the Los Alamos National Laboratory (Robert Macek, Tai-Sen Wang, and Paul Channell), with particular emphasis on the electron-proton instability in the Proton Storage Ring and the Spallation Neutron Source, the Massachusetts Institute of Technology (Chiping Chen), and Lawrence Livermore National Laboratory (Steven Lund). Recent investigations by the Princeton beam dynamics group have included:
(a) development of a kinetic model of the electron-proton (e-p) two-stream instability in high-intensity proton linacs and storage rings based on the nonlinear Vlasov-Maxwell equations[1, 2, 3]; (b) development and application of 2D and 3D multispecies nonlinear perturbative simulation techniques

based on the Vlasov-Maxwell equations for investigation of intense beam stability and transport properties[4, 5]; (c) development of a nonlinear kinetic stability theorem that identifies the class of *stable* distribution function for intense beam propagation over large distances[6, 7]; (d) development and application of a kinetic formalism based on the nonlinear Vlasov-Maxwell equations to describe the equilibrium and stability properties of intense ion beams propagating through a periodic focusing lattice[8, 9, 10, 11]; (e) development of a Hamiltonian averaging technique and canonical transformation for investigating the general class of periodically-focused beam distribution functions that solve the nonlinear Vlasov-Maxwell equations[12, 13, 14]; (f) development and application of simplified macroscopic fluid models[15, 16] of intense beam propagation; and (g) investigations of phase-space structure for test-particle motion and mechanisms for halo formation by collective mode excitations in high-intensity ion beams[17, 18, 19].

We summarize below selected highlights of recent technical advances.

4.12.2 Three-Dimensional Kinetic Stability Theorem for High-Intensity Beam Propagation

Global conservation constraints obtained from the nonlinear Vlasov-Maxwell equations have been used to derive a three-dimensional kinetic stability theorem for an intense nonneutral ion beam (or charge bunch) propagating in the z-direction with average axial velocity $v_b = const.$ and characteristic kinetic energy $(\gamma_b - 1)mc^2$ in the laboratory frame. The particle motion in the beam frame ('primed' coordinates) is assumed to be nonrelativistic, and the beam is assumed to have sufficiently high directed axial velocity that $v_b \gg |v'|$. Space-charge effects and transverse electromagnetic effects are incorporated in the analysis in a fully self-consistent manner. The nonlinear Vlasov-Maxwell equations are Lorentz-transformed to the beam frame, and the applied focusing potential is assumed to have the (time-stationary) form $\psi'_{sf}(\mathbf{x}') = (\gamma_b m/2)[\omega^2_{\beta\perp}(x'^2 + y'^2) + \omega^2_{\beta z} z'^2]$, where $\omega_{\beta\perp}$ and $\omega_{\beta z}$ are constant focusing frequencies. It has been shown that a sufficient condition for linear and nonlinear stability for perturbations with arbitrary polarization about a beam equilibrium distribution $f_{eq}(\mathbf{x}', \mathbf{p}')$ is that f_{eq} be a monotonically decreasing function of the single-particle energy, i.e., $\partial f_{eq}(H')/\partial H' \leq 0$. Here, $H' = \mathbf{p}'^2/2m + \psi'_{sf}(\mathbf{x}') + \phi_{eq}(\mathbf{x}')$, where $\phi_{eq}(\mathbf{x}')$ is the space-charge potential. This theorem represents a very powerful result since it identifies the class of beam distribution functions that can propagate quiescently over large distances. Most notably, it applies to perturbations about beam equilibria $f_{eq}(H')$ with arbitrary wave polarization and initial amplitude; to continuous beams that are radially confined and infinite in axial extent ($\omega_{\beta\perp} \neq 0$, $\omega_{\beta z} = 0$); to charge bunches that are radially and axially confined ($\omega_{\beta\perp} \neq 0$ and $\omega_{\beta z} \neq 0$); and to beams with arbitrary space-charge intensity consistent with the applied focusing potential $\psi'_{sf}(\mathbf{x}')$ providing confinement of the beam particles.

4.12.3 Kinetic Description of Electron-Proton Instability in High-Intensity Proton Linacs and Storage Rings

In a recent analysis, we have made use of the Vlasov-Maxwell equations to develop a fully kinetic description of the electron-ion two-stream instability driven by the directed axial motion of a high-intensity ion beam propagating in the z-direction with average axial momentum $\gamma_b m_b \beta_b c$ through a stationary population of background electrons. The ion beam has characteristic radius r_b and is treated as continuous in the z-direction, and the applied transverse focusing force on the beam ions is modeled by $\mathbf{F}^b_{foc} = -\gamma_b m_b \omega^2_{\beta b} \mathbf{x}_\perp$ in the smooth-focusing approximation. Here, $\omega_{\beta b} = const.$

is the effective betatron frequency associated with the applied focusing field, $\mathbf{x}_\perp$ is the transverse-displacement from the beam axis, $(\gamma_b - 1)m_b c^2$ is the ion kinetic energy, and $V_b = \beta_b c$ is the average axial velocity, where $\gamma_b = (1 - \beta_b^2)^{-1/2}$ is the relativistic mass factor. Furthermore, the ion motion in the beam frame is assumed to be nonrelativistic, and the electron motion in the laboratory frame is assumed to be nonrelativistic. The ion charge and number density are denoted by $+Z_b e$ and n_b, and the electron charge and number density by $-e$ and n_e. For $Z_b n_b > n_e$, the electrons are electrostatically confined in the transverse direction by the space-charge potential ϕ produced by the excess ion charge. The equilibrium and stability analysis retains the effects of finite radial geometry transverse to the beam propagation direction, including the presence of a perfectly conducting cylindrical wall located at radius $r = r_w$. In addition, the analysis assumes perturbations with long axial wavelength, $k_z^2 r_b^2 \ll 1$, and sufficiently high frequency that $|\omega/k_z| \gg v_{Tez}$ and $|\omega/k_z - V_b| \gg v_{Tbz}$, where v_{Tez} and v_{Tbz} are the characteristic axial thermal speeds of the background electrons and beam ions. In this regime, Landau damping (in axial velocity space v_z) by resonant ions and electrons is negligibly small. We introduce the ion plasma frequency-squared defined by $\hat{\omega}_{pb}^2 = 4\pi \hat{n}_b Z_b^2 e^2/\gamma_b m_b$, and the fractional charge neutralization defined by $f = \hat{n}_e/Z_b \hat{n}_b$, where $\hat{n}_b$ and $\hat{n}_e$ are the characteristic ion and electron densities. The equilibrium and stability analysis is carried out for *arbitrary* normalized beam intensity $\hat{\omega}_{pb}^2/\omega_{\beta b}^2$, and *arbitrary* fractional charge neutralization f, consistent with radial confinement of the beam particles. For the moderately high beam intensities envisioned in the proton linacs and storage rings for the Proton Storage Ring and the Spallation Neutron Source, the normalized beam intensity is typically $\hat{\omega}_{pb}^2/\omega_{\beta b}^2 \lesssim 0.1$. For heavy ion fusion applications, however, the transverse beam emittance is very small, and the space-charge-dominated beam intensity is much larger, with $\hat{\omega}_{pb}^2/\omega_{\beta b}^2 \lesssim 2\gamma_b^2$. The stability analysis shows that the instability growth rate $Im\omega$ increases with increasing normalized beam intensity $\hat{\omega}_{pb}^2/\omega_{\beta b}^2$, and increasing fractional charge neutralization f. In addition, the instability is strongest (largest growth rate) for perturbations with azimuthal mode number $\ell = 1$, corresponding to a simple (dipole) transverse displacement of the beam ions and the background electrons. For the case of overlapping *step-function density profiles* for the beam ions and background electrons, corresponding to monoenergetic ions and electrons, a key result is that there is no threshold in beam intensity $\hat{\omega}_{pb}^2/\omega_{\beta b}^2$ or fractional charge neutralization f for the onset of instability. Finally, for the case of *continuously varying density profiles* with parabolic profile shape, a semi-quantitative estimate is made of the (stabilizing) effects of the corresponding spread in (depressed) betatron frequency on stability behavior, including an estimate of the instability threshold for the case of weak density nonuniformity.

4.12.4 Hamiltonian Averaging Techniques Applied to the Nonlinear Vlasov-Maxwell Equations for Intense Beam Propagation Through an Alternating-Gradient Field Configuration

The nonlinear Vlasov-Maxwell equations have been used to describe an intense nonneutral ion beam propagating in the z-direction through a periodic focusing quadrupole or solenoidal field with transverse focusing force, $-[\kappa_x(s)x\hat{\mathbf{e}}_x + \kappa_y(s)y\hat{\mathbf{e}}_y]$, on the beam ions. Here, $s = \beta_b ct$ is the axial coordinate, $(\gamma_b - 1)m_b c^2$ is the directed axial kinetic energy of the beam ions, and the (oscillatory) lattice coefficients satisfy $\kappa_x(s + S) = \kappa_x(s)$ and $\kappa_y(s + S) = \kappa_y(s)$, where $S = const.$ is the periodicity length of the focusing field. The theoretical model employs the Vlasov-Maxwell equations to describe the nonlinear evolution of the distribution function $f_b(x, y, x', y', s)$

and the (normalized) self-field potential $\psi(x, y, s)$ in the transverse laboratory-frame phase space (x, y, x', y'). Here, $\hat{H}(x, y, x', y', s) = (1/2)(x'^2 + y'^2) + (1/2)[\kappa_x(s)x^2 + \kappa_y(s)y^2] + \psi(x, y, s)$ is the (dimensionless) Hamiltonian for particle motion in the applied field plus self-field configurations, where (x, y) and (x', y') are the transverse displacement and velocity components, respectively, and $\psi(x, y, s)$ is the self-field potential. The Hamiltonian is formally assumed to be of order ϵ, a small dimensionless parameter proportional to the characteristic strength of the focusing field as measured by the lattice coefficients $\kappa_x(s)$ and $\kappa_y(s)$. Using a third-order Hamiltonian averaging technique developed by Channell [P. J. Channell, Physics of Plasma **6**, 982 (1999)], a canonical transformation is employed[12, 13, 14] that utilizes an expanded generating function that transforms away the rapidly oscillating terms. This leads to a Hamiltonian, $\mathcal{H}(\tilde{X}, \tilde{Y}, \tilde{X}', \tilde{Y}', s) = (1/2)(\tilde{X}'^2 + \tilde{Y}'^2) + (1/2)\kappa_f(\tilde{X}^2 + \tilde{Y}^2) + \psi(\tilde{X}, \tilde{Y}, s)$, correct to order ϵ^3 in the 'slow' transformed variables $(\tilde{X}, \tilde{Y}, \tilde{X}', \tilde{Y}')$. Here, the transverse focusing coefficient in the transformed variables satisfies $\kappa_f = const.$, and the asymptotic expansion procedure is expected to be valid for sufficiently small phase advance ($\sigma < \pi/3 = 60^\circ$, say). Properties of axisymmetric beam equilibrium distribution functions, $F_b^0(\mathcal{H}^0)$, with $\partial/\partial s = 0 = \partial/\partial\Theta$, are calculated in the transformed variables, and the results are transformed back to the laboratory frame. Corresponding properties of the *periodically-focused* distribution function $f_b(x, y, x', y', s)$ are calculated correct to order ϵ^3 in the laboratory frame, including statistical averages such as the mean-square beam dimensions, $\langle x^2\rangle(s)$ and $\langle y^2\rangle(s)$, the unnormalized transverse beam emittances, $\epsilon_x(s)$ and $\epsilon_y(s)$, the self-field potential, $\psi(x, y, s)$, the number density of beam particles, $n_b(x, y, s)$, and the transverse flow velocity, $\mathbf{V}_b(x, y, s)$. As expected, the beam cross-section in the laboratory frame is a pulsating ellipse for the case of a periodic focusing quadrupole field, or has a pulsating circular cross-section for the case of a periodic focusing solenoidal field.

4.12.5 Application of 2D and 3D Nonlinear δf Simulation Schemes to Investigate High-Intensity Beam Dynamics and Stability Properties

A new particle simulation method based upon the nonlinear perturbative (δf) scheme has been developed to study the detailed transport and stability properties of intense ion beams, and to identify the parameter regimes for optimal beam propagation. The δf simulation scheme was initially developed for tokamak plasma simulations and has been extended for application to intense charged particle beams. In the δf-scheme, the particle distribution function f_b is separated into a background part f_b^0 and a perturbed part δf_b according to $f_b = f_b^0 + \delta f_b$. Here, the dynamics of the background particles associated with the distribution f_b^0 is assumed to be known, and the linear and nonlinear evolution of δf_b is computed numerically from the dynamics of a collection of simulation particles. The δf-scheme completely removes statistical noise associated with the representation of f_b^0 by a finite number of discrete particles, which is the merit of the δf-scheme in comparison with conventional particle-in-cell (PIC) simulations.

The δf simulation scheme has been used to confirm qualitatively that a Kapchinskij-Vladimirskij beam equilibrium propagating through a periodic quadrupole lattice is unstable in certain (high-current) parameter regimes, and to reveal the detailed mode structure in the plane transverse to the beam propagation direction[20]. The δf-scheme is found to be highly effective in describing detailed properties of beam stability and propagation over long distances. It has been shown that the KV beam equilibrium is indeed unstable in certain parameter regimes, particularly at sufficiently high beam current. Furthermore, the mode structure and linear and nonlinear evolution of the in-

stability have been explored over a wide range of system parameters. We have also extended the nonlinear δf simulation scheme to the case of intense beam propagation through a periodic focusing solenoidal field configuration. Applications have demonstrated quiescent, matched-beam propagation of a periodically-focused, high-intensity thermal equilibrium beam over hundreds of lattice periods[5].

Most recently, a 3D multispecies nonlinear perturbative simulation code, called the Beam Equilibrium, Stability and Transport (BEST) code, has been developed[4] to investigate collective processes such as the two-stream instability in high-intensity ion beams. Initial applications of this code to the electron-proton instability show that at sufficiently high beam intensity, the beam is subject to a strong transverse (dipole) instability involving two-stream interaction between the electrons and the proton beam. The instability growth rate is found to increase with increasing beam intensity and increasing electron concentration, and exhibits a sensitive dependence on the radial shape of the density profile of electrons over the beam cross-section. Typical numerical results are summarized in Fig. 4.22. It is expected that the BEST code will provide a useful scientific tool in identifying operating regimes that minimize the effects of the e-p instability in the Proton Storage Ring and the Spallation Neutron Source.

4.12.6 Kinetic Description of Intense Beam Propagation Through a Periodic Focusing Solenoidal Field

A kinetic model has been developed that describes intense nonneutral beam propagation through a periodic-focusing solenoidal field with axial component $B_z(z+S) = B_z(z)$, where $S = const.$ is the axial periodicity length. The analysis is carried out for a thin beam with characteristic beam radius $r_b \ll S$, and directed axial momentum $\gamma_b m \beta_b c$ large compared with the transverse momentum and axial momentum spread of the beam particles. Making use of the nonlinear Vlasov-Maxwell equations for general distribution function $f_b(\mathbf{x}, \mathbf{p}, t)$ and self-consistent electrostatic field consistent with the thin-beam approximation, the kinetic model is used to investigate detailed beam equilibrium properties for a variety of distribution functions. Examples are presented both for the case of a uniform solenoidal focusing field $B_z(z) = B_0 = const.$ and for the case of a periodic solenoidal focusing field $B_z(z+S) = B_z(z)$. The nonlinear Vlasov-Maxwell equations are simplified in the thin-beam approximation, and an alternative Hamiltonian formulation is developed that is particularly well-suited to intense beam propagation in periodic focusing systems. For the case of a uniform focusing field, the nonlinear Vlasov-Maxwell equations are used to investigate a wide variety of azimuthally symmetric intense beam equilibria, ranging from distributions that are *isotropic* in momentum dependence in the frame of the beam, to *anisotropic* distributions in which the momentum spreads are different in the axial and transverse directions. As a general remark, for a uniform focusing field, it is found that there is enormous latitude in the choice of equilibrium distribution function, and the corresponding properties of the beam equilibrium. Introducing the axial coordinate $s = z$, use is made of the nonlinear Vlasov-Maxwell equations to investigate intense beam propagation in a periodic solenoidal field $B_z(s+S) = B_z(s)$, in which case the properties of the beam are modulated as a function of s by the focusing field. The nonlinear Vlasov equation is transformed to a frame of reference rotating at the Larmor frequency, and the description is further simplified by assuming azimuthal symmetry, in which case the canonical angular momentum is an exact single-particle constant of the motion. As an application of this general formalism, the specific example is considered of a periodically-focused, rigid-rotor Vlasov equilibrium with step-

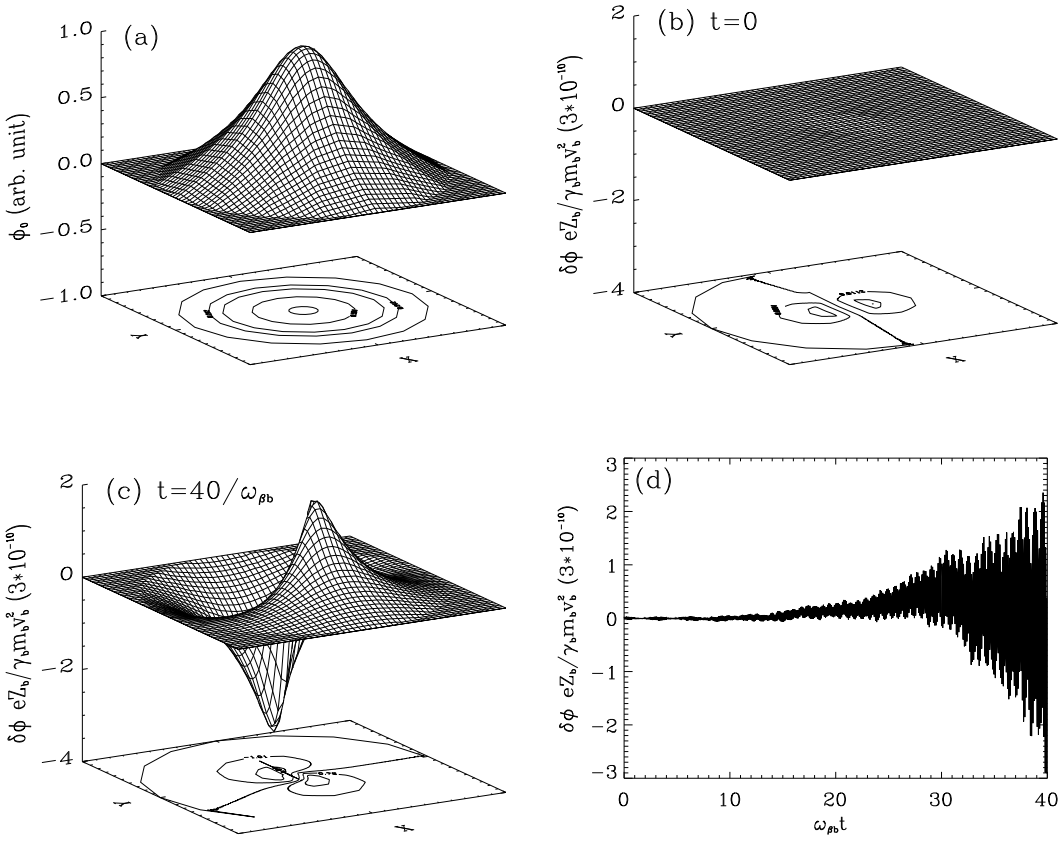

Figure 4.22: Illustrative plots of the e-p instability during the linear growth phase obtained numerically using the Princeton delta-f code for a high-intensity proton beam with $\hat{\omega}_{\beta b}^2/\gamma_b^2\omega_{\beta b}^2 = 0.5$, $\gamma_b = 1.85$, $(T_b/\gamma_b m_b V_b^2)^{1/2} = 1.5 \times 10^{-3}$, $f = \hat{n}_e/\hat{n}_b = 0.1$, $r_b/r_w = 0.22$, $T_e/T_b = 0.87$. Plots show transverse projections of the (a) dc space-charge potential ϕ_0, and perturbed space-charge potential $\delta\phi e Z_b/\gamma_b m_b V_b^2$ at (b) $t = 0$ and (c) $t = 40/\omega_{\beta b}$. In (d), the perturbed potential amplitude is plotted versus $\omega_{\beta b} t$. Note the strong dipole feature of the instability in (c).

function radial density profile and average azimuthal motion of the beam corresponding to a rigid rotation (in the Larmor frame) about the axial of symmetry. A wide range of beam properties are calculated, such as the average flow velocity, transverse temperature profile, and transverse thermal emittance. This example represents an important generalization of the familiar Kapchinskij-Vladimirskij beam distribution to allow for average beam rotation in the Larmor frame. Based on the present analysis, the Vlasov-Maxwell description of intense nonneutral beam propagation through a periodic solenoidal focusing field is found to be remarkably tractable and rich in physics content. The Vlasov-Maxwell formalism developed in this analysis can be extended in a straightforward manner to investigate detailed stability behavior for perturbations about specific choices of beam equilibria.

This research is supported by the U.S. Department of Energy, and in part by the LANSCE Division and Short-Pulse Spallation Source Project of Los Alamos National Laboratory.

References

[1] R.C. Davidson, H. Qin, and W. -S. Wang, Physics Letters **A252**, 213 (1999).

[2] R.C. Davidson, H. Qin, P.H. Stoltz, and T. -S. Wang, Physical Review Special Topics on Accelerators and Beams **2**, 054401 (1999).

[3] "Kinetic Description of the Electron-Proton Instability in High-Intensity Linacs and Storage Rings," R. C. Davidson, W. W. Lee, and T. -S. Wang, Proceedings of the 1999 Particle Accelerator Conference, in press (1999).

[4] "Multispecies Nonlinear Perturbative Particle Simulation of Intense Charged Particle Beams," H. Qin, R. C. Davidson, and W. W. Lee, Proceedings of the 1999 Particle Accelerator Conference, in press (1999).

[5] P.H. Stoltz, R.C. Davidson, and W.W. Lee, Physics of Plasmas **6**, 298 (1999).

[6] R.C. Davidson, Physical Review Letters **81**, 991 (1998).

[7] R.C. Davidson, Physics of Plasmas **5**, 3459 (1998).

[8] R.C. Davidson and C. Chen, Particle Accelerators **59**, 175 (1998).

[9] R.C. Davidson and C. Chen, Nuclear Instruments and Methods in Physics Research **415**, 370 (1998).

[10] R.C. Davidson, W.W. Lee, and P. Stoltz, Physics of Plasmas **5**, 279 (1998).

[11] C. Chen, R. Pakter, and R.C. Davidson, Phys. Rev. Letters **79**, 225 (1997).

[12] "Periodically-Focused Solutions to the Nonlinear Vlasov-Maxwell Equations for Intense Beam Propagation Through an Alternating-Gradient Field," R. C. Davidson, H. Qin, and P. J. Channell, Physical Review Special Topics on Accelerators and Beams **2**, in press (1999).

[13] "Periodically-Focused Intense Beam Solutions to the Nonlinear Vlasov-Maxwell Equations," R. C. Davidson, H. Qin, and P. J. Channell, Physics Letters **A252**, in press (1999).

[14] "Periodically-Focused Solutions to the Nonlinear Vlasov-Maxwell Equations for Intense Beam Propagation Through an Alternating-Gradient Quadrupole Field," H. Qin, R. C. Davidson, and P. J. Channell, Proceedings of the 1999 Particle Accelerator Conference, in press (1999).

[15] S. M. Lund and R. C. Davidson, Physics of Plasmas **5**, 3028 (1998).

[16] R. C. Davidson, P. Stoltz, and C. Chen, Physics of Plasmas **4**, 3710 (1997).

[17] "Production of Halo Particles by Collective Mode Excitations in High Intensity Beams," S. Strasburg and R. C. Davidson, Proceedings of the 1999 Particle Accelerator Conference, in press (1999).

[18] "Production of Halo Particles by Excitation of Collective Modes in High-Intensity Charged Particle Beams," S. Strasburg and R. C. Davidson, submitted for publication (1999).

[19] "Phase Space Structure for Intense Charged Particle Beams in Periodic Focusing Transport Systems," C. Chen, R. Pakter, and R. C. Davidson, Physics of Plasmas, submitted for publication (1999).

[20] W. W. Lee, Q. Qian, and R. C. Davidson, Physics Letters **A230**, 347 (1997).

4.13 Budker INP Activities on High Intensity High Brightness Hadron Beams

D. Pestrikov pestrikov@inp.nsk.su Budker Institute of Nuclear Physics
630090 Novosibirsk
Russian Federation

For more than 30 years the activity in the Budker INP in the field of the generation of the high brightness hadron beams is associated with the studies of the so-called electron cooling [1] and its applications. During about last 10 years the Institute does not operate any storage ring with hadron beams or cooling devices, so that the main part of this activity was shifted to the works, which are performed in collaborations with other laboratories (mostly in Germany, Italy, Sweden and USA). Correspondingly, the main part of the activity is in performing the research and development works for the mentioned collaborations as well as theoretical studies related to these works.

A general description of one of such works – Conceptual Design Study for a high-luminosity electron–nucleon collider, which was performed within the framework of the collaboration with GSI (Darmstadt, Germany), was recently reported in these Newsletters [2].

4.13.1 Electron cooling device for the GSI heavy ion synchrotron

Another work, which was done in the collaboration with GSI was the design, subsequent manufacturing and commissioning of the electron cooling device for the heavy-ion synchrotron SIS at GSI. It was performed within the framework of the intensity upgrade program for the heavy ion synchrotron SIS and electron cooler [3]. The design, manufacturing and initial tests of this cooling device was performed in the Budker INP, while its performance tests as well as commissioning in the heavy ion synchrotron were conducted in GSI (Darmstadt). The main parameters of this cooling device are listed in the following Table:

Electron energy	keV	up to 35
Cathode diameter	mm	25.4
Cathode temperature	K	1200
Electron current	A	up to 2
magnetic field expansion factor		1–8
Gun perveance	μPerv	2.9
Magnetic field strength	T	up to 0.06
Length of cooling section	m	3.36
Magnetic field parallelism	mrad	$\leq$0.04
Collection efficiency	%	≤ 0.01
Vacuum pressure	mbar	$\leq 1 \times 10^{-10}$

The tests of this device showed that nearly all design parameters were achieved, or even exceeded [4].

4.13.2 Intensity limitations in cooled beams

The works in this direction were continued studying the so-called effect of electron heating. This phenomenon was initially discovered in the CELSIUS cooler ring and indicates itself in an increase of the particle losses during their accumulation in ion storage rings with electron cooling [5]. The nature of this phenomenon is not clear yet as well as it is not clear, if the limitation occurs due to some leading instability, or due to contributions from different instabilities of the beam during its cooling. One of the suspects is an instability (or instabilities) of coherent oscillations of the stored beam due to its interaction with the cooling device. The cooling device is one of dissipative elements of the vacuum chamber. Collective interaction of the coasting stored beam with such an element results in instabilities of certain beam oscillation modes. The interaction of the bunched beam with the cooling device may produce instability of coherent oscillations of the ion beam at least in the case, when the average velocities of the ion and electron beams differ by the amount exceeding the velocity spread in the electron beam (see, for example, in Ref.[6]). However, the observed particle losses can also occur due to a more conventional instability.

4.13.3 Fast linear charge density monitor

The new-type linear charge density with a pico-second time resolution was designed and successfully tested at BINP [7]. The device detects deflections of the weak continuous electron beam in the electro-magnetic field of the studied beam (for more detail see in the Letter from P. Logatchov and A. Starostenko in this issue). It can be used for measurements both in linear accelerators and storage ring. Due to high time resolution this device enables study of both stationary parameters of the bunch linear density and the variations of these parameters during, say, coherent oscillations of the bunch.

Initial tests of this device which were conducted at VEPP-3 (BINP) showed that it can be a reliable and very useful tool for studies of the longitudinal beam dynamics.

References

[1] G.I. Budker. Atomnaja Energia, **22**, p. 346, 1967.

[2] D. Pestrikov. ICFA Beam Dynamics Newsletter, **18**, December 1998.

[3] L. Groening, M. Steck et al. Performance test at the SIS Electron Cooling Device. In Proc. of the EPAC 1998.

[4] M. Steck, K. Blasche, et al. Commissioning of the Electron Cooling Device in the Heavy Ion Synchrotron SIS. In Proc. of the EPAC 1998.

[5] Reistad D., Hermansson L., Bergmark T., Johansson O., Simonsson A., Burov A.V., "Measurements of Electron Cooling and "Electron Heating" at CELSIUS, Proc. Workshop on Beam Cooling and Related Topics, Montreux, Switzerland 4-8 Oct.1993, CERN 94-03, 26 April 1994 PS Division, pp.183-187.

[6] N.S. Dikansky, D.V. Pestrikov. Physics of Intense Beams and Storage Rings. AIP PRESS, New York, 1994.

[7] P.V. Logatchov, P.A. Bak, N.S. Dikansky, A.A. Starostenko, et.al. "Nondestructive Single Pass Monitor of Longitudinal Charge Distribution in an Ultrarelativistic Electron Bunch." PAC-99, New York, April 1999.

4.14 High Intensity High Brightness Proton Machine Tables

W. Chou chou@fnal.gov For the ICFA Working Group

During the past three years, the ICFA Working Group on High Intensity High Brightness Hadron Beams has compiled and maintained five machine tables. The parameters were provided by each lab at the ICFA mini-workshops. These tables are available on the web and are printed below. Some parameters may be out-of-date. There are also typos. The readers are encouraged to take a look at these tables and send us updated information and corrections.

4.14.1 Table 1: Performance of proton machines

Machine	$E_{\rm max}$ (GeV)	$N_{\rm tot}$ (10^{12})	$N_{\rm b}$ (10^{12})	$A_{\rm b}$ (eV-s)	$\epsilon^{\rm H}_{rms}$ (μm)	$\epsilon^{\rm V}_{rms}$ (μm)	$N_{\rm b}/A_{\rm b}$ (10^{12}/eV-s)	$N_{\rm b}/\epsilon_{rms}$ ($10^{12}/\mu$m)	$N_{\rm b}/(A_{\rm b}\epsilon^{\rm H}_{rms}\epsilon^{\rm V}_{rms})$ (10^{10}/eV-s/μm^2)
Existing:									
BNL AGS	24	63	8	4	10	10	2	0.8	2
CERN PS	14	25	1.25	0.7	12.5	10	1.8	0.11	1.4
CERN SPS	450	46	0.012	0.5	10	7	0.024	0.0014	0.03
KEK PS	12	3.6	0.4	2	5	15	0.2	0.04	0.27
FNAL Booster	8	4	0.05	0.1	3	3	0.5	0.02	5.6
FNAL MR	150	20	0.03	0.2	2	2	0.15	0.02	3.8
DESY III	7.5	1.2	0.11	0.09	5	3	1.2	0.03	8.1
PETRA II	40	5	0.08	0.12	8.7	6.2	0.7	0.01	1.2
PSR	0.797	23	23	1.25	6.5	13.4	18	2.3	21
ISIS	0.8	25	12.5	0.6	47	47	21	0.27	0.94
Planned:									
AGS for RHIC	25	0.4	0.4	0.3	1.5	1.5	1.3	0.3	59
PS for LHC	26	14	0.9	1.0	2.8	2.8	0.9	0.3	11
SPS for LHC	450	24	0.1	0.5	3.5	3.5	0.2	0.03	1.6
FNAL Main Inj	150	60	0.12	0.1	2	2	1.2	0.06	30
KEK JHP	50	200	12.5	5	55	55	2.5	0.2	0.08
$\mu\mu$ Proton Dr	16	100	25	2	35	35	12.5	0.71	1.0

4.14.2 Table 2: Particle losses

Machine	Cyc. Time [s]	Circ. [m]	Injection Loss [kJ]	Accel. Loss [kJ]	Trans. Loss [kJ]	Extr. Loss [kJ]	Beam Energy at Ext. [kJ]	Prc. Loss [%]
BNL Boos.	0.13	200	0.4 (H-,0.2)	0.3	-	0.3 (F, 1.5)	5.4	19.0
BNL AGS	3.6	800	3.2 (B, 1.5)	2.5	2.60 (7.4)	7.3 (S, 25)	240	6.5
FNAL Boos.	0.07	474	0.05 (H-,0.4)	0.2	0.12 (4.3)	0.16 (F, 8)	5.1	10.4
FNAL MR	2.4	6282	10.0 (B, 8.0)	5.0	4.0 (16.7)	- (F, 150)	600	3.2
FNAL Tev.	60	6282	- (B, 150)	-	-	32 (S, 800)	3200	1.0
CERN PSB	1.2	157	0.1 (S, 0.05)	0.16	0.0	0.1 (F, 1)	4.8	7.5
CERN PS	1.2	628	0.24 (B, 1.0)	0.1	0.0	0.4 (F, 13)	62	1.2
KEK PSB	0.05	38	0.002 (H-, 0.04)	0.004	-	0.008 (F, 0.5)	0.16	8.6
KEK PS	3.0	340	0.03 (B, 0.5)	0.36	0.15 (5.4)	0.96 (S, 12)	5.8	25.9
RAL ISIS	0.02	163	0.006 (H-, 0.07)	0.03	-	0 (F, 0.8)	2.6	1.4
LANL PSR	0.04	90	0.022 (H-, 0.8)	-	-	0.003 (F, 0.8)	2.9	0.9

4.14.3 Table 3: Transverse emittance evolution and measurements

.

.

.

.

.

.

4.14.4 Table 4: RF parameters and beamloading

Machine	Circ. Current (A)	Rep Rate (Hz)	f_{rf} (MHz)	Q_{unload} /Q_{load}	R_{sh} per cavity (kΩ)	Power per cavity (kW)
KEK PS	0.4-0.6	0.25-0.4	6-8	?/20	5	22
KEK Booster	0.7-2	20	2.2-6	?/16	1.2	46
JHF MR	6.6-6.8	0.3	3.4-3.5	1/0.7	0.5	250(400)
JHF Booster	4-7	25(50)	2-3.4	1/0.7	0.5	250(400)
CERN PSB	2	0.8	(C02) 0.6-1.8	40/4	3/0.3	80
			(C04) 1.2-3.6	100/7	10/0.7	30
			(C16) 6-16	80/10	6/0.7	15
CERN PSB (High beam intensity operation)	2	0.8-0.4	(C10) 2.7-9.5	100	6/0.6	80
			(C200) 199.8	2000	70(14)	25
			(C40) 40.05	10^4	300(3)	400
			(C80) 80.1	1.5×10^4	900(6)	400
CERN PS (e^+/e^- accel.)	10mA when operating; 2A when shorted	0.8	114.5	5×10^4	10^4	60
AGS	3.5	0.3	2.7-3.2	50/5	16/1.6	75
AGS Booster	3.5 @ extr.	7.5	1.7-2.8	26/10	2.5	264
RAL ISIS	2.7	50	1.3-3.1	100/25	1.7	300
LANL PSR	10	20	2.795	10/10(?)	0.1	15 kW average @ 2% duty factor
Fermilab Main Injector	0.43	0.4	52.81-53.1	4500/?	360	200

RF Parameters and Beamloading (part 2)

Machine	Voltage per cavity (kV)	No. of cavities	h	No. of filled buckets	ϵ_L (eV-s)	Class
KEK PS	30	4	9	9	0.4	AB push-pull
KEK Booster	15	2	1	1	0.4	AB para-push-pull
JHF MR	16(20)	18(14)	17	16	3	AB
JHF Booster	16(20)	25(20)	4	4	1	AB
CERN PSB	8	1	1/ring	1	1.2	AB
	8	2	1/ring			AB
	6	9	1/ring			AB
CERN PSB (High Beam)	80	8, 10, 12, 14, 16, 18, 20	10+1	8, 16, 4, or 1	1.5 0.8	AB
	30	438-420 @ 14 GeV	8	0 or 420	0.1	
	300	84 @ 26 GeV	1	84	0.4	AB
	300	168 @ 26 GeV	2	(84)		AB
CERN PS (e^+/e^- accel.)	500	240	2	8		B
AGS	40	?	8	8	2-4 per bunch	AB
AGS Booster	45	2	2	2	2	AB1
RAL ISIS	14	12	2	2	0.4	
LANL PSR	12	1	1	1	1	AB
Fermilab Main Injector	240	588	18	504	0.1	C

RF Parameters and BeamLoading (part 3)

Machine	Beam Loading Issues	Compensation Method	Comments
KEK PS	Re-bunching after de-bunching for slow beam extraction	Detuning the cavities	Q value is at injection ϵ_L value at injection
KEK Booster	2 fs oscillation	2 fs dumping feedback	4 tetrodes/cavity adiabatic capture ϵ_L value at extraction
JHF MR	Y=0.3	Not decided	Length=40cm, HG cavity
JHF Booster	Y=0.3	Not decided	HG or ferrite cavity
CERN PSB (C02)	Heavy beam loading during adiabatic capture @ 50 MeV	Wide-band feedback	Main accelerator system
(C04)		Wide-band feedback and short circuit relay	Used for bunch shaping (bunching factor improvement)
(C16)	Very little beam loading (small beam current component @ h=9)	Wide-band feedback and short circuit relay	Used for controlled longitudinal blow-up during acceleration (h=9 operation and phase modulation at 3 fs)
CERN PSB (High beam intensity operation) (C10)	Heavy beam loading during injection and gymnastics and longitudinal transient beam loading	Wide-band feedback and 1 turn delay feedback and short circuit relays	Main acceleration system and beam gymnastics by grouping cavities in groups
(C200)	Beam loading during capture @ 14 GeV	Damping lines and Amplifier reflection	Used for longitudinal controlled blow-up on flat top and for rebunching on h=40 @ 14 GeV
(C40)	Beam loading during capture @ 26 GeV and bunch rotation	Wide-band feedback and short circuit chamber	Used for rebunching @ 26 GeV for LHC and bunch rotation
(C80)	Bunch rotation @ 26 GeV	Wide-band feedback and short circuit chamber	Used for bunch rotation @ 26 GeV. Capable of e^+/e^- acceleration or h=168
CERN PS (e^+/e^- acceleration.)	Moderate beam loading when accelerating e^+/e^-. "shorted" when high beam intensity	2 short circuit arms across nosecones when no voltage is required	Active only during acceleration of e^+/e^-. "Short circuit" arms move first resonance to 175 MHz and reduced Q (10^3)
AGS	1/4 turn delay. Proportional RF feedback		
AGS Booster	No feedback; beam resistance is small enough for Y$<$2		Ferrite Phillips 4M2; ferrite resistance: 6.5 kΩ per cavity
RAL ISIS	cancellation of injection transient	Fast feedforward (low power)	
LANL PSR	Small beam loading effect	AGC(Automatic Gain Control) at low level RF	Cathode follower amplifier
Fermilab Main Injector	Beam induced RF voltage during multi-batch coalescing; n = –1 mode instability due to detuning; phase modulation due to abort gap; 2nd type Robinson instability	RF feedforward Narrow-band damper Direct RF feedback (being planned)	

4.14.5 Table 5: H^- injection parameters

Machine	Type	Method of Injection		Injection Energy (MeV)	N total ($\times 10^{12}$)	Rep Rate (Hz)
		Long	Trans			
Existing Machines						
ISIS	RCS	No painting	v- bumper, falling B-field	70	25.0	50
PSR	Compressor ring	Synchronous fixed freq. 250° phase width	Foil stripping double offset, vertical painting	800	31.0	20
KEK PSB	RCS combined function	No painting	Painting under study	40	2.5	20
FNAL Booster	RCS	DC ∼1 eVs		401.5	5.1	15
AGS Booster	Synchrotron	3 eV-s painted	100π	200	peak 23 inj 45	5-75
IPNS	RCS	Constant E, no chopping	Bumped magnet	50	3	30
DESY III						
Planned						
SNS	Accumulator ring	Flexible, zero dispersion	8 bump magnets, h- and v-bumps	1000	200	60
ESS	Two accumulator rings	Momentum painting, rf steering	h-painting via dispersion, 4 v-bump magnets	1334	234 per ring	50
JHF Booster	RCS FODO	No Painting	H-V painting	200	50	25
AUSTRON	RCS	No painting	H-V painting on falling B	130	40	50
CERN 2GeV PS	Synchrotron	Bunch to bucket	H^- charge exchange	2000	15	0.83
CERN SPL/CPS	Synchrotron	Chopped linac beam	Corner foil w/fixed bump	2000	32	0.83
NSP	Two storage rings	Not decided (maybe no)	Painting	1500	210 per ring	50

H^- Injection Parameters (part 2)

Machine	**Synch freq (kHz)**	Q_h/Q_v	ΔQ_{sc}	**Aperture** (π mm-mrad)	**Trans. H/V emittances (100% unnorm πmm-mrad)**	
					Start Inject.	End Inject.
Existing Machines						
ISIS	∼2-4	3.7/4.2 varying	-0.4	500/400	300/300	100/100
PSR	1-1.5 depending on buncher voltages and ramp	3.2/2.2	-0.2	5 cm radius	3 (97%)	35/49 (95%)
KEK PSB	3.7	2.17/2.30	-0.23	665/109	20/20	293/52
FNAL Booster	454	6.7/6.8	0.4	4.16 cm	H9π V12π 100% beam	
AGS Booster	2.5	4.8/4.9	0.5 at 15TP	90mm H 70mm V	3π round	100π round
IPNS	2-5			5×10 cm		
DESY III						
Planned						
SNS	∼1.0	5.82/4.0-6.0	-0.1	310 acceptance	0.25 (rms), assuming 0.45 (rms, norm) from linac	paint 120 with collimators at 180-210 π mm-mrad in both planes
ESS	0.9	3.7/4.24	-0.05	480/480	2.45	150/150
JHF	6.6	6.8/5.8	-0.35	collimators 312π μ mm.mrad $\frac{\Delta p}{p} = \pm 0.5\%$	2.8/2.8 (90%)	214
AUSTRON	∼0.7	4.45/4.28	-0.4	680	476/476	
CERN 2GeV PS					1/1	5/5
CERN SPL/CPS	∼1	6.25/6.33	-0.2	50	1/1	5/5
NSP		2.75/2.75 (Triplet B) 4.8/4.7 (FODO)	-0.1	530	200	200

H^- Injection Parameters (part 3)

Machine	Long emit (eV-s)	Bunch length (ns)	$\frac{\Delta p}{p}$	Foil thickness & peak temp.	Foil hits	Injection tunrs	Injection loss (%)
Existing							
ISIS	0.6		$\pm 8 \times 10^{-3}$ max	Al_2O_3, 120 × 40 mm^2, 500°K		150	stripper loss 1.5%
PSR	0.6	250	±0.3%	Graphite 450 μg/cm^2	45	2305	0.1% H^0 first turn loss
KEK PSB			1% max	Carbon 60μg/cm^2		80	∼10%
FNAL Booster				carbon 300μg/cm^2		13	5%
AGS Booster	3	600	0.3%	carbon		300	15%
IPNS				Carbon 55-60μg/cm^2		~ 130	10-12% (inj. + capture)
DESY III							
Planned							
SNS	7	600	±1%	Carbon 200-400μg/cm^2, < 2000°K	~ 5	1160	$< 2 \times 10^{-4}$
ESS	5.8	400	5×10^{-3}	Carbon 545μg/cm^2, ~ 2500°K	6-7	1000	0.02%
JHF	1.5			Corner or single edged supported 200μg/cm^2	3-4	250	$\leq 5\%$
AUSTRON	0.5	350	$\pm 2 \times 10^{-3}$			126	$< 1\%$
CERN 2GeV PS				Carbon 450μg/cm^2, 2200°K		110-250	0% (simulated)
SPL/CPS				Carbon, corner 450μg/cm^2, 2200°K		125-150	0%
NSP			±0.36%	Carbon 500μg/cm^2		2780	$< 10^{-4}$

H^- Injection Parameters (part 4)

Machine	Chopping	2nd Harmonic rf ($\delta = V_2/V_1$)	H^0,H^- dump	Electron collection	Simulation codes	Comments
Existing						
ISIS	No	h=2/h=4 system for upgrade, var. δ (0.6 max)	internal	Yes	TRACK1D TRACK2D	50% upgrade planned
PSR	Trav. wave chopper at 750 keV, 70%	None	0.6% H^0 2.6% H^-	None	ACCSIM	
KEK PSB	No	None	None	None		$B_f = 0.33$
FNAL Booster	No	No	Yes	Yes		
AGS Booster	Fast 180^o buncher	$\sim$0.5	carbon block	None		Harmonic=1
IPNS	No	No (proposed)	Yes	No		
DESY III						
Planned						
SNS	MFBT chopper	First harmonic 27kV, second harmonic 13kV	Yes	Yes: e^- stopper at 230πmm-mrad, water cooled	SAMBA ACCSIM SIMPSONS	
ESS	60%	Var. voltage ($V_1 = 27$kV max) $\delta = 0.49$	Yes	Yes	TRACK1D TRACK2D	Figures given for 1997 reference model
JHF	60%	0.6	Yes	Not yet	ACCSIM	
AUSTRON			Yes	Yes	AGILE LONG1D ACCSIM	
CERN 2GeV PS	43%	No	Yes	Yes	TRACK1D wavelet code ACCSIM	h=21
SPL/CPS	43%		Yes	Yes	TRACK1D wavelet code ACCSIM	h=21
NSP	60%	Testing	Yes	Yes		5MW, two rings, possible laser stripping upgrade

5: Workshop and Conference Reports

5.1 The 17th ICFA Workshop on Future Light Sources

Kwang-Je Kim Kwangje@aps.anl.gov APS/ANL
9700 South Cass Avenue, Argonne
IL 60439-4800

5.1.1 Workshop Organization

The 17^{th} ICFA Workshop on Future Light Sources was held at the Advanced Photon Source (APS) Conference Center at Argonne National Laboratory on April 6-9, 1999. About 160 participants, including nearly 120 participants from the U.S., Europe, and Asia, and 40 participants from Argonne, gathered to discuss the prospects of new light sources.

This Workshop is a sequel to the 10th ICFA workshop held at ESRF, Grenoble, France in 1996. It is one of the ongoing activities of the ICFA Beam Dynamics Subpanel on Future Light Sources, chaired by K.-J. Kim. The Subpanel members are A. Ando, M. Cornacchia, M. Eriksson, S. Fang, S. Kamada, S. Krinsky, G. Kulipanov, C.C. Kuo, J.-L. Laclare (Vice Chair), C. Pellegrini, M. Poole, A. Renieri, J. Rossbach, L. Teng, R. Walker, A. Ropert, and A. Wrulich.

The Workshop program was developed by the Program Committee, chaired by J. Galayda. Program Committee members are S. Sinha, B. Tonner, H. Padmore, J.-L. Laclare, M. Cornacchia, A. Lumpkin, J. Rossbach, H. Kitamura, S. Krinsky, and G. Neal.

5.1.2 Invited Talks

J.-L. Laclare, Summary of the 1996 Grenoble Workshop
C. Pellegrini, Status and Development of SASE FELs
D. Nguyen, Overview of Gun and Linac FEL Experimental Results
V. Litvinenko, Storage Ring-Based Light Sources
H. Kitamura, Advanced Insertion Device Practices and Concepts
R. Schoenlein, Femtosecond X-ray Science at the ALS: Recent Results and Future Plans
H. Backe, Research with Coherent X-Rays at the Mainz Microtron MAMI
L. DaSilva, Status and Near Future of Soft X-ray Lasers
G. Materli, The X-ray Scientific Case
E. Johnson, The Demands of Fourth Generation UV Sources and Science

5.1.3 Background

Third-generation synchrotron radiation facilities have been highly successful with respect to both machine operations and scientific output. This success derives from the high brightness of the spontaneous emission from undulators in the straight sections of optimized electron storage rings. The brightness (in units of photons per second per mm^2 per $mrad^2$ per 0.1% relative bandwidth) is about 10^{20} in the wide spectral range from visible to hard x-ray wavelengths. Additional characteristics are tunability of the spectrum and adjustability of the polarization. The photon beams consist of $\sim$100-ps-long bunches. The peak brightness during the bunch duration is about 10^{23}.

Among the several possibilities for next-generation light sources, the most exciting is the one based on self-amplified spontaneous emission (SASE). SASE is intense, coherent radiation generated by amplifying the initial spontaneous emission via an extremely high free-electron laser (FEL) gain process. SASE in the x-ray region is made possible by using a system consisting of a photocathode rf gun, a bunch compressor, and a high-energy linear accelerator (linac). The Linac Coherent Light Source (LCLS) is a proof-of-principle demonstration project for production and use of the SASE at 1 Angstrom using the Stanford Linear Accelerator Center linac [1]. Given the positive experience from the LCLS, a "fourth-generation" user facility employing a superconducting linear accelerator, such as the one proposed by the DESY group [2], may be constructed. The R&D preparing for the conceptual design of the LCLS was recently endorsed by the BESAC Committee on Novel Coherent Light Sources [3]. In view of these developments, a major part of this Workshop was devoted to issues related to SASE-based light sources in the hard x-ray region.

The peak brightness of the x-ray SASE is projected to be about 10^{33}, about ten orders of magnitude larger than that of the third-generation sources. The beam is completely coherent transversely, that is, diffraction limited. The bunch length is about 100 femtoseconds, three orders of magnitude shorter than that of the third-generation sources. Since the bunch repetition rate is about 100 Hz, the average brightness is 10^{22}, 100 times that of the third-generation sources. A higher average brightness could be achieved by employing a superconducting rf accelerator with higher repetition rates.

[1] LCLS Design Study Report, SLAC-R-51 (April 1998).

[2] Conceptual Design of a 500 GeV e+e- Linear Collider With Integrated X-Ray Facility, DESY 1997-048 (May 1997).

[3] Report of Panel on Novel Coherent Light Sources for DOE, Basic Energy Sciences Advisory Committee (February 1999).

5.1.4 Summary of Working Group Activities

Working Group I: Scientific Opportunities for Coherent X-Ray Sources (D. Moncton, Leader)

Working Group I (WG I) was concerned with the scientific opportunities of high brightness and short time resolution that will be possible with the LCLS type of next-generation light source. Further development of advanced experimental techniques (e.g., imaging, multiphoton methods, pump-probe methods, and correlation spectroscopy), now in various stages of development in current third-generation synchrotron radiation facilities, was considered. Also discussed were scientific opportunities in a variety of scientific disciplines such as biology, condensed matter/materials science and technology, chemical science and technology, atomic and plasma physics, and fundamental physics. For a thorough discussion of these diverse topics, WG I participants were divided into several subgroups.

Working Group II: Linac-Based High Gain FELs (I. Ben-Zvi, Leader)

The high-gain FEL process that gives rise to SASE is well understood theoretically, thus establishing a set of criteria on electron beam and undulator qualities. These criteria become progressively more stringent as the wavelength becomes shorter. A proof–of-principle high-gain exper-

iment was carried out by the UCLA/Los Alamos National Laboratory collaboration achieving an FEL gain of 105 for 16 μm radiation. SASE experiments in the visible and ultraviolet wavelengths will be carried out in the near future by the Low-Energy Undulator Test Line (LEUTL) group at the APS, the TESLA Test Facility group at DESY, and the VISA collaboration at Brookhaven National Laboratory. Critical issues for accelerator development and possible new ideas were discussed by WG II.

Working Group III: Ring-Based Sources (M.E. Couprie, Leader)

It is generally accepted at present that the linac-based SASE will be the source of choice for the fourth-generation x-ray facility. However, storage ring-based sources will still be at the forefront of photon beam research for at least another decade. The brightness of a storage ring-based source could be improved by employing a larger circumference, higher current, and damping wigglers. Such a ring could be operated in top-up mode to overcome lifetime reduction. It is possible that a brightness enhancement of two orders of magnitude or higher could be achieved in this way. However, the time resolution will, at best, remain the same as that of current storage ring facilities. These and other issues for the ring-based sources were discussed by WG III.

Working Group IV: Insertion Devices for Future Light Sources (J. Bahrdt, Leader)

Undulators for hard x-ray SASE are long, typically about 100 m. For ease of construction, they will be assembled from 2- to 5-m-long segments. Several optimization issues arise, such as how to introduce focusing, the choice of magnetic design (pure permanent magnet, hybrid, superconducting device,...), etc. The tolerance on the straightness of the electron trajectory is extremely tight, which can only be met with beam-based techniques. WG IV discussed these issues as well as other more general topics of undulator development, such as circularly polarizing devices and the in-vacuum devices for producing hard x-rays from moderate energy rings.

Working Group V: Photon Optics for Future Light Sources (A. Freund, Leader)

Development of optical elements and detectors matched to the unique properties of the fourth-generation sources is crucial. Possible damage of samples due to the intense beam is another critical issue that requires extensive R&D. WG V deliberated these problems.

Working Group VI: New Ideas Employing High-Power Lasers
(W. Leemans, Leader)

High-power lasers have been important in the context of fourth-generation light source development in several ways—as a driver of the low-emittance photocathode gun, as a possible seed laser for the high-gain harmonic generation scheme (an alternative to the SASE), and for providing a scientific model for ultrafast or nonlinear phenomena at optical wavelengths. High-power lasers have also been used to develop compact radiation sources based on either electron-laser interaction or plasma-laser interaction. These issues were discussed in WG VI.

Working Group VII: Photon-and Electron-Beam Characterization (G. Neil, Leader)

Adequate diagnostics for electron beams and x-ray beams are vitally important for developing and operating fourth-generation light sources. The resolution requirements for LCLS are very tight in view of the small emittance and short bunch length. The diagnostics in most cases are sufficiently well developed for application to 1-Angstrom SASE. However, significant R&D will be necessary

in some key areas such as nonintercepting techniques and temporal diagnostics. These issues were investigated by WG VII.

5.2 The 6th ICFA Mini-Workshop on Injection and Extraction

C.R. Prior, G.H. Rees c.r.prior@rl.ac.uk Rutherford Appleton Laboratory, U.K.

The sixth in a series of mini-workshops arranged under the auspices of ICFA took place in England between February 24th and February 26th 1999. The venue was the Cosener's House in Abingdon, near Oxford, which provided a picturesque setting amidst the remains of a 10th century Benedictine abbey beside the River Thames. At various times there were up to 54 participants at the sessions. Thirty of these came from overseas and ensured a strong representation of the major accelerator laboratories throughout the world.

The theme of the meeting was topics in injection and extraction, but was limited, because of the wide range of issues involved, to questions concerning high intensity proton machines. These are topical issues, particularly in view of current interest in spallation neutron sources. Discussion ranged from developments in the US with regard to the SNS, through progress in Europe on the ESS, in Japan at JAERI/KEK and at JHF, to work at other participating laboratories such as CERN, LANL, BNL and ANL. Most of the participants were very closely involved in either problems in the extraction of protons or the creation of proton beams from H^- through charge exchange injection. One session was devoted to the former and two sessions (the whole of the first day) were spent on the issues of H^- injection using stripping foils in both existing and proposed machines. The recent promotion of resonant laser beams, as a potential mechanism for stripping avoiding some of the pitfalls of foils, was also topical and merited a session in its own right.

In the light of experience from previous mini-workshops, parallel sessions were avoided and plenty of time was allowed for discussion. There were no specific working groups, but the issues raised (and the convivial company) meant that many problems of common interest were kept under scrutiny until well into the night.

On the final day, following a tradition at ICFA mini-workshops, a table was prepared showing a comparison, for different machines around the world, of those injection and extraction parameters which had been subject to discussion. This is appended after the following session summary reports.

5.2.1 Session I: H^- Injection

Chair: H. Schönauer (CERN)

Although five of the six presentations in the session included the term H^- Injection in their titles, the topics of the individual talks differed as widely as the machines, reflecting the fact that the machines are individuals too. Hence the review of the past 35 years of H^- injection by G. Rees constituted a good introduction, including a classification scheme and many hints and reminders of the potential pitfalls that one cannot find in accelerator courses. It is worth noting that H^- injection designs span a range from a few up to 16000 injected turns (TRIUMF KAON Accumulator Ring).

D. Fitzgerald reported on the long-awaited direct H^- injection in PSR (proposed in 1987 by R. Macek). The goal was an increase of the average proton current from 70 to 100 μA with a simul-

taneous reduction of loss by a factor of five, to 0.1%. The upgrade embraces a number of modifications such as uncoupling the injection line, a merging magnet, injection bumpers and C-magnets to ease extraction. Commissioning included optimization of the foil thickness and in-house production of the foils aiming at substantial improvement in lifetime. The 'mCADAD' technique can now produce foils up to 130 μg/cm^2 that operate for 40-200 days, about six times longer than commercial products. Performances achieved after only a few weeks of commissioning are an average current of 100 μA accompanied by an average loss of 0.25%. An important observation is that the mysterious PSR e-p instability is still alive and well, now occurring at a 20% lower threshold.

Recent developments in H^- injection in the KEK Booster were reported by I. Sakai. Horizontal painting (4 bumpers) has been in operation since 1998 with the goal of producing flat beams to (i) reach $3.2\,10^{13}$ p/p (at present $2.2\,10^{13}$ p/p) in the 'high-intensity' mode for nuclear physics, and (ii) reduce the vertical emittance in the 'low-intensity' mode for the 12 GeV PS. While the flat beam can indeed be produced at low intensities - even hollow beams have been observed - a still unidentified phenomenon limits the horizontal emittance at higher intensity.

Y. Irie reported on H^- injection studies for JHF. A simulation comparison between corner foils and 'single-edge supported' foils showed superior results for the latter. Different painting strategies ('correlated' bumps for corner foils and 'anti-correlated' K-V like for the single-edge supported foils) may contribute to this result. It was also found that large-amplitude horizontal bumps perturb the vertical beta function. The effect can be reduced by edge correction of the bumpers. The consequences of an upgrade raising the injection energy from 200 to 400 MeV were studied. The loss due to decay of H^0 increases from $8\,10^{-5}$ to $1.3\,10^{-4}$.

H^- injection for the IPNS upgrade, a project proposed in 1995, was presented by Y-L. Cho. It has regained interest as its unconventional approach was recently proposed as an alternative to the mainstream design adopted for the SNS. The challenge of raising the beam power of a rapid cycling synchrotron to 1 MW and beyond is handled by high injection energy (400 MeV, possibly 600 MeV) and acceleration to high extraction energy (2.2 GeV). Even at this injection energy, fairly large emittances ($375\,\pi$ mm mrad) are required to keep the space-charge detuning within the conservative limit of -0.15. Other unconventional features are the use of a lattice quadrupole as a merging magnet, a working point below the integers (6.8, 5.7) and almost full buckets during acceleration. If losses at RF capture of the chopped linac beam and during acceleration can be kept at tolerable levels, the synchrotron approach promises economies when compared with the linac/compressor ring scenario.

W. Chou proposed a simple low-energy chopping technique. The unwanted portion of the linac beam is accelerated by an induction cell and subsequently filtered out by the narrow transmission band of the RFQ. This solves the space problem usually encountered by magnetic deflectors at the expense of the discarded part of the beam being lost on the RFQ structure. For the induction cell, ferrites proved to be unsuitable while 8 kV pulses per core at 2.5 MHz have already been achieved with Finemet material. A prototype is scheduled to be tested later in 1999 at HIMAC.

5.2.2 Session II: H^- Injection

Chair: W. Chou (FNAL)

5.2.2.1 Introduction

There were eight presentations in this session:

1. Y.Y. Lee: H^- injection at AGS booster and SNS
2. D. Olsen: Space charge issues in H^- ring injection
3. C. Prior: H^- injection for the European Spallation Source
4. M. Popovic: H^- injection at FNAL and muon collider
5. H. Schönauer and E. Griesmayer: H^- injection and RF trapping for AUSTRON
6. P. Knaus: H^- injection for PS booster
7. H. Schönauer: H^- injection of SPL 2GeV beam into CPS
8. A. Jason: Electron-foil interaction

The transparencies of these presentations are available in the proceedings. Here topics are selected to summarize the work reported in the talks.

5.2.2.2 Technical topics

Longitudinal painting The design for the European Spallation Source (ESS) injects a mismatched beam with a momentum error. During the 1000-turn injection period, longitudinal phase space painting is carried out by ramping the momentum linearly so that the momentum error of the injected beam increases from 0-2 10^{-3} to 2-4 10^{-3}. At the same time, RF frequency steering controls the stable region of phase space so that both halves of the bucket are filled. At the end of the injection, one obtains a well-matched beam with large momentum spread.

The AGS booster also uses momentum ramping ($\dot{B} = 4$ T/s) for injection painting. An interesting feature is that partial painting (*i.e.*, the chopped beam injected into the right hand half of the bucket instead of filling the whole bucket length) gives a beam with better quality. This is because the synchrotron oscillation gives rise to a hollow beam in the bucket and a more uniform distribution along the longitudinal axis.

In the study of injection for the SNS, it is claimed that the linac beam needs to have a large momentum spread ($\sigma_E = 4$ MeV for an injection energy of 1 GeV) in order to achieve a uniform particle distribution in longitudinal space. It is also necessary that injection errors must be small. The SNS requirements are 0.5° and 0.5% for RF phase and amplitude errors, respectively.

There was insufficient time for detailed discussion of a dual harmonic RF system beyond mention in individual talks. However, this is well known to have the advantages of: (i) reducing the RF trapping losses and, (ii) improving the bunching factor in the transverse plane. For stationary buckets, the bunching factor can be computed as a function of the voltage ratio $\delta = V_2/V_1$. For moving buckets, however, the best choice of δ is often determined by simulations. A common choice seems to be near 0.5.

Transverse painting ISIS uses the falling side of the $B(t)$ curve and large dispersion in the injection region to paint the beam in the horizontal plane. The advantage is that no additional hardware

is needed for painting. Vertical painting is effected simply by a steering magnet, and is possible because the ISIS foil has a large vertical dimension.

In the ESS, transverse painting in the horizontal plane is automatically achieved through the coupling into momentum space via a non-zero dispersion at the injection point. In the vertical plane, closed orbit bump magnets are used to improve the transverse distribution and keep the recirculating protons away from the stripping foil. For machines which inject in dispersion-free regions, the use of bump magnets, in either one or both planes, is the principle method of painting, sweeping the closed orbit while keeping the injection point fixed. For example, in the IPNS Upgrade design, the four orbit bump magnets for H^- injection are each individually powered, and the bumped orbit can be varied during the injection period. This is also the method used by the SNS. It has four bump magnets in each plane, which makes the injection scheme flexible. The KEK PS booster, on the other hand, employs two fast bump magnets to sweep the closed orbit. These magnets are in addition to the regular four orbit bump magnets for H^- injection, which have fixed field strength during the injection.

The simplest "painting" is realized at the CERN PS. It makes use of the fact that the fractional betatron tune Q_x is close to $\frac{1}{4}$. Thus, a 4-turn painting can automatically be done in the horizontal plane without need for special hardware.

One issue that needs further discussion is the "brush" size for the painting. Because the transverse emittance of the circulating beam is much larger than that of the injected linac beam, one might ask if a small emittance for the linac beam is absolutely necessary. The answer is probably yes. One reason is that a large size injected beam would mean a large number of subsequent hits on the foil, which is likely to lead to overheating.

Foil physics The choice of material and thickness is an important issue in foil design. A common material for the foil is carbon, which has a high melting temperature. Diamond-coated graphite has excellent vacuum properties and does not generate dust. The thickness of the foil is a more complicated issue. A thicker foil would increase the stripping efficiency, but it would also create heating and emittance dilution problems. Moreover, a thicker foil also implies more intrinsic injection losses through Coulomb scattering and nuclear reactions. Clearly, a choice has to be made that achieves a careful balance.

Both analytical and numerical methods are available for calculating the temperature rise ΔT and the emittance dilution $\Delta\epsilon$. Results were presented for ΔT and $\Delta\epsilon$ as functions of the foil thickness for the injection of a 2 GeV H^- beam into the CERN PS.

When an H^- beam is injected into an accumulator ring (*e.g.,* the ESS or SNS), a low-field lattice dipole can be used to bend the H^- and proton beams in opposite directions. The foil is placed inside the dipole. The ESS chooses 0.177 T, which causes the $n > 6$ Stark states to strip magnetically, whereas the $n < 4$ states stay as H^0 and are removed. Intermediate states strip after some delay and may be accepted, lost or become halo. The SNS uses a 0.31 T dipole field to strip $n \geq 4$ states. It is found that the position of the foil is important for reducing the fraction of $n = 4$ and 5 states lying outside the acceptance.

H^0 and H^- dumps are needed near the injection region. A further consideration is a device to collect electrons. The ESS design has a water cooled copper and graphite collector adjacent to the foil. The dipole field bends the electrons onto the collector. The PSR has no place for such a collector, but it suffers severely from the so-called e-p instability and would benefit from an electron collector at the injection region. The following method has been suggested for the PSR: to place a

6.5 cm radius circular coil above the stripping foil and drive 7 kA of current into the coil. This coil will generate multipole magnetic fields near the beam centre. The electrons will undergo a downward spiralling motion and eventually hit the magnet surface.

Recent work on the ESS has produced an alternative scheme based on stripping using an undulator and a resonant laser optical system. (See the summary report of laser stripping session by R. Macek.) There are therefore now two lattice designs. One is the baseline model that employs a foil, the second is a racetrack type lattice that can accommodate both foil stripping (in a region of reasonably high dispersion) and laser stripping (where the dispersion is zero).

Simulations Injection simulation is an important part of any design study. The ESS uses TRACK1D and TRACK2D, both written by C. Prior, for longitudinal and transverse simulations including space charge effects. The results are widely accepted. The SNS has spent a considerable effort to improve the code ACCSIM. The bench comparison with TRACK1D gives good agreement. It has also been compared with the beam profile measurement data at the PSR. At a beam intensity of $3\,10^{13}$, if space charge is neglected, the simulation gives a strange double-hump profile in the vertical plane. However, when the space charge is included, the double-hump disappears and the simulation agrees well with the measurement.

The SNS also uses simulation to study halo formation. In this instance, halo is defined as those particles outside an emittance of 180 π mm mrad. Halo formation can be due to parametric resonances. An interesting finding in the SNS simulation is that the halo has a strong dependence on the bare vertical tune. At certain tunes the halo reaches a peak, at others it becomes zero. The reason is unknown.

Several other codes, such as LONG1D (developed at TRIUMF) and ESME (developed at Fermilab), are also used for longitudinal injection simulations. TRACK1D has recently been extended to include treatment of micro-bunch structures with both momentum and phase ramping, and P. Knaus demonstrated its use to study the longitudinal dynamics of a linac beam with a micro-bunch structure. This has been applied to H^- injection into the CERN PS from a future 2 GeV superconducting proton linac (SPL). Separate work on a space charge solver using wavelet techniques, which allow careful study of injected beams with sharp edges, gives comparable results.

Other interesting topics

AUSTRON

The design for AUSTRON uses a 50 Hz resonant power supply. Simulation shows 10.2% particle losses during RF trapping and early acceleration. However, when a dual-frequency (33 Hz + 100 Hz) Praeg circuit replaces the 50 Hz single resonance circuit, it is found that the loss is reduced to 0.48%. The reason is not clear. (Note: Although Praeg's circuit was proposed in 1983, it has not yet been applied to any existing machine.)

Another feature of AUSTRON is the use of two rings: a rapid cycling synchrotron ($h = 1$) at 50 Hz and a storage ring ($h = 4$) at 10 Hz. The latter can accumulate four bunches from the former and thus addresses a range of needs of the user community: from lower intensity at higher repetition rate to higher intensity at lower repetition rate.

Proton Driver and Muon Collider

The proton driver under design at Fermilab is a high intensity rapid cycling synchrotron (10^{14} protons per cycle at 15 Hz). Its main purpose is to serve the high energy physics (HEP) community. As a comparison, most other high intensity proton machines serve the nuclear physics (NP) community. This means that, in contrast to the past when the HEP was mainly interested in high

brightness beams for high luminosity, high intensity beams will be in demand by the HEP as well. In the case of the proton driver, highly intense muon beams will be generated, which can be used either for collision (in a muon collider) or for neutrino sources (in a muon storage ring).

5.2.2.3 Conclusions

The idea of charge exchange H^- injection was raised many years ago and has been applied successfully in many machines for over 30 years. The challenge to the new generation of high intensity machines is to reduce injection losses, which usually form the major part of the total beam loss in a machine. Painting, both longitudinally and transversely, is an effective way of reducing space charge effects and minimizing losses. RF capture of a chopped beam also gives better efficiency than adiabatic capture. To employ a 2nd harmonic RF system to flatten the RF bucket shape is another commonly used scheme. Compensating the capacitive space charge impedance by an inductive insert is an interesting new venture, though not discussed at the workshop owing to time limitations. Foil physics is well understood. Simulations seem to be able to handle all the important effects, including space charge.

The general feeling is that we are in an increasingly strong position regarding the development of H^- injection studies. Although there remain a number of outstanding design questions, the knowledge, experience and tools at our disposal should enable us to address each of the issues properly in the near future.

5.2.3 Session III: Injection with Laser Stripping

Chair: R. Macek (LANL)

Multi-turn injection using stripping foils has well known limitations from elevated foil temperatures and from beam losses associated with the beam-foil interactions. For the next generation of high intensity proton rings, it would be highly advantageous to inject without the use of foils and thereby avoid these particular problems. Laser stripping is an old suggestion for foil-less injection but the "brute force" concept, photo-ionization, is very difficult even with present laser technology. The first step, neutralization of H^- by photo-ionization may be possible but field stripping is easier and would be the obvious choice. The second step, photo-ionization of H^0 (ground state) is the most difficult since it has a non-resonant cross-section of $\sim 10^{-17}$ cm^2 and therefore requires more than 15 MW/cm^2 of laser power at < 90 nm [in H^0 (g.s.) rest frame] for a $\sim$1 m interaction region. As a consequence, some "tricks" are needed for a practical system.

This need for an enabling innovation has stimulated new ideas and concepts for laser-aided injection, two of which were discussed in this session. These were (a) the laser and undulator charge exchange injection concept (LUCE) proposed by Y. Suzuki (JAERI), and (b) a proposal from I. Yamane (KEK) which incorporates the Rabbi oscillation in exciting H^0 (g.s) to H^0 (3p state). Both concepts make use of the following three basic sequential steps:

1. $H^- \rightarrow H^0$ (g.s.) $+ e$ [Field stripping in either a gradient magnet or undulator.]
2. H^0 (g.s.) $+ \gamma \rightarrow H^0$(3p) [Resonant excitation by a laser photon of the right frequency.]
3. H^0 (3p) $\rightarrow H^+ + e$ [Field stripping in either a gradient magnet or undulator.]

Step (1) occurs before the injection region of the ring while steps (2) and (3) occur in the injection section of the ring. The JAERI and KEK proposals differ somewhat at each step. In LUCE, tapered undulator fields of several periods are used both for the neutraliser [step (1)] and the ioniser [step (3)] whereas in the KEK scheme, single-period, high-gradient magnets are suggested for step (1) and step (3). A key difference between the two proposals is the approach to step (2), the laser excitation of H^0 (g.s) to H^0 (3p). In LUCE, there are repeated sections of low-field regions where H^0 (g.s) is effectively excited incoherently to a significant population of H^0 (3p) [$\leq \frac{1}{2}$ of the intensity of H^0 (g.s) entering the region]. Each excitation section is followed by an undulator half period where the H^0 (3p) is field-stripped to H^+. A small ramp to the field in the excitation region sweeps the Stark states across the laser line thereby ensuring overlap of all resonant atomic Stark lines with the narrow laser line width. Repeated excitation and stripping of the H^0 beam (with sufficient laser power) can result in a small fraction of H^0 remaining after the last undulator section. The LUCE concept also makes use of an intricate system of mirrors to reuse the laser light $\sim$80 times in order to reduce the average laser power requirements to manageable levels of 5 kW average (400 kW peak).

In contrast, Yamane's scheme makes use of a π-pulse condition for the Rabbi oscillation to excite a larger fraction of the incident H^0 (g.s) to H^0 (3p) in just one region. A significant portion of H^0 (g.s) ($\sim$20-30%) remains after the excitation region and will need to be disposed of. Required laser power is estimated at several hundred W/cm^2 (average). Careful matching of the laser light with the angle and momentum correlation of the beam is needed to ensure that laser line width overlaps the Doppler broadened atomic line widths of the various momentum components of the beam.

P. Drumm discussed ESS studies for laser injection, which would employ a variation of the LUCE concept. The proposed ESS lattice has been modified to accommodate laser injection as well as to increase the circumference of the ring. The new layout will also keep the foil stripping injection capability as a backup in another section of the ring. Paul presented results of calculations showing a very significant contribution of Stark splitting to emittance growth in the ioniser magnets.

E. Baynham presented results from superconducting magnet design studies for the ionization undulator, which have been carried out at RAL. Conductor configurations have been found which show (in numerical calculations) acceptable field variation along the beam in the low field region in a magnet with acceptable aperture. Given the novelty and the many technical and practical issues associated with laser injection, a proof-of-principle test or experiment is highly desirable before commitments are made to implement such a far reaching proposal. To this end, a collaboration of personnel from JAERI, RAL and LANL are preparing a proposal for a staged, proof-of-principle experiment using the 800 MeV H^- beam from the LANSCE linac. Sufficient space appears to be available in the Line B tunnel where Lines B and C separate. As currently envisioned, the experiment would include a half-period undulator for the neutraliser, an ioniser (made using two C-magnets) with one excitation region and a single-pass laser beam in head-on collisions with the H^0 beam. Also included are magnets to separate the species and detectors to measure various beam profiles and intensities. Several options exist for a suitable and tunable laser with the final choice to be made later after more evaluation. The experiment would produce measurements of the neutralization and ionization rates and the divergence/emittance growth at each step separately (neutralization and ionization steps) and overall. A multi-mirror system is not planned for the proof-of-principle experiment.

In conclusion, the ideas for laser injection discussed in this session show considerable promise

in providing multi-turn injection without the use of stripping foils. Laser injection may well be the enabling technology for rings of 5 MW and higher beam power being considered for the next generation short pulse spallation sources. No intractable obstacles have come up yet, although many challenges have been identified. A key difficulty is with the laser excitation step. The KEK scheme needs a practical system for angular dispersion matching of the beam and laser. The LUCE concept needs a complex multi-mirror system to gain a factor of $\sim$80 in time-averaged photon density. Design studies and prototype activity for the mirror system are planned. Additional study and R&D activities on several other issues are sorely needed. The proof of principle experiment being proposed by the JAERI/RAL/LANL collaboration is an important next step.

5.2.4 Session IV: Fast and Slow Extraction

Chair: M. Chanel (CERN)

5.2.4.1 Introduction

The type of extraction which is used in a given machine depends on the demands of the customers (physicists or the next machine), the characteristics of the machine (the number of extraction channels), the optimization of the machine time and schedule, and of course the performance of the accelerator itself. The different schemes which can be used are generally a mixture of the following types of extraction:

- fast extraction of one or more bunches in less than one turn,
- fast-fast-slow extraction, where the whole beam, or part of it, is extracted in roughly ten to one hundred turns,
- Slow-fast extraction taking some milliseconds
- Slow extraction, which gives spills of some hundred milliseconds to 10 sec.
- Ultra slow extraction, which takes much longer, at least minutes, even some hours.

The following paragraphs review the techniques used to improve the quality of the extracted beam, based on the five talks given in the session:

1. C. Steinbach, K. Cornelis: Slow extraction at high intensity.
2. M. Tomizawa: Slow extraction for JHF.
3. Y. Irie: Fast extraction at KEK.
4. K. Brown: AGS slow and fast extraction.
5. J. Johnstone: FNAL slow and fast extraction.

5.2.4.2 Fast extraction

Fast extraction is realised by a combination of a kicker and a septum or a Lambertson magnet. The phase between the two should be as close as possible to $\pi/2$ mod$[2\pi]$. The kicker magnet, which defines the number of bunches which are extracted, should have very fast rise and fall times, a constant current without ripple during the time the beam is kicked, and no current during the passage of the bunches which should stay in the machine. At the KEK-PS, the pulse provided by the Blumlein network [3] has been improved in terms of rise-time by adding a capacitor to earth at the middle of the PFN line. The residual magnetic field, after the pulse, has been reduced by adding a matching capacitor. One should note that this machine uses the same straight section for slow and fast extraction by moving in (for one physical period) the kicker or the electrostatic septum. At the AGS [4] up to six bunches ($45\,10^{12}$ protons) are extracted bunch by bunch into the same extraction channel in 0.2 sec. For this very high intensity operation, it has been demonstrated that the kicker material can support a large amount of particle loss without damage. Generally, experimenters want high intensity and short bunches, which remain stable during acceleration. There is a need to have VHF and non-adiabatic quad mode pumping. A major problem is mis-firing or jitter in the kicker firing time, which may induce large losses. This is due to beam-induced noise (up to 1000's of volts) causing the thyratron to fire at the wrong time. Reducing the gas pressure in the main discharge tube prevents the conduction occurring at voltages which are too low.

5.2.4.3 Slow extraction

Slow extraction uses, in an elegant and controlled way, the mechanism of betatron amplitude growth when the particle is sitting on a resonance. Half integer and third integer resonance are used. The tune of the beam is set close to the resonance and then the particles are driven onto this resonance. The way the beam is driven onto the resonance gives the extraction time or, conversely, the extraction time needed dictates the way the beam has to be driven onto the resonance. When the tune is close to the resonance two areas are defined: the first where particle motion is stable and the beam remains with no growth in amplitude, though the motion may be somewhat deformed; the second where the amplitude grows. In the latter case, particles in phase space tend to move close to lines called separatrices and their oscillation amplitudes grow exponentially. When the increase of amplitude over two turns (half integer) or three turns (third integer) is sufficient, these particles pass through an electrostatic septum and, finally, magnetic septa which extract them from the machine.

The method of fast-fast slow extraction consists of kicking the beam (or part of it) from the stable area to the unstable area. Particles diffuse to the electrostatic septum in 10-20 turns (half integer) up to 100-200 turns (third integer). This has been used in the SPS (CERN). Beam is extracted every two or three turns.

For fast-slow extraction, the beam is driven onto the resonance by changing the tune of the machine using a "kicker-quad". It is powered by a discharge power supply to give good rise time; then the current is slowly ramped to control the spill shape and finally the current is reduced to stop the extraction as required (for example, only part of the beam may need to be extracted). Spills of some msec may be contemplated in this way. Another way is by the acceleration or deceleration of the beam, when the change of tune is obtained by the chromaticity. The extracted beam is then bunched.

For slow extraction, which is the most common type, the tune is changed to cross the resonance.

(At AGS-BNL [4] and PS-CERN [1] the main current of the combined function magnets is changed; at FERMILAB Main Ring [5] the main quadrupole current is the driving element; while for JHF [2] only two quads will be powered.) The shape of the spill is adjusted by controlling the current in the varying elements. Spills of up to 10 sec are obtained in this way. To ease the control of the spill shape, the beam is de-bunched prior to extraction. A recommended procedure is to increase the momentum spread just before de-bunching [1] (changing the stable phase of the RF by 180° for a short time, then back, and finally de-bunching after almost a synchrotron period).

For ultra-slow extraction, particles are driven onto the resonance through chromaticity by stochastic acceleration (or deceleration). Spills of some minutes to hours can be contemplated (LEAR-CERN). The minimum spill length [2] obtained with good efficiency is of the order of 1 msec (50 msec) if the half (third) integer resonance is used. The percentage of beam which remains in the machine can also be controlled by the strength of the resonance and the tune change rate [1].

The ripple on the spill, generally at the line frequency and associated harmonics, is of major concern for all the machines. If the ripple has stable amplitude and phase over time, it can be reduced by a feed forward system. An adapted quadrupole (no iron), powered by a current representing the different frequencies observed in the spill, can be used. Nevertheless a feedback system can be added using the measured spill to control the current in the quadrupole. An alternative method consists of accelerating the particles arriving in the vicinity of the resonance in such a way that there are always enough particles on the resonance. Empty bucket channelling is often used. High frequency RF cavities [1] are excited in a continuous wave at an harmonic of the revolution frequency corresponding to the position of the resonance. During extraction particles are squeezed in between empty buckets while they enter resonance. This is some kind of Venturi effect (the speed of the water is increased when the tube diameter is reduced). But some high frequency structure will appear on the spill. Another method is to replace these empty buckets using a strong noise power at the same frequency. This is applicable for ultra-slow extraction at low energy.

The spill reproducibility depends on what happens prior to extraction, and especially on the beam stability. To avoid instability, in addition to ensuring correct setting of the chromaticity, the momentum spread of the beam is very often increased before and after transition by longitudinal blow-up [1, 4]. Stability is also of major concern in avoiding losses.

The losses in the machine itself or in the extraction line during extraction have to be minimized. The electrostatic septum [4] should be set to a position where the motion of the particle in the machine is still “linear”. The particles execute large amplitude oscillations, and resonances can easily perturb their motion. The half integer resonance seems less sensitive to octupolar fields than the third integer resonance [2].

5.2.4.4 Conclusions

Accelerator physicists have developed many tools to provide particle physicists with the type of beam and spills they want, from one bunch of ~ 5 ns to spills of some hours. The never-ending search for quality, reproducibility, stability, no losses, no ripple, flat spills etc. makes life constantly exciting.

6: Activity Reports

6.1 Non-destructive Single Pass Monitor of Longitudinal Charge Distribution

P.V. Logatchov logatchov@inp.nsk.su Budker INP, 630090 Novosibirsk
A.A. Starostenko astar@inp.nsk.su Russia

During our studies for electron-positron factories we came across a very interesting and, as we believe, very promising possibility of a non-destructive and very fast monitoring of the linear density in relativistic bunches. Although initially being developed for electron, or positron beams, the monitor can be used for measurements related to hadron beams too. As longitudinal dynamics are a usual concern in obtaining of high brightness beams, we think that general information concerning this new monitor could be interesting for the beam dynamics community.

First experimental tests of a single pass non-destructive monitor of the linear charge density in an intense relativistic bunch have been held at the Budker INP in Novosibirsk. The method is based on the scanning of deflections of a thin, low current and continuous electron beam in the electromagnetic field of an intensive relativistic bunch. The data processing after such measurements results in the instantaneous linear charge distribution of the tested bunch. The probe beam–with particle energies within the range 20-100 kV–was injected in the vacuum chamber of the accelerator in the direction perpendicular to the motion of the tested intensive relativistic bunch. This type of an electron beam probe is suitable for both circular and linear accelerators. The basic advantages of this method are:

- non-destructive method for intensive relativistic bunch
- single pass method
- low distortion of the main vacuum chamber impedance
- picosecond resolution for short bunch
- reasonable processing time

The monitor can be used to measure both static (linear density, bunch length, etc.) longitudinal parameters of the bunch and their dynamical variations.

6.1.1 Basic idea of the method.

The idea of this method is based on the following. A thin probe beam moves with the offset parameter ρ (see in Fig. 6.1) along the X-axis, which is orthogonal to the direction of the relativistic bunch motion (Z axis). The results of scanning are detected on the screen, which is placed parallel to the Y—Z plane at the distance L from Z axis. The center of the relativistic bunch is located at the origin at time $t = 0$ whereas the testing beam has uniform density along X and the diameter $d \ll \rho$. Here, we assume ρ exceeds the typical transverse size of the relativistic bunch. At time

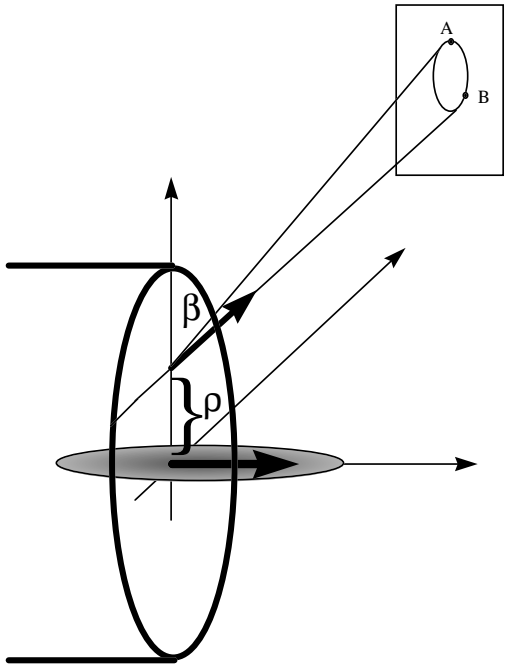

Figure 6.1: The basic scheme of the method.

$t = 0$, every testing beam particle corresponds to a certain x -coordinate. Then x will be used instead of time $x = \beta ct$. For a particle which has a coordinate x at $t = 0$ the total deflecting angle in Y direction due to effect of the electric field of the relativistic bunch reads

$$\theta_y(x) = \frac{2\rho r_e}{\beta} \int\limits_{-\infty}^{+\infty} \frac{n(z)}{\rho^2 + (x + \beta z)^2}\, dz. \tag{6.1}$$

Here, $r_e = e^2/mc^2$ is the classical electron radius, $\beta = v_x/c$ is the normalized probe beam velocity, x is the coordinate of probe beam particle at $t = 0$, $n(z)$ is the relativistic bunch linear density along Z axis. This formula takes into account a relative movement of both beams. The expression for the deflecting angle of the particle in Z direction due to magnetic field can be written as:

$$\theta_z(x) = 2r_e \int\limits_{-\infty}^{+\infty} \frac{(x + \beta z)n(z)}{\rho^2 + (x + \beta z)^2}\, dz. \tag{6.2}$$

As a result, the probe beam traces the closed curve on the screen. Assuming the constant current I of this beam, we derive the simple relationship between the coordinate x and the charge distribution $q(l)$ along the indicated curve on the screen from point A to point B:

$$x = \frac{\beta c}{I} \int\limits_{A}^{B} q(l)\, dl. \tag{6.3}$$

Integrating the charge along the curve from point A up to point B we find the x – coordinate Eq.(6.3) and correspond to it certain angles $\theta_z(x)$ and $\theta_y(x)$ at point B. Since the dependencies $\theta_z(x)$ and $\theta_y(x)$ are determined, it is possible using any of these functions to restore the linear density of the tested bunch $n(z)$:

$$n(z) = \frac{\beta^2}{4\pi^2 r_e} \int\limits_{-\infty}^{+\infty} \theta_y(k) e^{\mathrm{i}kz\beta + |k|\rho}\, dk \tag{6.4}$$

where

$$\theta_y(k) = \int\limits_{-\infty}^{+\infty} \theta_y(x) e^{\mathrm{i}kz}\, dx \tag{6.5}$$

It is necessary to emphasize that dependencies Eq. (6.1), Eq. (6.2) and Eq. (6.4) are valid only for relativistic bunch with $\gamma \gg 1$ and for

$$\theta_y^{max} \ll 1. \tag{6.6}$$

The last condition specifies the requirement that the perturbation of longitudinal motion in the probe beam by the electric field of relativistic bunch is small.

6.1.2 First results, time resolution and future applications.

The experimental setup and result of the first experiments was described in Ref.[1]. An example of the phosphor screen image of the bunch at VEPP-3 storage ring and processed linear charge density distribution are shown in Fig. 6.2. single turn picture of the bunch is obtained by the 10 ns gate

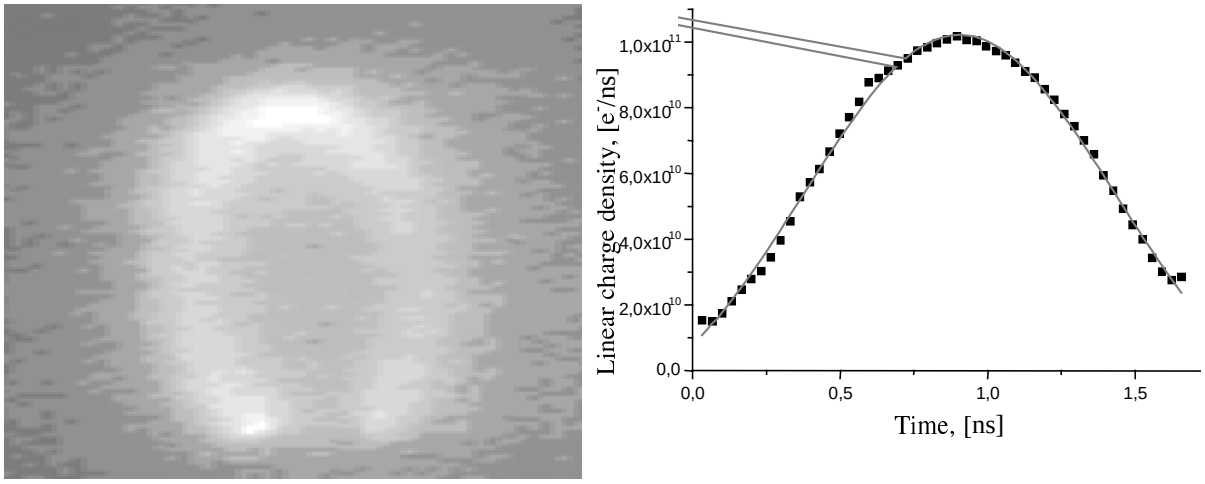

Figure 6.2: The picture of 1.2 GeV electron bunch at VEPP-3 and processed linear charge density distribution (dots). The solid line is a result of the best Gaussian fitting to experimental dots.

pulse on the Micro Channel Plate (MCP). MCP acts as a fast shutter and as an image intensifier. The probe electron beam was deflected from bottom to top (clockwise on the loop at the screen) as then relativistic bunch current increases from zero to maximum and goes back to the original

position as the current decays to zero. The non-deflected position of the probe beam spot (on the bottom of the screen) is shielded by Faraday Cup electrode. It helps to avoid the MCP saturation and to measure 5 μs duration probe beam current.

In order to hold measurements with good time resolution one need either the probe beam current value and the transition function of the incident charge to the image brightness in registration system. This system consist of MCP, phosphor screen, and digital CCD photocamera.

The minimum charge density value on the MCP surface for 1 mA probe beam current and 20 ps relativistic bunch is about 3×10^{-15} C/mm^2. It is possible to reach and measure this value of the surface charge density using linear scanning system (approximately 5 mm/ns - linear velocity of spot on the screen) and decreasing probe beam current down to 1 μA. The pulse shape measurement on deflecting plates with probe beam energy and current measurements give the value of the surface charge density on the MCP input. So, one can measure the transition function of registration system and restore the time from the image. The measurements shows that transition function does not change significantly on the surface of the registration system.

The most important parameter for any diagnostic method is a resolution, in this case - time resolution. At first the method is based on an ultra relativistic configuration of bunch fields, it gives an opportunity for fast picture processing. Real field is different from ideal one and the difference decreases as one over gamma. So the gamma-factor should be higher then 30 (for less then 3% error). The next factor is a finite angle resolution due to a finite probe beam size on the screen. It is possible to reach $0.3mm$ spot size for $1mA$ probe beam current at the beam energy $80keV$. On the other side the modulation of longitudinal probe beam velocity due to x component of bunch electric field increase the time error value. This phenomenon determines the maximum deflection angle and the maximum peak bunch current. Taking into account all this phenomena one can fix the bunch parameters range for better then 10% time resolution of this method:

- bunch peak current: $10A - 250A$,
- bunch length : $20ps - 2ns$,.
- gamma factor > 30.

One can use this kind of device out of these parameters area as a qualitative sensor for accelerator tuning. Experienced operators can say a lot about the longitudinal bunch dynamics just looking at the device display.

Another interesting application of this method is turn by turn pictures of particular bunches. One can place on the screen a few pictures of the same bunch. For example after the 10th, 20^th, 30^th, 40^th turn, or after the first, second, third, fourth turn and so on. It is possible to use for that purpose additional deflecting plates. Also, there is a possibility to detect the transverse position of the bunch center as a function of coordinates along the bunch comparing the pictures of two probe beams: one below and one above the relativistic bunch. The Electron beam probe used as a Beam Position Monitor was already tested Ref.[2]. The device with five pictures on the screen and two probe beams is under construction now. It should be installed on the VEPP-4 collider this year.

References

[1] P.V. Logatchov, P.A. Bak, N.S. Dikansky, A.A. Starostenko, et al. "Nondestructive Single Pass Monitor of Longitudinal Charge Distribution in an Ultrarelativistic Electron Bunch." PAC-99, New York, April 1999.

[2] John A. Pasour and Mai T. Ngo "Nonperturbing Electron Beam Probe to Diagnose Charged-particle Beams", Rev. Sci. Instrum. 63(5), May 1992.

6.2 Beam Dynamics Activities at CERN on CLIC

G. Guignard Gilbert.Guignard@cern.ch CERN

6.2.1 Colliding Main Beam and related topics

The focus of the CLIC study was changed from a 0.5-1 TeV linear collider to a 0.5-5 TeV collider. The increased energy reach became possible after making several important modifications to the RF power generation system. The parameters have been optimized for a center-of-mass energy of 3 TeV and follow the general scaling laws for the rational design of an e+e- linear collider that were derived. In order to limit the overall extension of the complex to less than 35 km it has been assumed that the collider will operate at a loaded accelerating gradient of 150 MV/m, what is only possible with an RF operating frequency of 30 GHz. The revised CLIC parameter list has a luminosity of $10.6 \cdot 10^{34} cm^{-2} s^{-1}$ at 3 TeV, with 150 bunches per pulse and an overall wall plug power of 206 MW.

6.2.1.1 Bunch compressor design

To restrict transverse wakefield effects the number of particles per bunch and the bunch length have been reduced to $4 \cdot 10^9$ and $30 \mu m$ respectively for a multi-bunch spacing of 20 cm. Considering that the damping ring delivers at 2 GeV a bunch which is 3.0 mm long, such a bunch length in the linac implies a total compression by a factor 100. The compressor design is based on a two-stage compression in order to limit the total energy spread (kept below 1.5 %). The first stage is placed at 2 GeV before the injector linac, which decreases the relative momentum-spread via the acceleration from 2 to 9 GeV. Its compression rate of 12 requires a total RF voltage of 103 MV at 3 GHz and a magnetic chicane length of 15 m. The second stage is planned at the very beginning of the main linac, to benefit from both higher gradients and a larger RF frequency. Its compression rate of 8.33 implies a total RF voltage of 1026 MV and a chicane length of 30 m. These parameters look reasonable and the high order effects in the longitudinal plane are small. Multibunch effects may however require some cures.

6.2.1.2 Main linac emittance preservation and trajectory correction

Simulations in the linac show that, under the conditions mentioned above, a normalized vertical emittance at the interaction point of 10^{-8} radm can be obtained. The parameters for the lower energies (0.5 and 1 TeV) are in general less demanding than for 3 TeV. Beam dynamics studies have

focused on single and multibunch emittance preservation in the main linacs for the 3 TeV machine. The overall emittance blow-up is kept to a reasonable value by the use of local bumps which are created at about 10 positions along the linac by displacing laterally a few upstream cavities and which aim at minimizing the emittance measured downstream. In order to obtain a good beam stability with small emittances, the lattice has to be optimized to take into account both static and time-varying mis-alignments. Simulations of the effects of ground-motion, and beam and quadrupole jitter show that after a certain time (typically a few days) the use of bumps and the application of the one-to-one correction scheme are insufficient to keep the emittance small; the whole machine has then to be re-aligned using a beam-based correction with some repositioning of the support girders. Two such corrections have been studied, the ballistic alignment method and the multi-step lining-up. Both assume that the linac is divided in bins which are corrected one after the other. In the first method, the quadrupoles are switched-off except for the first one, and the beam centered in the monitor at the end of the bin by a steering coil in the first quadrupole; the positions of the other trajectory monitors are then redefined such as to be centered on the beam; a one-to-one or few-to-few correction brings then the quadrupoles (all switched on again) near the line defined by the beam. The second method relies on small changes of the quadrupole strengths in the bin and on measurements of trajectory differences as in the dispersion-free correction; the off-sets of the quadrupoles (never switched off) relative to the injection line (defined by a beam that would go straight) are deduced from these measurements and a least square fit of the beam position measurements allows a good estimate of the injection parameters; the beam is then steered toward a line close to the average center of the linac and all the monitors, automatically followed by the girders on which they are installed and supporting the cavities, are displaced toward this line (by nullifying their measurements. Effects on the correction of imperfections such as beam and quadrupole jitters, magnet tilts, earth field and field errors are being investigated.

6.2.1.3 Theory of single bunch stability

A new analytical treatment of the dynamics of a single bunch in the presence of wakefields and quadrupole misalignments in the linac has been developed. It complements the information provided by simulation programs and offers a better understanding of how the key parameters affect the stability of the main beam. The analysis, based on a perturbation method with partial expansions worked out for this theory, leads to closed expressions for the transverse off-sets inside the bunch, the tune shifts with momentum and the emittance growth. Results exhibit the expected near resonance dynamics due to the wake-fields and reproduce well the oscillations inside the bunch associated with the de-coherence of the motion linked to the spread in the betatron oscillation frequency.

6.2.1.4 Multi-bunch and damped structures

To obtain stable beams with multiple bunches requires a careful design of the accelerating structure to achieve a strong damping of the long-range transverse wakefields. Design studies have focused on the new Tapered Damped Structure (TDS). Each cell of the TDS is damped by its own set of radial waveguides resulting in a Q of 16 for the lowest dipole mode and the structure has a detuning spread of 5.4 %. Analytical solutions for the electric field profile in such a structure with variations of the group velocity, the shunt impedance per unit length and the quality factor have been

worked out in the presence (or absence) of beam loading for a design-given average accelerating gradient. The results offer a useful complement to the common relations widely used for constant impedance, constant group velocity structures. A new ”wave number” method of calculating the wake has been developed to improve the understanding of the interaction of a beam with a damped periodic structure. The method which is based on the direct computation or measurement of the propagation characteristics of the higher order modes will provide a second independent estimation of the TDS wakefield. Particle tracking is carried out in order to make sure that the corresponding field attenuation is sufficient.

6.2.2 Power Generating Drive Beam and related topics

The proposed multi-drive-beam-generation scheme has been further studied which uses a conventional normal-conducting fully-loaded 937 MHz linac to produce the initial bunch trains. An 8 A, 91 ms beam with an energy of about 1.2 GeV is required and can be generated with an efficiency of about 97 %. Two alternating ways of generating this train of bunches are being presently considered. The first creates the bunches directly using a photo-injector, while the second uses a conventional injector consisting of a thermoionic gun and a sub-harmonic buncher. The 937 MHz linac is powered by conventional long pulse klystrons. After acceleration, the beam passes through a complex composed of a delay-line combiner and two combiner rings, where groups of leading bunches are delayed to fill in the gaps between trailing bunches. The net effect is to convert the long beam pulse to a periodic sequence of drive beam pulses with gaps in between. Each pulse has 32 times the initial current, while the bunch spacing is 32 times smaller. This sequence of pulses is distributed from the end of the linac against the main beam direction down a common transport line. Pulsed kicker magnets deflect each pulse at the appropriate time into a turn around. After the turn-around each drive beam pulse is decelerated in a 700 m long sequence of low-impedance decelerating structures, and the resulting output power is transferred to the main linac where it is used to accelerate the high-energy beam. At the end of each 700 m long section the drive beam pulse is dumped and a new one takes over the job of accelerating the main beam. The complex can be upgraded or downgraded to other energies by simply changing the initial pulse length.

6.2.2.1 Beam stability in the accelerator

In the drive beam accelerator beam stability is very important. Particular attention has been given to the focusing required, the amount of cavity damping and de-tuning needed, injection and quadrupole jitter effects, alignment tolerances, and steering.

6.2.2.2 Isochronous lattice in the combiner ring

Preliminary layouts of isochronous lattices for the delay-line and the combiner-rings have been proposed. Two possibilities have been studied to some details. The first one is based on a FODO lattice with missing dipoles in the arcs (similar to the arcs of the re-circulating linac of Jefferson’s laboratory), with additional chicanes for path length adjustment and two long straight sections for injection and ejection. The fixed length of the whole ring circumference, imposed by the gaps between drive-beam pulses, makes the matching and tuning of this lattice difficult though probably possible. The chromaticity correction with sextupoles has been considered and the non-linear variations of

the isochronicity for off-momentum particles analyzed. The second solution offers the advantage of being more compact (3 dipoles per 90° arc instead of 4). It is based on isochronous achromats made of three equally-long dipoles separated by two quadrupole doublets, which control the dispersion such as the overall integral of D/ρ in the dipoles be zero. Each such module bends the beam by 90° and is related to the next by a quadrupole triplet that controls the betatron functions. The same triplets offer the facility to easily match the modules to the straight sections and the chicanes. Preliminary analysis indicates that chromaticity correction is not more difficult than in the other solution but further investigations are necessary for a valuable evaluation of the two retained lattices.

6.2.2.3 Turn-arounds, chicanes and bunch-compressors

The same 3-bend, isochronous achromats considered for the combiner rings can be used in the turn-arounds mentioned in the general description. One module bending on the right say by 90° and three others each bending on the left by 90°, with triplets in between, obviously form a turn-around loop. The chicanes for the path length adjustment are planned to consist of three successive dipoles with a finite deviation such as to make the system more sensitive to fine adjustments. The bunch compressors require special characteristics due to the unusual energy correlation in the drive-beam bunches (head of the bunch with higher energy than the tail). Different layouts have been studied. The present trend favors again the use of an initially-isochronous, achromatic 3-bend modules, de-tuned in such a way that the R56 coefficient becomes different from zero in order to break the isochronicity. This offers the considerable advantage to make both the compression as well as a the stretching of the bunches possible by tuning, the latter being probably needed in some places where the coherent synchrotron radiation effects are a concern.

6.2.2.4 Drive beam stability in the decelerator

For the drive beam decelerator, the studies have focused on the control of the beam size and eventual beam losses for cavities without rotational symmetry, for non-linearly varying wakefields with transverse displacement, for strong energy variations along the train, and for a large bunch energy spread. Effects of drive-beam de-phasing susceptible to generate the RF power ramp needed for beam-loading compensation were investigated. Development studies continue on the 30 GHz power generating transfer structures. The work first concentrated on a four-channel structure with inner diameters of 20 and 24 mm and R'/Q values of 100 and 62 Ohm/m respectively. Six-channel and eight-channel structures with larger apertures were also investigated and the corresponding drive-beam stability checked numerically. The effect of field non-uniformity clearly decreases for the same damping of the dipole-mode, when the number of channels increases. Hence, in the case of a six-waveguides transfer structure, simulations show that the Q-value of the dipole mode could be slightly relaxed with respect to the four-channel configuration and that the natural layout where three accelerating structures are fed by one transfer structure (which means longer modules, each with six main linac cavities) is acceptable.

6.2.3 Present and Future Test Facilities.

The present CLIC test facility (CTF2) is made of two parallel beam lines, to reproduce at low energy (40-50 MeV) the conditions for nominal-power transmission from the transfer structures to the accelerating structures at 30 GHz. A drive beam of 755 nC in 48 bunches has been generated and about 375 nC transmitted in the decelerating part. The probe beam made of a 1nC bunch is used to check the so provided acceleration. The design of a future test facility (CTF3) is studied in view of demonstrating (at low energy also) the feasibility of the new drive beam generation system briefly described above and based on a fully loaded linac and combiner rings.

6.2.3.1 Beam dynamics investigations in CTF2

Beam-modeling has been pursued for the existing CTF2 configuration. It was recently aiming at a better knowledge of the influence on the beam transport of the RF forces and the wakefields (longitudinal and transverse) of the high-charge 3GHz-structures (HCS) of the injection line. Multiparticle tracking was therefore carried on with different codes including these effects as well as the space charge forces for the nominal charge per bunch, 48 bunches per train and a setting of the focusing-triplets approaching the nominal. Results indicate that the space-charge effects dominate at low energy, but that wakefield and space-charge forces are comparable in the HCS. Beam transmission through the 3 GHz transport line and then through the 30 GHz modules equipped with transfer structures for power-generation tests is being studied for comparison with the observation. Other investigations concerned the analysis of the emittance measurements done during the bunch compression in CTF2. They were done with different charges and energy correlations versus the bending angle in the bends of the compressor. To explain the large emittance increase which reaches its maximum when the compression is maximum, only the coherent synchrotron radiation(CSR) and to a lesser extend the longitudinal space charge forces can be invoked. Recent simulations of CSR effects which include transients and some shielding effect (parallel plates) indicate that CSR is the most likely candidate for the emittance growth observed.

6.2.3.2 Isochronicity tests in the EPA ring.

The CTF3 combiner ring has to be isochronous in order to preserve the length of the very short bunches (3 to 5 ps) required for testing the power generation scheme of CLIC (see above). The existing EPA (electron-positron accumulator) ring of the LEP injection system was used to demonstrate the feasibility of keeping the rms length of such micro-bunches well below 10 ps for several turns. To achieve this, the orbit length must be constant at all momenta present in the bunch and the control of the orbit length dependence on the momentum deviation can be done by adjusting the strength of multipole magnets. Expressions were derived for the change of the first, second and third order length derivatives of the closed orbit with respect to $\Delta p/p$. They are only functions of the strength increment and of the local dispersion amplitude in the quadrupoles, sextupoles and octupoles, respectively (note that similar expressions can also be applied in transfer lines). In EPA, the use of these expressions to set the existing quadrupoles and sextupoles made it possible to keep the orbit length variation below 20 mm in the momentum range of ± 0.5 %. Simulations show that by installing an octupole the variation might be reduced to 1 mm approximately. During the experiment in EPA with the isochronous optics, the micro-bunch structure was observed with a streak camera. No significant increase of the bunch length could be observed after ~ 40 turns.

6.2.3.3 Longitudinal beam dynamics in CTF3

In CTF3, one of the main challenges is the combination in an isochronous ring of short (1.5 mm rms), high charge (2.3 nC) electron bunches, using an injection scheme based on RF deflectors. After extraction from the combiner ring, bunches must be compressed in length to about 500 mm, rms. A first evaluation of the longitudinal dynamics of the bunches along the whole complex (beginning after the bunching system, at an energy of 10 MeV and ending at the ring extraction at 180 MeV about), has been made using a semi-analytical approach with macro-particles. The correlation in longitudinal phase-space needed for the final compression is obtained through a combination of off-crest acceleration and short-range wake-fields in the injector linac. Bunches then make one to five turns in the ring before being extracted. The distortions introduced in the phase space by coherent synchrotron radiation (CSR) emission and by the residual momentum compaction have been included in the model. Results show that CSR is indeed a limiting factor for the final bunch length, but should not prevent from reaching the nominal requirements. The performance of the system can be further enhanced by stretching the bunches to a length of 2.5 mm rms before injection into the ring, taking an advantage of the reduction of CSR emission due to the beam pipe shielding effect. Detailed simulations of the CSR process, transients included, is still needed in order to confirm the first results.

Further documentation and information about the studies summarized above are available in the form of CLIC notes, which can be consulted on the Web at the following site:

http://www.cern.ch/CERN/Divisions/PS/CLIC/Publications/CLICNotes.html

6.3 Inverse Compton Scattering and Its Application

T.Hirose hirosecomp.metro-u.ac.jp Department of Physics
Tokyo Metropolitan University
1-1 Minamiohsawa Hachioji
Tokyo 192-0397, Japan

6.3.1 Introduction

Compton scattering, scattering of a photon with an electron at rest, was discovered in 1923 by A. H. Compton and formulations on the basis of relativistic quantum dynamics were given by V.O. Klein and Y. Nishina[1] in 1928. Since then, Compton scattering has been utilized in wide areas of fundamental researches such as material science, nuclear and particle physics and so forth. Particularly, the Compton scattering experiments, by the use of synchrotron radiations, offer a useful mean to study momentum distributions of electrons in materials. In the case of particle physics, γ-rays are scattered on protons, thus called "proton Compton scattering ". On the other hand, inverse Compton scattering (ICS), in which low energy photons are scattered off high energy electrons, was first discussed by E. Feenberg and H. Primakoff[2] in 1948 with regard to the interaction of cosmic-ray primaries such as electrons with sunlight or starlight. In 1963, two proposals[3, 4] were presented in order to create experimentally high- energy γ-rays through ICS, in which laser lights were backscattered by relativistic electrons. It was also pointed out that the γ-rays produced

in this manner was partially polarized if polarized laser lights were utilized[4]. Immediately after these proposals, numbers of proof-of-principle experiments were designed[5, 6]. In Levedev Physical Institute of Academy of Science, back scattered γ-rays per an accelerator pulse, 0.42 ± 0.08 were observed in a head-on collision of 1.79 eV laser photons generated by a ruby laser off 550 MeV electrons provided from an electron synchrotron[5].

Since these pioneer experiments, ICS has been routinely used for electron beam diagnostics. Meanwhile great progress has been achieved both for electron accelerators and laser facilities, which can create considerably high quality electron and laser beams in terms of time spread, intensity, beam emittance and so on. In addition, development of highly advanced synchronization technology between laser and electron beams enables us to control collisions of two beams to subpicosecond accuracy. Consequently the highly efficient ICS is realized, so that it can offer us possibilities of utilizing x-rays with higher peak flux and shorter time duration than those obtained from conventional synchrotron sources. Unique features of ICS may be put together as follows.

- ICS offers scattered photons with considerable high-energy, although, in ordinary Compton scattering, the energy of scattered photons cannot exceed that of incident photons .
- Photon energy is controlled by the kinematical condition of a collision process ; high energy photons are generated in a colinear geometry i.e. a head-on collision, while ultra-short pulses, at the cost of the energy and the production rate, are obtained in a transverse geometry where laser and electron beams are collided at an angle of 90 degree.
- Highly polarized photon beams can be generated by utilizing polarized laser lights. Furthermore, if the energy of back scattered photons is higher than twice an electron mass, highly polarized positrons and electrons are created through pair-creation process (see discussions in sec. 3.3).
- Scattered photons are well collimated and are tunable over the broad range of a photon spectrum by changing either a collision angle, or an electron (or laser) energy.
- Ultrabright lasers cause a non-linear effect which results in producing photons in higher harmonics[7].

Indeed, the generation and application of high-brightness, quasi-monochromatic x-rays and γ-rays are fast developing fields of science and technology, and thus, render great contributions to open multidisciplinary research fields including fundamental sciences as well as industrial and medical applications. In this article, I review a recent development of ICS and discuss applications of ICS to various fields of science.

6.3.2 Inverse Campton Scattering

6.3.2.1 Fundamental Properties

In the following, discussions will be mainly addressed for the ICS at the colinear geometry, in which laser photons are anti-parallel to electron beams, corresponding to a head-on collision. According to the kinematics of the ICS, the energy of a back scattered photon, k_2 is

$$k_2 = \frac{4k_1{E_e}^2}{{m_e}^2 + 4k_1E_e} \tag{6.7}$$

where k_1 is the energy of incident lasers, E_e is the kinetic energy of an electron and m_e represents the electron mass. For example, for collisions between 2.33 eV photons (corresponding to the second harmonics of a Nd:YAG laser) and 1.26 GeV electrons, the energy of backscattered photons (or γ-rays in this case) is 54 MeV. For the convenience of memory, the simple formula derived from Eq.6.7, being valid for ${m_e}^2 > 4k_1E_e$, is

$$k_2 = 4k_1\gamma^2 \tag{6.8}$$

where γ is the Lorentz factor defined as E_e/m_ec^2. Indeed, the magnitude of a correction to Eq.6.8 is 2% for 100 MeV electrons and 1 μm lasers. Through these equations, it is clearly demonstrated that the energy of back scattered photons increases in proportional to the electron energy squared. Since laser fields in ICS may be regarded as a virtual wiggler with a period of $10^4 - 10^5$ times shorter than an ordinary magnetic undulator, the ICS can provide extremely higher energy photons than a conventional synchrotron source for a given electron energy. Eq.6.8 is equivalently represented using the wave lengths λ_2 and λ_1 for an electron and a laser :

$$\lambda_2 = \lambda_1/4\gamma^2 \tag{6.9}$$

Employing the relation,

$$\beta = (1-\gamma^2)^{1/2} \sim 1 - 1/2\gamma^2, \tag{6.10}$$

we obtain

$$\lambda^2 = (1-\beta)\lambda_1/2 \tag{6.11}$$

indicating that only photons ahead of electrons can be emitted as suggested by the factor (1 - β). For example, if the electron would travel with the speed of light, no photons had an opportunity to emerge beyond the electron ($\beta = 1$). The backscattered photons are well collimated within a cone of $\theta \sim 1/\gamma$ and thus are emitted into a solid angle, $2\pi\theta^2$. An interaction time, during which an electron and a laser pulse interact, is given by

$$t_{int} = (t_L + t_e)/2 \tag{6.12}$$

where t_L and t_e represent the time duration of the laser and electron pulses. In the case of one electron, the difference of speed between the electron and the photons spreads the backscattered photon-pulse over the interaction time and thus the photon pulse duration is given by

$$\Delta t_{ph} = (1-\beta)t_{int} \sim (t_L + t_e)/4\gamma^2 \tag{6.13}$$

For actual cases, in which electrons form a bunch, the total pulse duration t_{ph} is represented by

$$t_{ph} = t_e + \Delta t_{ph} = t_e(1 + 1/4\gamma^2) + t_L/4\gamma^2 \sim t_e + t_L/4\gamma^2 \tag{6.14}$$

Here, for the practical case where $t_e \gg t_L/4\gamma^2$, the relation $t_{ph} \sim t_e$ is obtained, thus indicating that the photon pulse length is essentially determined by the electron bunch length. According to classical electrodynamics, radiation is emitted by an electron oscillating in external electromagnetic fields provided from a laser. As is well known, the total power radiated by a single electron is

$$P = 2e^2\dot{v}^2/3c^3 \tag{6.15}$$

where e is the electric charge and $\dot{v}$ is the acceleration vector. The formula 6.15, the familiar Lamor result for a nonrelativistic accelerated charge, can be generalized as the Lorentz invariant form, which is valid for arbitrary velocities of electrons. Using the laser beam power P_L and the laser beam radius r_L, Eq. 6.15 is modified as

$$P = (64/3){r_e}^2\gamma^2 P_L/{r_L}^2 \tag{6.16}$$

where $r_e = e^2/mc^2$ stands for a classical electron radius. For the electron ensemble as a bunched beam, the electron beam radius r_b should not exceed the laser beam radius r_L, so as to efficiently exploit the total electron bunch charge. Under the assumption that $r_b < r_L$ and the interaction length extends over the overlap distance defined by ct_{int}, the total power P_T radiated from this electron bunch is derived as

$$P_T \sim 10{r_e}^2\gamma^2 P_L t_L/et_e{r_L}^2 \tag{6.17}$$

Thus, the numbers of x-ray photons per pulse is given by

$$n_x(photon/pulse) \sim (P_T/h\nu_x)t_e \sim 8{r_e}^2 E_L Q\lambda_1/3her_L{}^2. \tag{6.18}$$

where $E_L = P_L t_L$ is the laser pulse energy and Q is the electron bunch charge[8]. The important indication of Eq.6.18 is the fact that the longer wave-length is more advantageous to generate larger number of photons. In the above discussion, it is implicitly assumed that the laser intensity is so weak that the nonlinear regime does not occur. However, in various current researches where ultra-intense laser beams are employed, we are forced to take account of the nonlinear effect . In the nonlinear regime, Eq.6.8 is modified as

$$k_2 = 4k_1\gamma^2 n/(1 + a^2). \tag{6.19}$$

where n is the harmonic number and a is the dimensionless laser strength parameter, defined as the normalized amplitude of a vector potential of incident laser fields, $a = eA/mc^2$. The scattering takes place in the linear regime when $a \ll 1$, and the nonlinear regime becomes dominant when $a > 1$. In the nonlinear regime, x-rays are generated in both fundamental and higher harmonics. Actually, a state-of-the-art laser system based on chirped-pulse amplification can deliver ultrashort pulses (< 1 ps) at extremely high power (> 10 TW) and intensity ($> 10^{18}\mathrm{W/cm}^2$), giving rise to $a \sim 1$ for a laser wavelength 1 μm. In this article, I will not go into details of the nonlinear effect. Reader, who are interested in this issue, may refer to Ref. [7].

6.3.2.2 Production of back scattered photons

At present, the most intense x-ray flux is generated from electron synchrotrons equipped with undulator (or wiggler) magnets, which provides periodic, transverse magnetic fields to make electrons move in a zigzag direction. The wavelength of x-rays generated along the electron beam axis is

$$\lambda_{\mathrm{x}} = \lambda_u/2\gamma^2 \tag{6.20}$$

where λ_u is the undulator wavelength. The ICS, in which the periodical electromagnetic field is also generated by the laser itself, is quite similar to this synchrotron radiation mechanism, so that the radiation in association with ICS may be called as a laser synchrotron source (LSS). If we assume typical values, $\lambda_u = 2$ cm, and $\lambda_1 = 1\mu m$, it may be expected, from the comparison of Eq.6.9 with Eq.6.20, that the LSS generates, for a fixed energy of electron beams, x-rays whose wavelength λ_2 is approximately 4 order shorter than λ_x of a conventional synchrotron light source(SLS). In another wards, for a given x-ray energy, the LSS requires the electron beams whose energy is about 200 times lower than that of the SLS ; for example, assuming above parameters, in the case of producing 1 keV x-ray, the LSS needs the electron beam energy of only 7.3 MeV, whereas the SLS requires that of 1.5 GeV.

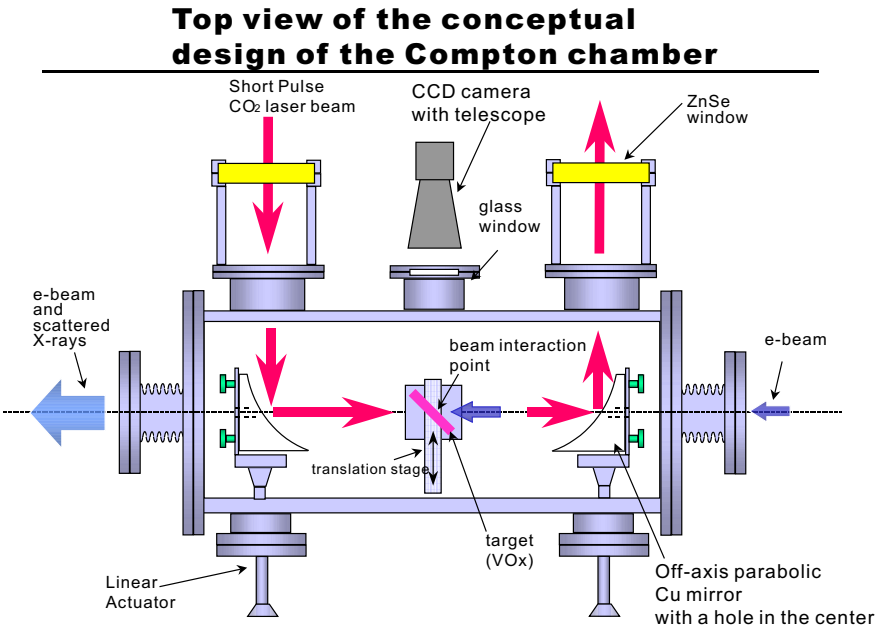

Figure 6.3: Cross sectional view of the Compton chamber.

In order to accomplish the high-luminosity ICS for the given laser energy and electron beam intensity, it is of importance to obtain a small spot size of the laser light at the collision point. For this objectives, a Compton chamber was constructed through the US/Japan joint research, in which Japanese institutes[1] and the BNL-ATF group have been cooperating. The Compton chamber is so designed that the head-on collision and a short focal length 15 cm are realized(see Fig. 6.3). The electron beams of 50 MeV, 0.5 nC/bunch are produced by a linear accelerator, in which the photo-cathode RF gun is installed and the electron bunch length 20 ps is created . The CO_2 laser system generates the laser pulse with the wave length 10.7 μm, the energy 1J and the pulse width 175 ps, corresponding to the power 6 GW; the nonlinear effect is still small, i.e. $a \sim 0.01$. Under these conditions, it is expected to obtain x-rays with the maximum energy 4.7 keV and, according to Eq.6.18, 7×10^8 x-rays per pulse. In the Compton chamber, off-axis parabolic mirrors, being precisely remote-controlled, is set to focus the laser lights ; the gaussian shape of an initial laser light is transformed into a cylindrical shape and then reflected by 90 degree on the off-axis mirror,

[1]Tokyo Metropolitan University, KEK, Waseda University and Sumitomo Heavy Industries Ltd.

at the center of which a hole of the 5mm diameter is available to stream out the electron beams and back scattered x-rays. At the collision point, a VO_2 foil is placed to measure the profile of electron and laser beams by taking advantage of the hysteresis property of the VO_2 foil with respect to temperature[9]; the adequate performance of the VO_2 foil was already verified. This chamber is being employed for Compton scattering experiments at BNL-ATF and later at KEK-ATF.

6.3.2.3 *Polarized gamma rays*

In comparison with conventional synchrotron lights, one of the unique feature of an LSS is that highly polarized photons are created through ICS of polarized laser lights scattered off non-polarized electrons, because of the small spin flip component in the head-on collision. For example, if 100 % circular-polarized laser-lights of the wave length 532 nm (second harmonics of a Nd:YAG laser) are back-scattered off electron beams of the energy 1.26 GeV, the magnitude of γ-ray polarization is calculated as a function of its energy as shown in Fig. 6.4. In this case, the circular polarization of initial laser lights is assumed to be right-handed corresponding to a helicity, $h = +1$ and thus, the back scattered γ-rays has a large component of a negative helicity, $h = -1$ towards the high energy end of γ-rays; at the maximum energy 54 MeV, 100 % of polarization is attained.

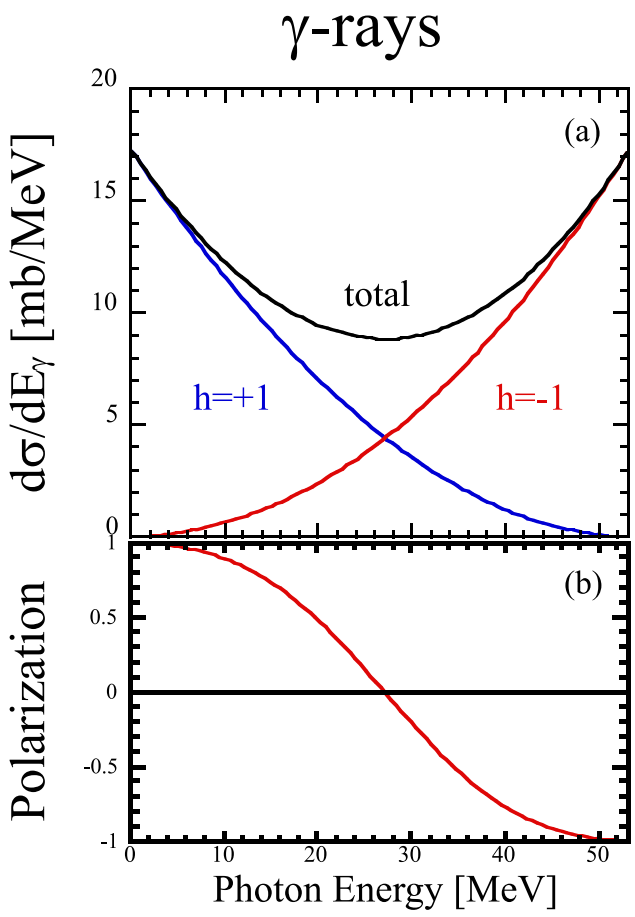

Figure 6.4: (a) Differential cross section of Compton scattering for γ-ray helicities $h = \pm 1$ and (b)γ-ray polarization, as a function of the γ-ray energy.

In several research institutes, the polarized γ-rays have been extensively utilized in nuclear physics and particle physics. In 1969, SLAC began to investigate a photoproduction experiment in a GeV energy region, using polarized γ-rays introduced into a hydrogen bubble chamber[10]. In 1980, INFN first exploited a storage ring of 1.5 GeV electrons, ADONE and studied details of technical aspects on laser Compton scattering for establishing a fundamental technique to create monochromatic, polarized γ-rays through tagging of scattered electrons. This facility, called LADON, was further upgraded to the TARADAN project in ESRF, in which 5 GeV electron beams were stored[11]. From around 1983, BNL has developed the laser electron gamma source, LEGS which generates highly polarized γ-rays in the wide energy range between 80 MeV and 470 MeV; the particular energy region is selected by varying the electron energy as well as the laser wave length obtained from Nd:YLF or Ar lasers and then, the final energy of γ-rays is determined on an event-by-event basis through tagging of a scattered electron[12]. In 1983, Budker Institute of Nuclear Physics at Novosibirsk started to develop the ROKK-1 facility at the VEPP-4 storage ring, and later from 1987, the ROKK-2 at the VEPP-3 storage ring was constructed for the generation of γ-rays with the energy range between 30 MeV and 270 Mev[13]. In 1994, to determined the parity of nuclear levels in $^{208}\mathrm{Pb}$ through elastic scattering of polarized photons, Electrotechnical Laboratory generated highly polarized(99%) photons[14] with the energy ranging from 1 to 10 MeV, using a Nd:YAG laser and the storage ring TERAS, which stores an electron beam with the energy between 200 and 750 MeV. Recently a multi-GeV photon beam system was constructed at the photon factory facility, SPRING-8; polarized γ-rays with the energy of 1-3.5 GeV will be obtained through the scattering of (3.5-6) eV laser photons off the 8 GeV electron beams[15]. Extensive studies with regard to quark nuclear physics are scheduled using the high energy, polarized γ-rays.

6.3.3 Polarized Positron Source

6.3.3.1 Physics objectives

The ICS is now extended, one step further beyond photon productions, toward creation of polarized positrons. It has been pointed out that, in future electron - positron collider experiments, the positron polarization as well as the electron polarization plays important roles in the detailed investigation of the standard model and in the discovery of exotic phenomena beyond the standard model[16, 17, 18]. A key aspect of observing a clean signal of important and interesting processes is how efficiently one can suppress dominant backgrounds of reaction processes predicted by the standard model. Indeed, for this objectives, highly polarized electron beams can offer a considerably efficient tool. However, owing to the fact that the magnitude of the electron polarization is not 100 %, we necessarily suffer contaminations arising from the processes with a large cross section. If a positron as well as an electron is polarized, we can significantly enhance the effective polarization defined as

$$P_{eff} = (P_1 - P_2)/(1 - P_1 P_2) \tag{6.21}$$

where P_1 and P_2 represent electron and positron polarizations, respectively. For example, if the positron polarization 80 % can be achieved in addition to the electron polarization 90 %, the effective polarization will be 99 %, being close to complete polarization of one beam particle. Furthermore, the positron polarization can reduce the measurement error of P_{eff} to a great extent; this

is actually an important aspect in high energy physics experiments because the error of P_{eff} directly influences the precision of determining some physical quantities. Detailed discussions on these issues are given in Ref. [18] and [19].

6.3.3.2 Basic experiment of polarized positron production

A new method of producing highly polarized positrons on the basis of ICS was proposed in Ref. [20]. In this case, ICS is again exploited to generate polarized γ-rays, which subsequently creates polarized positrons through pair creation process in a heavy material. The schematic illustration of the proposed method is shown in Fig. 6.5. Taking into account the results shown in Fig. 6.4, we calculate the differential cross section and the polarization of positrons, which are pair-created from polarized γ-rays injected on a W-target of 1 mm in thickness. The electron beam of 1.26 GeV/c with the intensity $6 \times 10^9 \mathrm{e}^-/\mathrm{pulse}$ and the pulse length 20 ps are extracted every 0.78 sec from the KEK-ATF damping ring[21] constructed as a test facility for JLC[22]. We used a Nd:YAG laser with the power 500 mJ in 6 ns pulse duration at the wavelength 532 nm (second harmonic). It is theoretically demonstrated that the 80% polarization is achieved if positrons with the energy higher than 23 MeV are selected. To test this proposed method, we have been performing a basic experiment and achieved the first observation of positron production via Compton-scattering and pair creation processes[19]. The production rate is in precisely agreement with the theoretical prediction.

The next step is to measure the positron polarization through Bhabha scattering of a positron on a magnetized iron target. For the attainment of three fundamental processes, i.e. Compton scattering, pair creation and Bhabha scattering at the same time, the large signal to background ratio should be essential, particularly at the Compton scattering; this is achieved by increasing drastically the luminosity of the laser-Compton scattering process as well as to suppress enormous amount of background. For this objectives, the Compton chamber will certainly render essential contributions because the short focal length 15 cm permits quite small spot size (less than 100 μm) of laser light at the collision point.

6.3.3.3 Conceptual design of polarized positron beam

In future colliding experiments at JLC[22], ultrahigh intensity positron beams, $0.7 \times 10^{10} \mathrm{e}^+/\mathrm{bunch}$ are required; therefore extremely high-intensity electron and laser beams must be provided for Compton scattering. In addition to this severe condition, we encounter another requirement with regard to the time structure of JLC beams, called multi-bunch beams, which is so complicated that the beam may consist of a macrobunch with a time spread 240 ns, repeated with 150 Hz, and each macrobunch contains 85 microbunches with the time interval 2.8 ns. To achieve these requirements, the electron linac should generate the electron beams of 5.8 GeV with the intensity $10^{11} \mathrm{e}^-/\mathrm{bunch}$. In order to increase numbers of backscattered γ rays, we choose a CO_2 laser, whose wave length 10.7 μm is relatively long, thus containing a large number of photons in a single pulse for a given energy. Such a combination of the electron beam and the CO_2 laser yields back scattered γ-rays with a maximum energy 60 MeV, and the large cross section is expected both for the Compton scattering and the pair creation on a tungsten (W) target, i.e. 658 mb and about 10b, respectively[23].

Extensive Monte-Calro study indicates that the laser energy per pulse about 10 J is needed to produce required numbers of positrons at JLC. In order to generate the 80 % positron polarization, we have to collect positrons with the energy higher than 25 MeV. If the laser energy 10 J is sup-

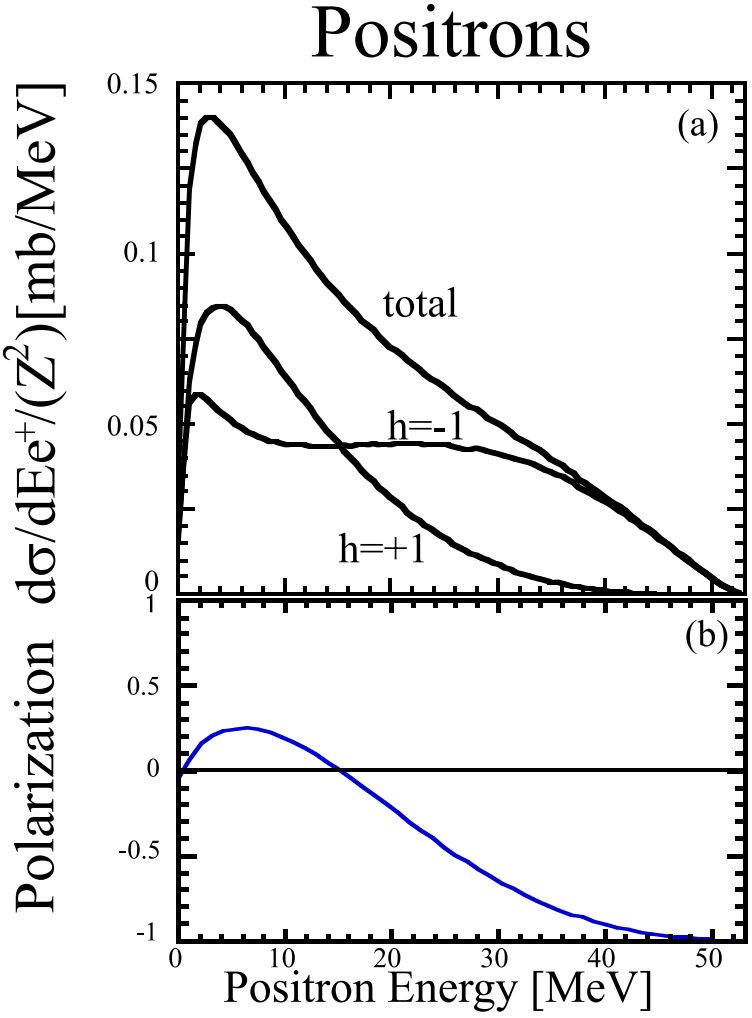

Figure 6.5: Schematic illustration of polarize positron generation via Compton scattering of circularly polarized laser lights off relativistic electron beams and pair creation of backscattered γ-ray.

plied by a single laser pulse with a diameter of 30 μm at the collision point, the large non-linear effects causes necessarily wider energy-spread and lower polarization for generated γ-rays. Hence the laser energy is split into 40 pieces of CO_2 laser pulses; each pulse, containing 250 mJ, collides successively 40 times with one electron bunch. Consequently, we install 40 units of the similar off-axis parabolic-mirrors to those used in the Compton chamber[24]. Fig. 6.6 shows the schematic design of the Compton scattering system to create multi-pulse γ-rays and the capture section to collect pair-created positrons. According to the Monte Carlo simulation, the capture efficiency 13.6 % can be achieved, resulting in the numbers of collected positrons $0.72 \times 10^{10} e^+/\mathrm{bunch}$ and the degree of polarization 70%; this meets almost the requirement of JLC[25]. In this figure, the wall-plug-power of the electron linac and the laser system is indicated. The spot size of the laser beam is 15 μm in sigma, so that the peak power of a laser pulse is $2.2 \times 10^{19} \mathrm{W/m^2}$, indicating that non-linear QED effect is relatively small and causes 10% depolarization of γ-rays[23, 26]. It is demonstrated that the laser-Compton scattering is also applicable to the determination of both longitudinal and transverse polarizations by measuring the asymmetry of angular distributions of Compton scattered γ-rays off the electron or positron immediately behind the interaction point[27].

6.3.3.4 Plasma channeling

To put our conceptual design to practical use, we have to overcome the most serious technical problem of realizing high average-power picosecond CO_2 lasers with high repetitions. The short pulse of 10 ps necessarily demands a high pressure (10 atm) CO_2 laser-system. However, the high pressure, high repetition laser does not exist yet, and multiple slicing of a CO_2 laser pulse and amplification of picosecond pulses, being consistent with the JLC bunch structure, have not been demonstrated to date. In order to ease these technological requirements imposed on the laser system, we are investigating the technical feasibility of confining the laser electron interaction in an extended plasma channel[28], in which ICS occurs. With respect to the laser channelings, there are a number of proposed schemes and demonstrations for high intensity laser pulses[29, 30, 31].

If the microbunch duration in the plasma channel is 1 ns, the channel length is 15 cm. Thus, keeping the average power of a microbunch as 3 kW (250 mJ $\times$ 85 bunches $\times$ 150 Hz), we may increase the micro-bunch energy in the plasma channel up to 2.5 J which is one order higher than the current value 250 mJ. Longer laser pulses permit lower pressure, which facilitates maintaining a high repetition rate discharge.

6.3.4 Discussion and Future Prospect

This article describes historical development of the inverse Compton scattering(ICS) experiments, with a stress on recent circumstances of its applications. The laser synchrotron source (LSS) based on ICS, in which intense lasers undergo a collision from relativistic electrons, offers us a mean to generate tunable, narrow band, polarized photons for applications in a wide variety of fundamental research fields as well as for more practical use in various industrial and medical areas. Actually, the LSS is furnished with numbers of unique and attractive features, especially compared with conventional synchrotron sources. First of all, it is very compact, because the photon energy supplied by an LSS is considerably high due to the fact that lasers can provide a virtual "undulator" with the extremely short wave length ($< 10\mu$m). In addition to the compactness, photons thus generated are near monochromatic, ultrashort, tunable over an entire x-ray spectrum from ultraviolet to γ-rays,

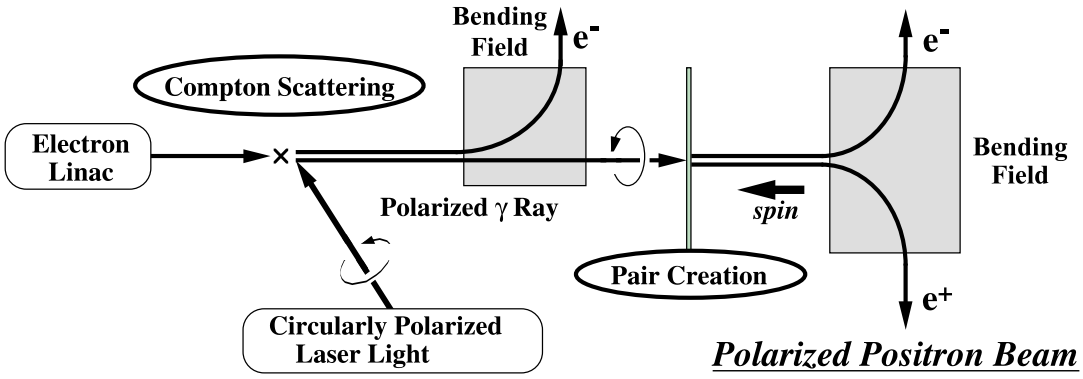

Figure 6.6: Schematic design of the Compton scattering system to create multi-pulse γ-rays and the capture section to collect pair-created positrons.

and highly polarized.

These specific features of an LSS would play an important role for diverse utilization of x-rays in multidisciplinary researches. In particular, intense short-pulse x-rays (< 1 ps) may permit fast exposure of x-rays on living bodies and thus reduce the risk in association with radiation damage. It is expected that short pulse x-rays in a particular spectral region, called the water window with the wavelength corresponding to a K-absorption edge between oxygen (2.3 nm) and carbon (4.4 nm), are able to achieve time resolving observation of a cell without killing it. In the past few years, technological challenges as an application of LSS have been made for the generation of polarized positrons, which offers a possible positron source for future linear colliders. Since a linear collider imposes stringent requirements to positron beams in terms of extraordinary high intensity and a sophisticated bunch structure, there might be a plenty of technical problems to be overcome. Extensive study has been made so far with regard to proof-of-principle experiments based on ICS and a conceptual design including the pisosecond CO_2 laser system, a positron capture system into subsequent accelerators[25, 26], and plasma chanelling in which ICS takes place[28].

Since the development of LSS and its application is rapidly advancing, it may be hard to predict details of its status even in near future. Certainly, future advance of LSS will depend on technical achievement of high quality laser and electron beams as well as precise sychronization technique for short laser and electron bunches. Here I will briefly mention two projects being currently underway, one at BNL and the other at Sumitomo Heavy Industries (SHI) Ltd. in cooperation with Femtsecond Technology Research Association. At BNL-ATF[8], the current electron linac and the CO_2 laser will be up-graded according to the following program. The first stage is almost available as follows: CO_2 laser;10 GW, 100 ps, 140 μm (radius at focus), electron linac;50 MeV, 0.5 nC, 10 ps, 2 mm-mrad(emittance), x-rays;4.7 keV, 10 ps (pulse duration), 2×10^8 photon/pulse, 2×10^{19} photon/s. A proof-of-principle experiment is being carried out. The second stage is more ambitious and thus attractive. The 5 TW, 3 ps, CO_2 laser and the electron beam with 70 MeV, 0.5 nC, 3 ps, 2 mm-mrad of an emittance are considered; this system is expected to generate 3 ps, 9.4 keV x-rays with 6×10^{10} photon/pulse and 2×10^{22} photon/s. At SHI, it has been planned to achieve extremely short and high energy x-ray pulses through Compton scattering at 90 degree. A 150 MeV microtron, being already constructed, will be upgraded by installing an improved RF gun activated by highly stabilized laser pulses for obtaining electron beams with a pulse duration 0.5 ps, electron charge 1.6 nC, an emittance of 1π mm-mrad and a focussed beam size 50 μm. Then, employing a solid state laser of 5 TW, 100 fs and a focussed beam size 50 μm, they will achieve 228 fs, 214 keV x-rays with 3×10^7 photon/pulse.

Finally, it may be remarked that laser-plasma collisions is also promising to generate very strong x-rays through higher harmonic interactions because the rapid progress of laser facilities will soon allow to provide ultra-intense laser beams. Indeed, studies of interactions between laser, beam and plasma will certainly offer unique and attractive capabilities for multidisciplinary researches, in which unexpected new phenomena may emerge.

References

[1] V. O. Klein and Y. Nishina: ZS f Phys.52 (1998) 853, ibid. 52 (1998) 869

[2] F. Feenberg and H. Primakoff: Phys. Rev.73 (1948) 449

[3] F. R. Arutyunian and V. A. Tumanian: Phys. Letters 4 (1963) 176

[4] R. H. Milburn: Phys. Rev. Letters 10 (1963) 75

[5] O. F. Kulikov et al.: Phys. Letters 13 (1964) 344

[6] C. Bemporad et al.: Phys. Rev.138 (1965) 1546

[7] E. Esarey, S. K. Ride and P. Sprangle: Phys.Rev. E 48 (1993) 3003

[8] I.V. Pogorelski: Nucl. Instru.& Method : A411(1998) 172

[9] A. Tsunemi, A. Endo, I. Pogorelsky, I. Ben-Zvi, T. Hirose, T. Omori, J. Urakawa and M. Washio: Contribution paper to CLEO Pacific Rim '99 Summary

[10] J.J. Murray and P.R. Cline: SLAC TN-67-19 (1967)

[11] M. Perger, B. Spataro, R. Bernabei, M.P. de Pascale and C. Schaerf:Nucl. Instru.& Method : A249 (1986) 299

[12] National Synchrotron Light Source, Activity Report 1996, BNL 52517

[13] G.Ya. Kezerashvilli, A.M. Milov and B.B. Wojtsekhowski: Nucl. Instru.& Method : A328 (1993) 506

[14] H. Ohgaki, T. Noguchi, S. Sugiyama, T. Yamazaki, T. Mikado, M. Chiwaki, K. Yamada, R. Suzuki and N. Sei: Nucl. Instru.& Method : A353 (1994) 384

[15] Spring-8 Laser-Electron Photon Collaboration, RCNP, Osaka Univ. 1997 October

[16] T. Hirose: Proc. of Int.workshop on physics and experiments with linear colliders (Morioka Iwate, Sep. 8-12, 1995) ed. A.Miyamoto Y.Fujii.T.Matsui and S.Iwata, (World Science, Singapore 1996), P.748-756

[17] T. Omori: Proc.of Int.workshop on New Kinds of Positron Sources for Linear Colliders (SLAC, March 4-7, 1997) SLAC-R-502, p. 285

[18] T. Omori: ACFA 1st Linear Collider Workshop (Tsinghwa Univ., November 27, 1998)

[19] K. Dobashi, T. Hirose, K. Kumita, Y. Kurihara, T. Muto, T. Omori, T. Okugi, K. Sugiyama and J. Urakawa: KEK Preprint 98-177 (1998), Preprint of Tokyo Metropolitan University TMU HEP/EXP 98-13 (1998), Submitted to Nucl. Instru.& Method.

[20] T. Okugi, Y. Kurihara, M. Chiba, A. Endo, R. Hamatsu, T. Hirose, T. Kumita, T. Omori, Y. Takeuchi and M. Yoshioka: Jpn. J. Appl. Phys.35 (1996) 3677

[21] ATF Design and Study Report, KEK Internal 95-4 (1995)

[22] JLC Design Study: KEK Report 97-1 (1997)

[23] T. Omori, K. Dobashi, T. Hirose, T. Kumita, Y. Kurihara, T. Okugi, K. Sugiyama, A. Tsunemi and M. Washio: Proc. of Asia Pacific Accelerator Conference, KEK, Oct. 1998, KEK Preprint 98-13, Preprint of Tokyo Metropolitan University, TMU HEP/EXP 98-10 (1998)

[24] A. Tsunemi, A. Endo, M. Washio, T. Hirose, Y. Kurihara, T. Omori and J. Urakawa: Proc. of Int. Conf. on Laser '97, New Orleans, Louisiana, USA. SRS Press, McLean, VA, 838 (1998)

[25] T. Hirose: Talk given at Int. Conf. on Laser'98 (Tucson, Arizona, USA, Dec. 7-11, 1998) Preprint of Tokyo Metropolitan University, TMU HEP/EXP 99-1(1999)

[26] T. Omori: Proc. of 1st ACFA Workshop on Physics/Detector at the Linear Collider (Tsinghua University, Beijing, The People of Republic of China, Nov. 26-27, 1999) KEK Preprint 98-237

[27] H. Ishiyama, T. Hirose, T. Kumita, Y. KUrihara, T. Okugi and T. Omori: KEK Preprint 96-141, Preprint of Tokyo Metropolitan University, TMU HEP/EXP 96-10 (1996)

[28] I. V. Pogorelski, I. Ben-Zvi and T. Hirose: BNL Report 65907, October 1998

[29] Y. Ehrlich, C. Cohen, A. Zigler, J. Krall, P. Sprangle and E. Esarey: Phys. Rev. Lett. 77 (1996) 4186

[30] C. D. Durfee and H. M. Milchberg: Phys. Rev. Lett. 71 (1993) 2409

[31] I. V. Pogorelski, W. D. Kimura and Y. Liu: 6th Workshop on Advanced Accelerator Concept, Jun 12-18, 1994, Lake Geneva, WI, AIP 335 (1995) 419

6.4 University of Illinois Summer Course on Accelerators

Frederick Mills `fredmills@aol.com` Department of Physics
Deborah Errede University of Illinois at
Urbana-Champaign

Accelerators: Theory and Applications (Physics 498ACC)
Semester: Summer 1999
Time: M 1:00 p.m.- 4 p.m. Tu 9:00am - 12:00 noon
Place: 147 Loomis
Call Number: 00783
Credit: 1 Unit

6.4.1 Prospectus

This course introduces the basic concepts in accelerator theory and practice. After a brief review of classical mechanics, the following topics are developed; longitudinal and transverse motion of particles in linear and nonlinear fields in linear and circular accelerators; effects of synchrotron radiation on particle motion; collective motion of particle beams. Applications in Particle, Nuclear, Surface, and Condensed Matter Physics, Chemistry and Biology will be discussed. Since accelerators are important resources for these fields, their understanding will enable curious scientists better to understand the requirements of their apparatus and to contribute to the direction of the future of their field.

Prerequisites include Hamiltonian Mechanics (PHYCS 225/326 or PHYCS 414) and Electromagnetic Theory (PHYCS 335/336 or PHYCS 411/412).

6.4.2 Syllabus

Date	Subject	Guest Lecturer
June 14	Review of Mechanics	
June 15	Pendulum Motion	
June 21	Accelerator Coordinates	
June 22	Betatron Oscillations	
June 28	Lattice Calculations	
June 29	Radio Frequency Acceleration	
July 5	No Class Meeting, Holiday	
July 6	Synchrotrons and Linacs	
July 12	Synchrotron Radiation	
July 13	Linear e+-e- Colliders	Robert Siemann, SLAC
July 19	Resonances, Extraction	
July 20	Collective Effects	
July 26	Hadron and Muon Colliders	Alvin Tollestrup, Fermilab
July 27	Synchrotron Light Sources & Spallation Neutron Sources	Robert Kustom, ANL
August 2	Student Reports	
August 3	Student Reports	
August 7	Summer Term Ends	

http://web.hep.uiuc.edu/home/derrede/498ACC/

References

[1] Edwards and Syphers, An Introduction to the Physics of High Energy Accelerators

[2] Henri Bruck, Circular Particle Accelerators

[3] K. Wille, Physik der Teilchenbeschleuniger (in German)

[4] C. Bovet et al, A Selection of Formulae and Data Useful for the Design of A.G. Synchrotrons

[5] A. Chao and M. Tigner, Handbook of Accelerator Physics and Engineering

[6] P. Bryant and K. Johnson, The Principles of Circular Acceleratos

[7] M. Month and M. Dienes (eds), Physics of Particle Accelerators, AIP Conference Proceedings 153 Volume I and II

[8] M. Month and M. Dienes (eds), Physics of Particle Accelerators, AIP Conference Proceedings 184 Volume I and II

[9] F. Mills (ed), Advanced Accelerator Concepts, AIP Proceedings 156

[10] A. P. Wills, Vector Analysis with an Introduction to Tensor Analysis

[11] M. Stanley Livingston, Particle Accelerators

[12] R.R. Wilson and R. Littauer, Accelerators: Machines of Nuclear Physics

6.5 New Doctoral Theses in Beam Dynamics

6.5.1 Marco Venturini

Author: Marco Venturini (venturin@physics.umd.edu)

Institution: University of Maryland

Date: July 1998

Title: Lie Methods, Exact Map Computation, and the Problem of Dispersion in Space Charge Dominated Beams

Supervisors: Alex Dragt (dragt@physics.umd.edu), Physics Department, University of Maryland, and Martin Reiser (mreiser@glue.umd.edu), Institute for Plasma Research, University of Maryland

Abstract: The Dissertation consists of three parts. The first part contains a discussion of two possible ways to compute Lie transformations based on the theory of normal forms and the Scaling, Splitting, and Squaring algorithm, and implementation of the latter in the code MARYLIE5.0. The second part is devoted to fringe field modeling and accurate computation of transfer maps using a realistic description of the magnetic fields in terms of numerical data or spinning coil measurements. Applications to the study of the beam dynamics in the Large Hadron Collider and University of Maryland Electron Ring are discussed. Finally, in the third part the focus is on space charge effects in circular lattices and in particular on the the interplay between space charge and dispersion. Here I work out a novel set of equations that provides the natural generalization of the standard rms envelope-equations to include the effects of a thermal energy spread and bending magnets.

6.5.2 Maria Paz Zorzano

Author: M.P. Zorzano (Maria.Paz.Zorzano@cern.ch)

Institution: DESY

Present affiliation: CERN

Date: 10 March 1999

Title: Numerical Integration of the Fokker-Planck Equation and Application to Stochastic Beam Dynamics in Storage Rings.

Supervisors: Dr. H. Mais (mais@solar01.desy.de), DESY-Hamburg, Dr. L. Vazquez (lvazquez@eucmax.si UCM-Madrid.

This work has been developed within the European network "Nonlinear Problems in Beam Dynamics and Transport" as part of a collaboration between the University Complutense de Madrid (UCM) and the laboratory Deutsches Elektronen Synchrotron (DESY). The Ph.D. was presented at the School of Physics of the UCM on 10 March, 1999.

Abstract: The Fokker-Planck equation has been used to describe the stochastic dynamics of particles. This partial differential equation has been integrated using a finite difference scheme and an ADI technique. The integration scheme has been successfully applied to problems of 2, and 3 dimensions, plus time, with absorbing and/or periodic boundary conditions. Since the biggest limitation is the CPU time a parallel version of the scheme has been implemented.

We have studied the influence of noise on some particular problems of accelerator physics as for example betatron motion with beam-beam interaction and longitudinal dynamics subject to nonlinear influences such as double RF systems. We have also collected several examples where the effect of noise is not a simple diffusion: a “noise induced transition” can stabilize a point which in the deterministic system was unstable and the phenomenon of “stochastic resonance” increases the systems response to an external modulation.

7: Forthcoming Beam Dynamics Events

7.1 The 8th ICFA Mini-Workshop: Two-Stream Instabilities

An ICFA Mini-Workshop on "Two-Stream Instabilities in Particle Accelerators and Storage Rings" will take place at Santa Fe, NM, USA, February 16 -18, 2000.

Two-stream instabilities such as e-p in proton rings, ion-beam instabilities at electron accelerators, or electron cloud-induced effects observed at various accelerators can be serious limitations to the performance of high-intensity rings. This international workshop, which is being organized by LANL and ANL, aims at bringing together the separate communities working on various aspects of two-stream instabilities for the purpose of sharing observations, experiences and insights.

The accelerators for which these issues are of interest include but are not limited to:

- high intensity proton rings (PSR, LHC, BNL Booster, drivers for SNS, ESS, JHP and the muon colliders)
- B-factories (PEP-II, KEK-B)
- photon factories (KEK PF)
- e^+e^- rings and colliders (BEP-C, CESR, APS, Bates storage ring)

The topics to be covered include observations and measurements of various instability characteristics, experiments on causes, studies of cures, theory and simulations including benchmarking with measured data, study of mechanisms for and diagnostics of electron cloud generation, surface effects, beam-induced multipactor, and instability diagnostics.

Organizing Committee (as of 8/4/99):

Katherine Harkay (ANL, co-chair), Robert Macek (LANL, co-chair) Arch Thiessen (LANL), Dan Fitzgerald (LANL), Miguela Sanchez (LANL-administration), Bob Kustom (ANL), Richard Rosenberg (ANL), Miguel Furman (LBNL) and others, in particular ones from abroad, to be added later.

A draft program, invitations to attend and registrations forms will be issued in October 1999. For further information contact:

Robert Macek (505-667-8877, macek@lanl.gov)
or Miquela Sanchez (505-667-2778)
LANL, LANSCE-DO, MS H848, Los Alamos, NM 87545, USA.

or contact Katherine Harkay (630-252-9758, harkay@aps.anl.gov)
Argonne National Laboratory
Advanced Photon Source, Bldg 401
9700 South Cass Ave. Argonne, IL 60439, USA

7.2 The 9th ICFA Mini-Workshop: Longitudinal Emittance Control

This is the first announcement of a mini-workshop to be held at CERN, Geneva, Switzerland from March 6th to March 9th 2000, on the subject of "Longitudinal Emittance Control."

This mini-workshop will be held under the auspices of the ICFA Working Group on High Intensity High Brightness Hadron Beams, and is organised by the PS and SL divisions of CERN.

The purpose of the workshop is to study methods for identifying the causes of and preventing unwanted increases in longitudinal emittance in hadron machines, and also the tools available for producing controlled emittance and distribution changes.

The first case includes, for example, instability signal analysis, source identification, feedback systems, Landau damping and the use of higher harmonic RF systems in general. In the second case resonant excitation, and the many types of RF gymnastics can be cited.

Workshop organizing committee:

T.Linnecar and E.Shaposhnikova, SL division,
R.Cappi and R.Garoby, PS division.

7.3 JINR Accelerator School

Problems of Charged Particle Acceleration International School for Young Scientists

14-22 September, 1999, Dubna, Russia

The Joint Institute for Nuclear Research is organizing the School for young scientists on problems of charged particle acceleration. The School topics will cover technical and theoretical aspects of the problem and can be of interest for staff of accelerator laboratories, university physics departments and seniors specializing in physics of particle accelerators.

The topics will include:

1. Heavy Ion Physics.
2. Synchrotron Radiation Sources and Free Electron Lasers.
3. Synchrotron Radiation Researches and Instrumentation.

Organizing Committee :

Chairman - A.Sissakian (JINR), **Co-Chairman** - I.Ivanov (JINR), L.Ignatova (JINR), S.Ivanova (JINR - University Centre), V.Kazacha (JINR), **Secretariat** - V.Novikova (JINR), **Scientific Secretary** - N.Tokareva (JINR), V.Zhabitsky (JINR).

Accommodation and meals for all the participants will be provided by the Organizing Committee. Travel expenses are to be covered by the participants. Further information and registration procedure can be obtained via WWW at:

http://www.jinr.ru/conferences/overview.html

or by contacting:

Co-Chairman, Dr. Igor Ivanov
Joint Institute for Nuclear Research, Laboratory of Particle Physics
141980 Dubna, Moscow Region, RUSSIA
Tel. : (095) 926 2269 (096) 216 3057
Fax : (096) 216 5767 telex : 911621 Dubna RU
e-mail: ivanov@sunse.jinr.ru

Scientific Secretary Dr. Nadezhda Tokareva, tokareva@sunse.jinr.ru

Secretariat Mrs. Valentina Novikova, novikova@cv.jinr.ru
Fax:(096) 216 5891 (096) 216 5599

7.4 Second Announcement: BDO '99

Sixth International Workshop on Beam Dynamics & Optimization

Saratov State University

Saratov, RUSSIA September 6–10, 1999

Organized by : Saratov State University[1] named after N.G. Tschernyshevsky

- Faculty of Physics, Department of Electrical & Radio Engineering
- Nuclear Physics & Accelerators Laboratory, Joint Institute of Nuclear Research (Dubna), St. Petersburg State University
- Institute of Computational Mathematics & Control Processes
- Faculty of Applied Mathematics & Control Processes, D.V. Efremov Institute of Electrophysical Apparatus (St. Petersburg), Peoples' Friendship University of Russia.

The series of the BDO Workshops is supported by Russian Foundation for Basic Research and Russian Federal Program "Integration".

ORGANIZING COMMITTEE
chairman - D.I.Trubetskov (Russia), **co-chairman** - D.A. Ovsyannikov (Russia), S.N. Andrianov, Yu.A. Budanov, N.S. Edamenko, A.B. Kurzhanskii, B.P. Murin, V.V. Petrenko, V.P. Stepanchuk, V.A. Teplyakov, M.F. Vorogushin, I.P. Yudin, E.P. Zhidkov, V.I.Zubov (Russia), A.N. Dovbnya (Ukraine), H. Mais (Germany), M. Berz, G. Gillespie, R. Jameson (USA), Y. Yamazaki (Japan)

PROGRAM COMMITTEE
chairman - D.A. Ovsyannikov (Russia), V.A. Belyakov, B.I. Bondarev, V.P. Gorbachev, N.V. Egorov, O.I. Nikonov, R.V.Polyakova, Yu.A. Svistunov, I.P. Yudin, A.V. Zherebtsov (Russia), F. Meot (France),

[1] http://www.sgu.ru/

Yu. Tur (Ukraine), R. Ryne, A. Todd (USA), S. Kawata (Japan)

LOCAL ORGANIZING COMMITTEE
chairman - V.P. Stepanchuk (Russia), **workshop coordinator** - V.P. Gorbachev, I.V. Alekseev, A.Yu. Balaev, S.N. Belyaev, S.B. Frolov

SCOPE
The objective of the Workshop is to bring together mathematicians, physicists and engineers to present and discuss recent developments in the area of mathematical control methods, modeling and optimization, theory and design of charged particle beams. This Workshop is the sixth event in a series which started in 1994.

MAIN TOPICS

- Nonlinear problems of beam dynamics: Mathematical modeling, nonlinear aberrations, including space charge forces and the self-consistent distributions problem, long time beam evolution, dynamic aperture and halo problems
- Methods of control theory in the problems for the beam and plasma dynamics optimization
- Mathematical modeling of the electro- and magnetic fields
- Computing problems for beam physics, object-oriented modeling
- Software for the beam dynamics and optimization

TIME AND LOCATION
The Workshop will be held in "the capital of Volga region" Saratov, Russia, September 6–10, 1999. It is carried out in the comfortable resort houses called "Salut" in the area of picturesque Saratov suburbs. The celebration of the 90^{th} anniversary Saratov State University starts at this time.

OFFICIAL LANGUAGES
Working languages : Russian, English. Simultaneous translation is planned.

ABSTRACTS and PROCEEDINGS
Proceeding on the theme of the Workshop will include: **Reviews** (40 min, 12 pages), **Reports** (20 min, 5 pages) and **Posters** (4 pages). Published Abstracts of the Workshop will be distributed at the BDO '99. Contributed papers will be included in the Workshop Proceedings that will be published after the workshop. Extended abstracts (1 page is maximum) should be e-mailed to us in LaTeX[2] or ASCII format.**These must be received no later than August 9, 1999.** Abstracts sent after the deadline will not be included into the Workshop Book of Abstracts, but will be included in the Workshop Program.

ACTIVITIES
A social program for participants and accompanying persons is planned. It will include visiting the

[2]Form for Abstracts : http://www-bd.fnal.gov/icfa/newsletter/aug99/bdoform1.ps

State Art Museum (named after N.A. Radischev and often called "The Hermitage of Volga region"), theaters, and a bus excursion to the historical places of Saratov and the Saratov region (where the landing of the first Cosmonaut took place).

FEES
The registration fee for the conference is following:
Participants : $250 US Ph.D. Students : $50 US
We are sorry but WE CANNOT ACCEPT CREDIT CARDS OR CHECKS. The registration fee covers the collection of abstracts and other printing materials, coffee and tea breaks and the basic cultural program. For participation, please fill in the form[3] and return it immediately to the Organizing Committee.

ACCOMMODATION
The resort houses (Salut) are available for the BDO workshop participants. Prices are $8 US per night for a double room and $4 US per night for a single room. It is not necessary to send payment for accommodation in advance. Payment will be accepted upon arrival. Unfortunately, the number of double rooms is limited. The deadline for reservation a double room is August 27, 1999. Resort house guests are provided with three meals a day, $4 US per day.

DEADLINES
Today : Please fill in the Registration Form and e-mail it to : bdo99.ph.sgu@oda.ssu.runnet.ru
Today : Please, fill in the Visa Form and e-mail it to : bdo99.ph.sgu@oda.ssu.runnet.ru
August 9, 1999 : Submission of Abstracts
August 27, 1999 : To reserve double room

BDO '99 LOCAL ORGANIZING COMMITTEE ADDRESS
chairman - V.P. Stepanchuk
E-mail : step.ph.sgu@oda.ssu.runnet.ru - or - StepanchukVP@info.sgu.ru
Phone: (8452) 514562

All correspondence should be sent to:

V.P. Gorbachev, BDO-99
Department of Electrical & Radio Engineering
Faculty of Physics
Saratov State University
83 Asrakhanskaya Street
Saratov, 410026
RUSSIA
Phone: (8452) 513836
E-mail: bdo99.ph.sgu@oda.ssu.runnet.ru - or - GorbachevVP@info.sgu.ru

Contact with the BDO '99 LOCAL ORGANIZING COMMITTEE by e-mail is preferable.

[3] http://www-bd.fnal.gov/icfa/newsletter/aug99/bdoform2.ps

More complete information about ”BDO-99” can be found in the Home Page of the Nuclear Physics & Accelerators Laboratory:
http://www.sgu.ru/nuke

8: Announcements of the Beam Dynamics Panel

8.1 Minutes of the 14th Meeting of the ICFA Beam Dynamics Panel

Kohji Hirata kohji.hirata@kek.jp Chairman
ICFA Beam Dynamics Panel

The 14th meeting of the ICFA Beam Dynamics panel was held at New York Marriott Marquis Hotel, New York City on 1 April 1999. The following panel members took part: W. Chou, K. Hirata, J.M. Jowett, K.-J. Kim, J.-L. Laclare, E. A. Perelstein, J. Wei, Y. Satunov (INP) for D.Pestrikov. Apologizes were received from P. Chen, S. Ivanov, H. Mais, L.Palumbo, D. Whittum and C. Zhang. M. Cornacchia (SLAC) and P. F. Tavares (LNLS) attended as observers.

1. Reports of Working Groups (WG):

   (a) W. Chou reported the activities of the "high intensity high brightness hadron beams" working group. The group had a meeting on March 31 at the PAC'99. The 7th mini-workshop will be held from September 13 to 15, 1999 at Fermilab. The topic is beam halo and scraping. In addition to that, three new mini-workshops are proposed for the next two years. They are: longitudinal emittance control and measurement (March 6-8, 2000 at CERN), two-stream beam instability (LANL, dates to be selected) and beam chopping (place and dates to be selected). Furthermore, one "full" workshop is proposed. (see below)

   (b) E. Perelstein has reported the activity. There is not remarkable activity recently in the "Tau-Charm Factory" working group, after the successful workshop in Frascati in 1997. The proceeding has been published.

   Considering the present situation for Tau-Charm factories, it was discussed and agreed that this working group will stop soon and will be re-formulated as "High Luminosity Factories".

   (c) K-J. Kim has reported the activity of the "future light source" working group. (see below)

2. Reports on Workshop Preparation:
   The preparation status of the 17th ICFA Beam Dynamics Workshop on "Concepts for Future Light Source" was reported by K-J. Kim. There will be seven working groups and roughly 150 participants were anticipated.

3. Future workshops:
   The following three workshops were agreed. Hirata will ask ICFA for their approval.

   (a) "Quantum Aspects of Beam Physics", early 2000 in USA was proposed by P. Chen. This follows the similar workshop in 1998 held in Monterey, which was highly successful and regarded important.

   (b) "X-Ray Free Electron Lasers and Their Applications", September 2000 in Arcidosso Italy was proposed by C. Pellegrini and M. Cornacchia through K-J. Kim. This subject belongs to the "Future Light Source" working group. Thus the panel approved it provided it is agreed in the working group meeting scheduled during the workshop in ANL, which was in a week. It was finally approved in this meeting.

(c) On "High Intensity and High Brightness Hadron Beams", September or October 2000 (place to be determined) was proposed by W. Chou based on the agreement in the working group. It is meant to be a full workshop held by the "high intensity high brightness hadron beams" working group. It was requested to the working group to have a full workshop once a while.

(d) A workshop in Brazil was proposed by P. F. Tavares which might be held in 2001. The panel encouraged it and asked K-J. Kim to discuss in his working group.

4. Guideline for the workshops:
   A discussion was made on the guide line of the Advanced ICFA Beam Dynamics Workshop. The guideline appears to be too rigid and might discourage to get ICFA sponsorship. The conclusion, however, was that the present guideline (see the minutes for the 11^th ICFA Beam Dynamics Panel Meeting, 1996) is valid and we keep it.

5. The Newsletter:
   The new editing system was discussed, which is as follows:

   Kohji Hirata and John M. Jowett serve as Editors in chief, who supervise each edition. W. Chou, S. Ivanov, H. Mais, Jie Wei, D. H. Whittum, and C. Zhang will serve as editors, each working as the main editor of each issue alternatively. The panel agreed with the new system.

   Another discussion was that, in the instruction of the newsletter, the "invitation only" is too much underlined. Actually, the submission of an article to the newsletter is open to everyone. The submission is understood as the proposal for the invitation. Hirata and Jowett will take care of the softening of the instruction.

   W. Chou has proposed that, in one of the future issues, he would like to collect the activity reports related to his working group. The panel encouraged this idea, provided that the issue has normal articles not exclusively be devoted to it. The style was discussed. Hirata has requested other working group leaders to think of similar effort.

6. Next Meeting:
   The next panel meeting will be held in the occasion of EPAC in 2000.

The panel thanks the organizing committee of PAC99 in particular its chairman Dr. W.T. Weng for providing the facilities for the fourteenth meeting and for the hospitality extended to them.

8.2 Minutes of the ICFA Working Group Meeting

Weiren Chou chou@fnal.gov Leader
ICFA Working Group on
High Intensity High Brightness
Hadron Beams

There was an ICFA Working Group Meeting on high intensity and high brightness hadron beams at the PAC'99 on March 31, 1999. Eleven group members or their representatives attended this meeting: R. Baartman (TRIUMF), S. Chattopadhyay (LBNL for J. Wurtele), W. Chou (FNAL), R. Davidson (PPPL), M. Giovannozzi (CERN for R. Cappi), W. Hofle (CERN for T. Linnecar), R. Macek (LANL for A. Thiessen), S. Machida (KEK), P. Martin (FNAL), D. Olsen (ORNL) and T.

Roser (BNL). K. Hirata (KEK) and N. Mokhov (FNAL) were also invited to the meeting. It was regrettable that some members missed this meeting because of a misprint of the meeting date on the PAC'99 bulletin.

1. The first part of the meeting was lab reports of activities on high intensity and high brightness hadron beams. The following talks were presented to the meeting:

   - R. Macek: PSR and APT
   - T. Roser: AGS
   - P. Martin: Main Injector
   - M. Giovannozzi: CERN PS
   - W. Hofle: CERN SPS
   - D. Olsen: SNS
   - S. Machida: JHF
   - R. Baartman: TRIUMF activities
   - S. Chattopadhyay: LBNL activities
   - W. Chou: Proton Driver for muon storage ring/muon collider

   Most of the talks were well prepared and served the purpose of information exchange among the labs.

2. W. Chou gave a report on the group activities in the past two years. This group has been doing two things:

   (a) Organizing ICFA beam dynamics mini-workshops:
   Since 1996, six mini-workshops have been organized:

      i. May 1996, Fermilab, transition crossing;

      ii. Dec 1996, KEK, beam losses;

      iii. May 1997, BNL, rf;

      iv. Nov 1997, CERN, transverse emittance preservation and measurement;

      v. Feb 1998, KEK, beamloading;

      vi. Feb 1999, RAL, injection and extraction.

      The next one (7th) will be Sept 13-15, 1999 at Fermilab. The topic is beam halo and scraping. The organizers are N. Mokhov and W. Chou.

(b) Compiling and maintaining proton machine parameter tables:
At this moment, there are five tables compiled:

- Table 1. Proton synchrotron performance;
- Table 2. Particle losses;
- Table 3. Transverse emittance evolution and measurements;
- Table 4. RF parameters and beamloading;
- Table 5. H- injection.

These tables have been published in the mini-workshop proceedings. They are or will soon be available on the ICFA web page.

3. There was a discussion on the plan for next two years. The group decided to propose the following new workshops to the ICFA:

(a) A ”full” ICFA workshop next year:
At the suggestion of K. Hirata, chairman of the ICFA beam dynamics panel, the group agreed to organize a ”full” ICFA workshop in September or October 2000. The subject is high intensity and high brightness hadron beams. The focus will be on circular machines. The place will be determined later. Unlike mini-workshops, this workshop will be open to general registration (i.e., not by invitation only) and will publish formal proceedings.

(b) Three new ICFA mini-workshops:

- Longitudinal emittance control and measurement, March 6-8, 2000 at CERN. The organizers are: T. Linnecar, E. Shaposhnikova, R. Cappi and R. Garoby.
- 2-stream beam instability, at LANL, dates to be determined. The contact persons are R. Macek and A. Thiessen.
- Beam chopping, place and dates to be determined.

4. August 1999 issue of the ICFA Beam Dynamics Newsletter:
This will be a special issue focusing on the problems related to high intensity high brightness hadron beams. W. Chou will be the editor. Every group member is invited to contribute a paper to this issue. Detailed instructions will be sent out later. (Note: In addition to these ”theme” papers, the ”normal” stuff such as letters to the editor, Ph.D. thesis topics and other articles will also be published in this issue.)

8.3 ICFA Beam Dynamics Newsletter

Editors in chief
Kohji Hirata (hirata@kekvax.kek.jp) and John M. Jowett (John.Jowett@cern.ch)

Editors
Weiren Chou (chou@adcon.fnal.gov),
Sergei Ivanov (ivanov_s@mx.ihep.su),
Helmut Mais (mais@mail.desy.de),
Jie Wei (wei1@bnl.gov),
David H. Whittum (whittum@SLAC.Stanford.EDU),
Chuang Zhang (zhangc@bepc3.ihep.ac.cn)

8.3.1 Aim of the Newsletter

The ICFA Beam Dynamics Newsletter is intended as a channel for describing unsolved problems and highlighting important ongoing works, and not as substitute for journal articles and conference proceedings which usually describe completed work. It is published by the ICFA Beam Dynamics Panel, one of whose missions is to encourage international collaboration in beam dynamics.

8.3.2 Categories of the Articles

It is published every April, August and December. The deadlines are 15 March, 15 July and 15 November, respectively.

The categories of articles in the newsletter are the following:

1. Announcements from the panel
2. Reports of Beam Dynamics Activity of a group
3. Reports of Beam Dynamics related workshops and meetings
4. Announcements of future Beam Dynamics related international workshops and meetings.

   Those who want to use newsletter to announce their workshops etc can do so. Articles should typically fit within half a page and include descriptions of the subject, date, place and details of the contact person.
5. Review of Beam Dynamics Problems

   This is a place to put forward unsolved problems and not to be used as the achievement report. Clear and short highlights on the problem is encouraged.
6. Letters to the editor

   It is a forum open to everyone. Anybody can show his/her opinion on the beam dynamics and related activities, by sending it to one of the editors. The editors keep the right to reject a contribution.
7. New Doctoral Theses in Beam Dynamics

   Please send announcements to the editors including the following items (as a minimum):

   (a) Name, email address and affiliation of the author,

(b) Name, email address and affiliation of the supervisor,
(c) Name of the institution awarding the degree,
(d) The title of the thesis or dissertation.
(e) Date of award of degree. (For a while, we accept the thesis awarded within one year before the publication of the newsletter.)
(f) A *short* abstract of the thesis is also very desirable.

8. Editorial

All articles except for 6) and 7) are by invitation only. The editors request an article following a recommendation by panel members. **Those who wish to submit an article are encouraged to contact a nearby panel member**.

The manuscript should be sent to one of the editors as a LaTeX file or plain text. The former is encouraged and authors are asked to follow the instructions below.

Each article should have the title, author's name(s) and his/her/their e-mail address(es).

8.3.3 How to Prepare the Manuscript

Here, the *minimum* preparation is explained, which helps the editors a lot. The full instruction can be found in WWW at

`http://www-acc-theory.kek.jp/ICFA/instruction.html`

where you can find the template also.

Please follow the following:

- Do not put comments (%) when sending the manuscript through e-mail. Instead, you can use \comm as \comm{your comments}. It is defined as \newcommand\comm[1]{}.
- Start with \section{title of your article}. **It is essential**.
- Then put your name, e-mail address and affiliation.
- It is *useless to include any visual formatting commands* (such as vertical or horizontal spacing, centering, tabs, etc.).
- Do not define new commands.
- Avoid TEXcommands that are not part of standard LATEX. These include the likes of \def, \centerline, \align, ...
- Please keep figures to a minimum. The preferred graphics format is Encapsulated Postscript (EPS) files.

8.3.3.1 Regular Correspondents

Since it is impossible for the editors and panel members to watch always what is going on all around the world, we have started to have *Regular Correspondents*. They are expected to find interesting activities and appropriate persons to report them and/or report them by themselves. We hope that we will have a "compact and complete" list covering all over the world eventually. The present *Regular Correspondents* are as follows

Liu Lin (liu@ns.lnls.br)	LNLS	Brazil
S. Krishnagopal (skrishna@cat.cat.ernet.in)	CAT	India
Ian C. Hsu (ichsu@ins.nthu.edu.tw)	SRRC	Taiwan

We are calling for more volunteers as *Regular Correspondents.*

8.3.4 Distribution

The ICFA Beam Dynamics Newsletters are distributed through the following distributors:

W. Chou	chou@adcon.fnal.gov	North and South Americas
Helmut Mais	mais@mail.desy.de	Europe* and Africa
Susumu Kamada	kamada@kekvax.kek.jp	Asia** and Pacific

(*) including former Soviet Union.
(**) For mainland China, Chuang Zhang (zhangc@bepc5.ihep.ac.cn) takes care of the distribution with Ms. Su Ping, Secretariat of PASC, P.O. Box 918, Beijing 100039, China.

It can be distributed on a personal basis. Those who want to receive it regularly can ask the distributor to do so. In order to reduce the distribution cost, however, please use WWW as much as possible. (See below).

8.4 World-Wide Web

The home page of the ICFA Beam Dynamics Panel is at the address

http://www-acc-theory.kek.jp/ICFA/icfa.html

(which happens to be in Japan). For reasons of access speed, there are mirror sites for Europe and the USA at

http://wwwslap.cern.ch/icfa/
http://www.slac.stanford.edu/grp/arb/dhw/dpb/icfa/icfa.html

All three sites are essentially identical and provide access to the Newsletters, Future Workshops, and other information useful to accelerator physicists. There are links to information of local interest for each area.

8.5 ICFA Beam Dynamics Panel Organization

The mission of ICFA Beam Dynamics Panel is *to encourage and promote international collaboration on beam dynamics studies for present and future accelerators.* For this purpose, we publish *ICFA Beam Dynamics Newsletters* three times a year, we sponsor *Advanced ICFA Beam Dynamics Workshops* and *ICFA Beam Dynamics Mini-Workshops,* and we organize *Working Groups* in the panel to promote several important issues.

Chairman K. Hirata
Chief Editors of ICFA Beam Dynamics Newsletter K. Hirata and J. M. Jowett

Editors of ICFA Beam Dynamics Newsletter W. Chou, S. Ivanov, H. Mais, J. Wei, D.H. Whittum, and C. Zhang

Distributors of ICFA Beam Dynamics Newsletter W. Chou, H. Mais, S. Kamada

Leader and Subleader of Future Light Source Working Group K. J. Kim and J. L. Laclare

Leader and Subleader of Tau-Charm factory Working Group E. A. Perelstein and C. Zhang

Leader of High-Brightness Hadron Beams Working Group W. Chou

WWW keeper K. Hirata, J. M. Jowett and D.H. Whittum

Panel Members

Ainosuke Ando (ando@lasti.himeji-tech.ac.jp)	Himeji Inst.Tech./SPRING8
Pisin Chen (chen@slac.stanford.edu)	SLAC
Weiren Chou (chou@adcon.fnal.gov)	Fermilab
Kohji Hirata (kohji.hirata@kek.jp)	SoKenDai/KEK
Albert Hofmann (Albert.Hofmann@cern.ch)	CERN
Ingo Hofmann (I.Hofmann@gsi.DE)	GSI
Sergei Ivanov (ivanov_s@mx.ihep.su)	IHEP (Protvino)
John M. Jowett (John.Jowett@cern.ch)	CERN
Kwang-Je Kim (Kwang_Je_Kim@macmail.lbl.gov)	LBNL
Jean-Louis Laclare (laclare@soleil.cea.fr)	SOLEIL
Helmut Mais (mais@mail.desy.de)	DESY
Luigi Palumbo (lpalumbo@frascati.infn.it)	Univ.Rome/LNF-INFN
Claudio Pellegrini (claudio@vesta.physics.ucla.edu)	UCLA
Elcuno A. Perelstein (perel@ljap12.jinr.dubna.su)	JINR
Dmitri Pestrikov (pestrikov@inp.nsk.su)	BINP
Jie Wei (wei1@bnl.gov)	BNL
David H. Whittum (whittum@SLAC.Stanford.EDU)	SLAC
Chuang Zhang (zhangc@bepc3.ihep.ac.cn)	IHEP(Beijing)